

NASA/TM-2010-216194



Investigation of Control System and Display Variations on Spacecraft Handling Qualities for Docking with Stationary and Rotating Targets

*E. Bruce Jackson, Kenneth H. Goodrich, and Randall E. Bailey
Langley Research Center, Hampton, Virginia*

*James R. Barnes
ARINC, Hampton, Virginia*

*William A. Ragsdale
Unisys Corporation, Hampton, Virginia*

*Jason R. Neuhaus
Langley Research Center, Hampton, Virginia*

NASA STI Program . . . in Profile

Since its founding, NASA has been dedicated to the advancement of aeronautics and space science. The NASA scientific and technical information (STI) program plays a key part in helping NASA maintain this important role.

The NASA STI program operates under the auspices of the Agency Chief Information Officer. It collects, organizes, provides for archiving, and disseminates NASA's STI. The NASA STI program provides access to the NASA Aeronautics and Space Database and its public interface, the NASA Technical Report Server, thus providing one of the largest collections of aeronautical and space science STI in the world. Results are published in both non-NASA channels and by NASA in the NASA STI Report Series, which includes the following report types:

- **TECHNICAL PUBLICATION.** Reports of completed research or a major significant phase of research that present the results of NASA programs and include extensive data or theoretical analysis. Includes compilations of significant scientific and technical data and information deemed to be of continuing reference value. NASA counterpart of peer-reviewed formal professional papers, but having less stringent limitations on manuscript length and extent of graphic presentations.
- **TECHNICAL MEMORANDUM.** Scientific and technical findings that are preliminary or of specialized interest, e.g., quick release reports, working papers, and bibliographies that contain minimal annotation. Does not contain extensive analysis.
- **CONTRACTOR REPORT.** Scientific and technical findings by NASA-sponsored contractors and grantees.

- **CONFERENCE PUBLICATION.** Collected papers from scientific and technical conferences, symposia, seminars, or other meetings sponsored or co-sponsored by NASA.
- **SPECIAL PUBLICATION.** Scientific, technical, or historical information from NASA programs, projects, and missions, often concerned with subjects having substantial public interest.
- **TECHNICAL TRANSLATION.** English-language translations of foreign scientific and technical material pertinent to NASA's mission.

Specialized services also include creating custom thesauri, building customized databases, and organizing and publishing research results.

For more information about the NASA STI program, see the following:

- Access the NASA STI program home page at <http://www.sti.nasa.gov>
- E-mail your question via the Internet to help@sti.nasa.gov
- Fax your question to the NASA STI Help Desk at 443-757-5803
- Phone the NASA STI Help Desk at 443-757-5802
- Write to:
NASA STI Help Desk
NASA Center for AeroSpace Information
7115 Standard Drive
Hanover, MD 21076-1320

NASA/TM-2010-216194



Investigation of Control System and Display Variations on Spacecraft Handling Qualities for Docking with Stationary and Rotating Targets

*E. Bruce Jackson, Kenneth H. Goodrich, and Randall E. Bailey
Langley Research Center, Hampton, Virginia*

*James R. Barnes
ARINC, Hampton, Virginia*

*William A. Ragsdale
Unisys Corporation, Hampton, Virginia*

*Jason R. Neuhaus
Langley Research Center, Hampton, Virginia*

National Aeronautics and
Space Administration

Langley Research Center
Hampton, Virginia 23681-2199

February 2010

Acknowledgments

The authors extend their thanks to Tom Aldrete, Karl Bilimoria, Eric Mueller, Chad Frost and former astronaut Bo Bobko of the NASA Ames Simulation Laboratory for their collaboration, astronaut Jim Dutton of Johnson Space Center for his assistance, and to members of the NASA Langley simulation staff, including Miguel Alvarez, Wayne Burge, Don Buhl, Victoria Chung, Tom Feigh, Dennis Frasca, Chris Harrison, Sonia Herndon, Jerry Karwac, Kemper Kibler, Ben Lewis, Nevin Oswald, Darrell Sacra, Ming-Yun Shih, Phil Smith, John Tulppo and Tom Wolters.

The use of trademarks or names of manufacturers in this report is for accurate reporting and does not constitute an official endorsement, either expressed or implied, of such products or manufacturers by the National Aeronautics and Space Administration.

Available from:

NASA Center for AeroSpace Information
7115 Standard Drive
Hanover, MD 21076-1320
443-757-5802

Abstract

This paper documents the investigation into the manual docking of a preliminary version of the Crew Exploration Vehicle with stationary and rotating targets in Low Earth Orbit. The investigation was conducted at NASA Langley Research Center in the summer of 2008 in a repurposed fixed-base transport aircraft cockpit and involved nine evaluation astronauts and research pilots.

The investigation quantified the benefits of a feed-forward reaction control system thruster mixing scheme to reduce translation-into-rotation coupling, despite unmodeled variations in individual thruster force levels and off-axis center of mass locations up to 12 inches. A reduced rate dead-band in the phase-plane attitude controller also showed some promise. Candidate predictive symbology overlaid on a docking ring centerline camera image did not improve handling qualities, but an innovative attitude status indicator symbol was beneficial.

The investigation also showed high workload and handling quality problems when manual dockings were performed with a rotating target. These concerns indicate achieving satisfactory handling quality ratings with a vehicle configuration similar to the nominal Crew Exploration Vehicle may require additional automation.

Contents

1	Summary	4
2	Introduction	4
3	Acronyms	5
4	Symbols	7
5	Vehicle Model	8
6	Simulation Implementation	8
6.1	Cockpit description	8
6.2	Aural cueing	8
6.3	Inceptors	9
6.4	Control Laws	11
6.4.1	Autopilot	11
6.4.2	Control mixing	12
6.4.3	Reaction control system model	15
6.5	Displays	15
6.5.1	Out-the-window display	16
6.5.2	Attitude Director Indicator	16
6.5.3	Navigation display	17
6.5.4	Rendezvous and Proximity Operations display	17
6.5.5	Docking Centerline Camera display	17
6.5.6	Scorecard display	21
6.5.7	Digital Autopilot Interface Display and Keyboard	23
7	Task Description	23
8	Experiment Protocol	24
8.1	Evaluation pilots	24
8.2	Schedule	25
8.3	Presentation order	25
8.4	Briefing	25
8.5	Training runs	25
8.5.1	Training for task 1 (stationary International Space Station (ISS) docking)	25
8.5.2	Training for task 2 (rotating target docking)	27
8.6	Data runs	27
8.6.1	Task 1: Stationary ISS docking	27
8.6.2	Task 2: Rotating target docking	28
8.7	Scoring	29
9	Experiment Results	30
9.1	Task 1 - Stationary ISS docking	30
9.2	Task 2 - Rotating target docking	32

10 Discussion of Results	33
10.1 Task 1 - Stationary ISS docking	33
10.1.1 Comparison of variants vs. the nominal Crew Exploration Vehicle (CEV) configuration baseline	33
10.1.2 Comparison of variants vs. a reversionary six degrees-of-freedom (6DOF) CEV configuration	40
10.1.3 Comparing reversionary 6DOF CEV to the baseline CEV	44
10.2 Task 2 - Rotating target docking	45
10.2.1 Test 16 - Yawing target	45
10.2.2 Test 17 - Pitching target	46
10.2.3 Test 18 - Pitching & yawing target at 0.4 deg/s total rate	47
10.2.4 Test 19 - Pitching & yawing target at 0.566 deg/s total rate	47
10.3 TDM mixer contamination	47
11 Conclusions	49
11.1 Task 1 - Stationary ISS docking	49
11.2 Task 2 - Rotating target docking	50
12 References	51
Appendix A - Metrical Data Plots	53
Appendix B - Autopilot Details	82
Introduction	82
Digital Autopilot (DAP) Configurations	82
Control modes	84
AUTO	84
INTRL	84
LVLH	84
Free	84
Manual modes	84
Rotational command modes	84
Translational command modes	85
Phase Plane implementation	85
reaction control system (RCS) mixer	88
Conclusion	89
Code listings	89
Appendix C - Pilot Briefing Slides	100

1 Summary

An investigation into the manual docking of a preliminary version of the Crew Exploration Vehicle (**CEV**) with stationary and rotating targets in low Earth orbit was conducted at NASA Langley Research Center (**LaRC**) in the summer of 2008 in a repurposed fixed-base transport aircraft cockpit. The study involved nine evaluation astronauts and research pilots.

The investigation quantified the benefits of a feed-forward reaction control system thruster mixing scheme to reduce translation-into-rotation coupling, despite unmodeled variations in individual thruster force levels and off-axis center of mass locations up to 12 inches. A reduced rate dead-band in the phase-plane attitude controller also showed some promise. Candidate predictive symbology overlaid on a docking ring centerline camera image did not improve handling qualities, but an innovative attitude status indicator symbol was beneficial.

The investigation also showed high workload and handling quality problems when manual dockings were performed with a rotating target. These concerns indicate achieving satisfactory handling quality ratings with a vehicle configuration similar to the nominal **CEV** may require additional automation.

2 Introduction

As part of the Constellation Program (**CxP**), the need for a crew-carrying spacecraft capable of operating in both low-Earth, Lunar and Martian orbits has been addressed by design of the Orion **CEV** spacecraft. The **CEV** is similar in shape to the earlier Apollo spacecraft used to place the first human on the Moon in July 1969 but somewhat larger.

The planetary landing Apollo and Orion missions are both called on to perform docking between two spacecraft; in the case of the Apollo Command Module, the other spacecraft was the Lunar Module which landed on and returned from the lunar surface. The Orion **CEV** will use a similar vehicle, the Altair lander, to reach the Moon's surface; the Mars lander is not yet named. In addition, Orion is required to be able to rendezvous and dock with the International Space Station (**ISS**).

The investigation of docking a manned spacecraft with another spacecraft has been underway since the early 1960s [1], [2], [3], [4], [5], [6]. The Apollo predecessor Gemini spacecraft were the first to be designed for and to achieve a successful docking in space (Gemini 6 with an Agena target vehicle in March 1966). Achievement of this milestone was preceded by extensive ground-based orbital docking simulations in which handling qualities were studied [1], [4], [5], [7].

In addition to docking with a relatively stable target such as the **ISS**, the Orion Systems Requirement Document [8] requires the **CEV** to be able to dock with a spacecraft rotating up to 0.4 deg/s. Earlier Gemini and Apollo studies may have addressed this issue [7], but it had not been examined for the **CEV** until [9], which looked at an oscillating and nutating **ISS**.

A fixed-base piloted simulation study was conducted at **LaRC** to investigate the effect of display and control law variations on the manual and semi-automatic docking of a spacecraft resembling the **CEV** with a large stationary target (the **ISS**) and a smaller rotating target (an Apollo Command/Service Module [**CSM**]). Two basic vehicle control configurations (with and without feed-forward rotational coupling compensation), autopilot (with and without rate command/attitude hold [**RCAH**]) and centerline docking camera overlay symbology variations were studied for the stationary **ISS** docking scenario; a baseline **CEV** was assumed for the rotating target docking task, which looked at rotation rates of at least 0.4 deg/s in single and dual axes. Variations in attitude control law dead-bands and off-nominal vehicle

configurations were also evaluated for the stationary [ISS](#) docking scenario.

Evaluation pilots in this study included nine active and former astronauts and research pilots. They were briefed on the experiment purpose, trained to perform a docking under nominal conditions, and were asked to perform and evaluate at least three dockings with each vehicle control, autopilot and overlay symbology combination, presented in unique (to each pilot) random order in a blind test. They were asked after each configuration to provide commentary and Cooper-Harper Pilot Ratings, based on their performance and amount of compensation required, and Task Load Index ratings based on their perceived work load.

The resulting objective and subjective measures of performance and crew task load were compared on a per-pilot basis for the stationary docking scenario to judge the relative effects of the configuration variations. The rotating target scenarios were evaluated for feasibility based on perceived workload and handling qualities.

In all, 286 dockings were attempted by nine pilots; 285 were successful.

3 Acronyms

6DOF	six degrees-of-freedom
A-DAP	digital autopilot high-authority setting
ADI	Attitude Director Indicator
ASI	Attitude Status Indicator
B-DAP	digital autopilot low-authority setting
CEV	Crew Exploration Vehicle
CDU	Control Display Unit
CHR	Cooper-Harper Rating
CLC	centerline camera
CM	center of mass
CSM	Command/Service Module
CxP	Constellation Program
DAP	Digital Autopilot
DB	dead-band
FF	feed-forward
FOV	field of view
HP	geopotential altitude
ISS	International Space Station
LaRC	NASA Langley Research Center
LaSRS++	Langley Standard Real-Time Simulation in C++
LCD	Liquid Crystal Display
LVLH	local vertical, local horizontal

LSAM	Lunar Surface Access Module
NA	not applicable
NAV	navigation display
PIO	pilot-induced oscillation
RCAH	rate command/attitude hold
RCS	reaction control system
RFD	Research Flight Deck
RHC	rotational hand controller
RMS	root-mean-square
RPOP	Rendezvous and Proximity Operations Program display
TDM	time-domain multiplexer
THC	translational hand controller
TLX	task-load index
UPNT	Universal Pointing mode
UTC	coordinated universal time

4 Symbols

Δp	Change in roll rate
Δq	Change in pitch rate
R	Distance between docking port centers
\dot{R}	Rate of change of distance between docking port centers
\bar{R}	Vertical axis of the local vertical, local horizontal (LVLH) frame, positive towards Earth's center
Δr	Change in yaw rate
ΔV	Change in linear velocity
\bar{V}	Orbital velocity axis, LVLH frame, positive in direction of motion
X, X_{body}	Longitudinal body axis, positive forward
$\Delta \dot{X}$	Change in velocity, longitudinal body axis
Y, Y_{body}	Lateral body axis, positive right
\bar{Y}	Lateral axis, LVLH frame, positive to right of direction of motion and normal to the orbital plane
$\Delta \dot{Y}$	Change in velocity, lateral body axis
Z, Z_{body}	Vertical body axis, positive down
$\Delta \dot{Z}$	Change in velocity, vertical body axis
θ	Pitch Euler angle of body with respect LVLH frame
ϕ	Roll Euler angle of body with respect to LVLH frame
ψ	Yaw Euler angle of body with respect to LVLH frame
$\Delta \omega$	Absolute change in angular velocity

5 Vehicle Model

The vehicle modeled was the [CEV](#), model 606C, as described in [10]. A fixed-mass condition corresponding to the first [ISS](#) docking opportunity was used for all data runs. Since the control system, aside from the positions and thrust levels of the [RCS](#), was not sufficiently defined for piloted operation, a control law and autopilot of limited capability was developed specifically for this experiment. The [RCAH](#) control system was based on the Space Shuttle with simplifications.

6 Simulation Implementation

The vehicle model was realized in NASA [LaRC](#)'s Langley Standard Real-Time Simulation in C++ ([LaSRS++](#)) simulation framework, described in [11]. The simulation equations of motion included an oblate rotating Earth model so orbital mechanics effects were apparent during the docking maneuvers. The docking studies were all conducted at an altitude of 333.4 km (180 nm) in an orbital plane corresponding to that of the [ISS](#) (51.6 degrees) and were performed from the $+\bar{V}$ axis (approaching the target from an initial position in front of the velocity vector, moving retrograde relative to the orbit of the target). The various targets were likewise in a full six degrees-of-freedom ([6DOF](#)) orbit with a constant rotational rate; in the case of the [ISS](#) target, the rotation rate matched the orbital rotation of the [LVLH](#) frame and thus appeared stationary to the approaching vehicle.

6.1 Cockpit description

Langley's Research Flight Deck ([RFD](#)) cab, a re-purposed advanced twin-engine transport cab with twin seating [12], was utilized for this experiment. The evaluation pilot sat in the right-hand seat.

A wide-angle collimated visual scene of approximately 200×40 degrees was projected in front of the cab. The forward and side windows were masked to represent the field of view of a standing pilot in the right side of the [CEV](#). This field of view provided out-the-window views of the approaching target vehicle but, in general, sight of the target's docking ring was obscured within five feet of docking due to the pilot offset from the centerline docking axis.

The observer(s) occupied the left-hand and jump seats of the [RFD](#) cab; the simulation operator was also located in the aft of the cab.

The [RFD](#) flight management system Control Display Unit ([CDU](#)) keyboard and display could be used by the evaluation pilot but was normally used by the test observer, at the request of the pilot, to select digital autopilot gain changes.

The weather radar range selection knob on the center aisle stand was re-purposed to allow either the evaluation pilot or the observer to change the field-of-view of the centerline docking camera from 5 to 80 degrees; it is anticipated some selectable field-of-view will be available in the actual [CEV](#).

Figure 1 shows an interior view of the [RFD](#) cab from behind the evaluation pilot's seat, as configured for this experiment.

6.2 Aural cueing

During docking maneuvers, an automated voice called out 20, 15, 10, and subsequent decreasing integer feet values, based on slant-range distance between docking ports for consistent aural cueing between pilots and runs. In addition, a tailored white noise (emanating



Figure 1: Picture of the right seat of the RFD

from a non-specific location) was used whenever a thruster fired, either in response to autopilot or manual command. Finally, a metallic bang sound was used at the moment of docking (relative X_{body} range crossed through zero) and the simulation run would end.

6.3 Inceptors

Apollo-like translational and rotational hand controllers were mounted in positions convenient for the right-hand pilot seat, as shown in figure 1. The translational hand controller (THC) was mounted on the left side of the pilot, while the rotational hand controller (RHC) was mounted on the right side of the pilot.

The THC, shown in figure 2a, allowed motion of the T-shaped handle in three axes: longitudinal (in-out), lateral (left-right) and vertical (up-down). Springs kept the controller in the central position. When moved more than approximately $1/2''$ (requiring approximately 1 lbf of force) in any axis, the T-handle would move out of the center, or detent, position, closing a discrete switch. Proportional deflection was not sensed. The T-handle could also be rotated ± 17 deg around the longitudinal axis (with some effort) to function as a switch; this motion was not used in this study.

The RHC, shown in figure 2b, allowed rotational motion about three axes: pitch, which rotated ± 15 degrees near the center of the grip; roll, which rotated ± 26 degrees about a pivot $3\frac{5}{8}''$ below the grip, and yaw, which rotated ± 34 degrees about the vertical axis of the handle. A small knob at the base of the controller which moved in the longitudinal direction was not used in this study. Breakout force was approximately 0.1 lbf in pitch and yaw, and 0.5 lbf in roll. Figure 3 gives the moment-vs.-displacement curve for all three axes of motion.

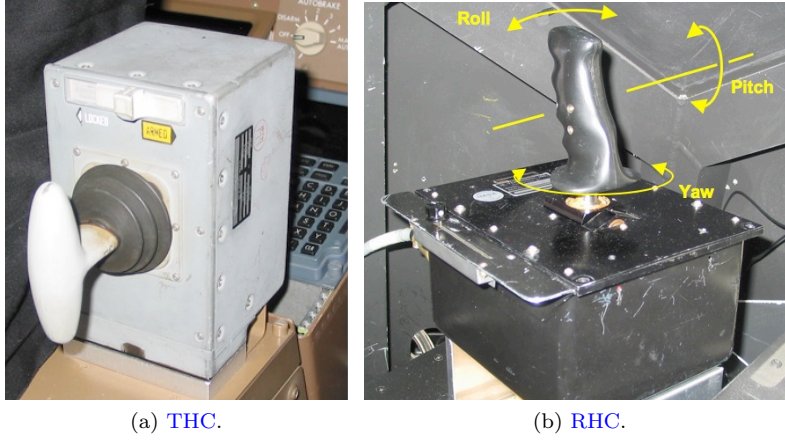


Figure 2: Translational and rotational hand controllers

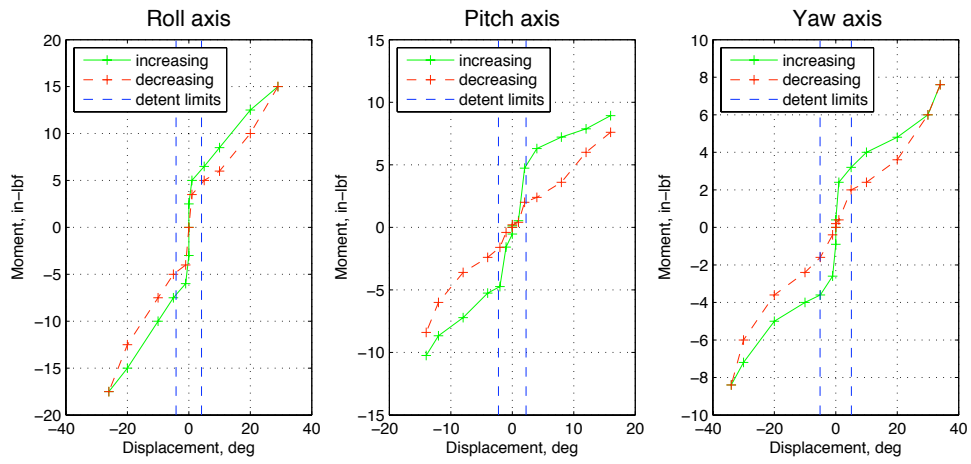


Figure 3: Rotational hand controller moment-displacement curves

6.4 Control Laws

Figure 4 shows the logic involved in selecting manual or automatic control of attitude, the control mixer, and the feed-forward compensation network. A more complete specification of the autopilot is found in Appendix B.

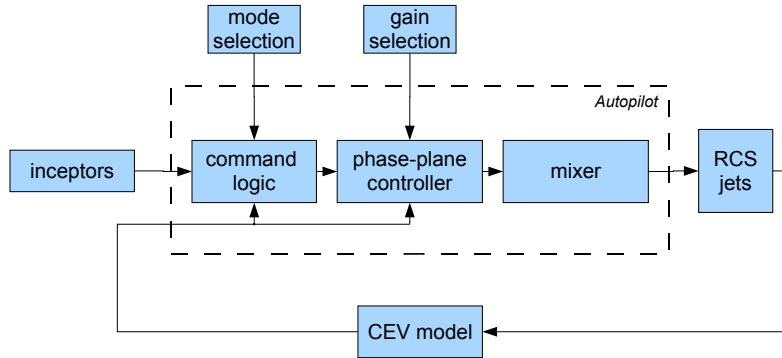


Figure 4: Overview of the control law configuration for the experiment

6.4.1 Autopilot

The tasks involved in this experiment were flown with an autopilot, which allowed selection of separate RCS command modes, either Pulse or Direct for translations and either Pulse or Discrete Rate for rotations, on a per-axis basis. These modes are described in more detail below.

In most tests, the tasks were flown with the autopilot in Pulse mode for translational axes and Discrete Rate mode for rotational axes. The increment of rotation ($\Delta\omega$) or translation (ΔV) commanded by movement of an inceptor out of detent depended on the autopilot gain set selected. An ‘A’ gain set provided larger rate responses than the corresponding ‘B’ gain set, in both rotation and translation.

Table 1 gives the commanded ΔV and $\Delta\omega$ magnitudes for the ‘A’ and ‘B’ gain sets.

Table 1: Command authority for Pulse command autopilot mode

Gain set	ΔV ft/s	$\Delta\omega$ deg/s
A	0.010	0.10
B	0.002	0.04

Pulse command mode - all axes. The RCS Pulse command mode allowed the pilot, for each translational and rotational axis, to command a fixed change in velocity (ΔV) or rotational rate ($\Delta\omega$) each time the appropriate inceptor was moved out of the center (detent) position. [Moving the inceptor back into detent had no effect.] The values of pulse size in translation and rotation were set based on the gain set chosen. In Pulse mode, the controller had to be moved back into and out of detent again to command an additional pulse.

When the three rotational axes were in [RCS](#) Pulse mode, the resulting configuration was sometimes referred to as a [6DOF](#) configuration, meaning the evaluation pilot had direct command in all six degrees-of-freedom of motion of the vehicle about the center of mass.

Direct command mode - translational axes. When [RCS](#) Direct command mode was selected for a particular translational axis, each movement of the translational inceptor out of detent in a particular axis resulted in constant [RCS](#) thrusting in the corresponding direction. The amount of acceleration was determined by the relative amount of acceleration available in that direction, a function of spacecraft mass and the maximum amount of decoupled thrust available in that direction (see section [6.4.2](#) below).

Discrete Rate command mode - rotational axes. When [RCS](#) Discrete Rate command mode was selected for a particular rotational axis, each movement of the rotational inceptor out of detent in a particular axis commanded a fixed (discrete) angular rate about the corresponding axis; the amount of acceleration was determined by the relative amount of [RCS](#) moment authority and the rotational inertia in that axis. When the inceptor was moved back into detent, the [RCS](#) system would fire in the opposite sense to null the resulting rate (in an [LVLH](#) sense). Once the rate had been nulled, the autopilot would then attempt to maintain the vehicle in the new attitude.

If the inceptor was moved more than 90% of full throw in a particular axis, the [RCS](#) thrusters would be commanded to fire continuously in that axis, like the Direct mode in the translational axes. When the inceptor was moved back below 90% of full throw, the achieved rate was maintained (by virtue of no additional [RCS](#) thruster firing). As before, when the inceptor was moved back into detent, the [RCS](#) system would fire to null rates and would then maintain the vehicle in the new attitude.

This command-response type control mode is also called rate command/attitude hold. In this report, the term ‘[RCAH](#)’ implies [RCS](#) Discrete Rate command mode in a particular rotational axis.

The [RCS](#) Discrete Rate capability was provided by a phase plane controller based on the Shuttle [RCAH](#) controller described in [13]; a schematic of the phase-plane control space is shown in figure [5](#). Additional information regarding the implementation of the [DAP](#) are given in appendix [B](#).

6.4.2 Control mixing

As documented in previous experiments [9] and [14], the unique reaction control system jet locations and orientations relative to the [CEV](#) center of mass and principal axes of inertia required that multiple jets must be fired to maneuver in any single axis (both in translation and rotation). Thus some sort of control mixing strategy was necessary to select which jets should be fired, preferably one that provided feed-forward compensation to lessen the resulting coupling of translational inputs into rotational axes.

An off-line optimization was performed to determine the most fuel-efficient set of jets required to generate any combination of rotation and translation motion in three senses (positive, zero, and negative) in each of six degrees-of-freedom (three in rotation and three in translation), yielding 3^6 or 729 combinations of the eight [RCS](#) jets. This optimization scheme provided the most fuel-efficient firings of available jets that would minimize translation-into-rotation coupling. The output of the optimizer specified the proportion of thrust of each jet to be used to match each possible command input combination, resulting in a 729×8 jet mixing table.

This mixing table was precomputed for a nominal center of mass, cross-products of inertia and nominal [RCS](#) thruster size and provided a proportional [RCS](#) firing solution. This firing solution theoretically would yield uncoupled motion in response to a six-element

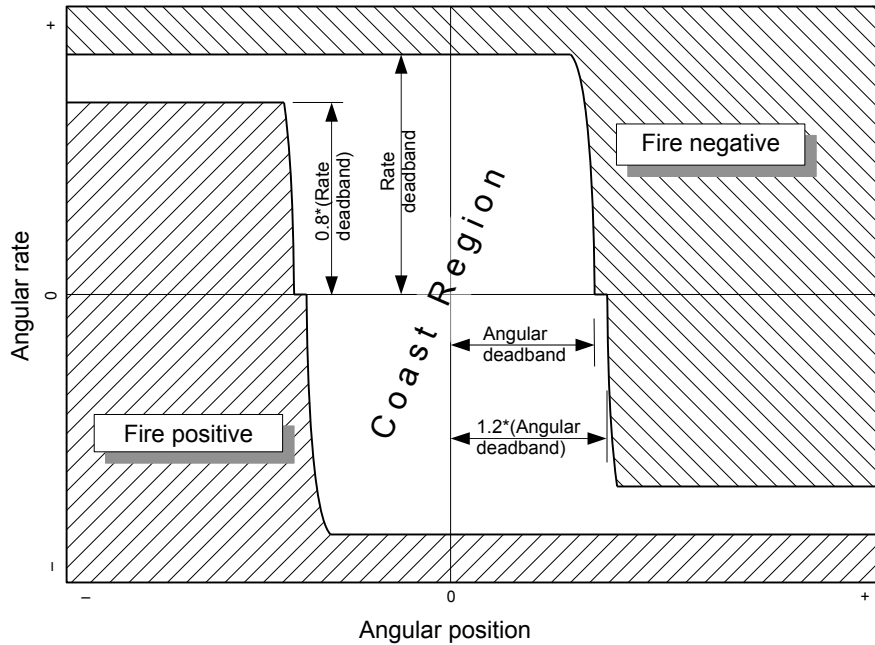


Figure 5: Schematic drawing of phase plane attitude controller

command vector (one element per axis indicating positive, zero, or negative translation or rotation in that axis), if proportional (throttle-able) RCS thrusters were available.

Time domain multiplexer. Since the RCS thrusters were not designed to fire proportionally (having a fixed thrust) the use of a time-domain multiplexer (TDM) strategy was used to achieve pseudo-proportional thrust. This was accomplished by quantizing the proportional firing commands (pre-calculated in the jet mixing table) into a repeating train of sixteen 40 ms-wide pulses for each thruster; the thruster(s) with the highest demanded thrust were fired continuously and the other RCS thrusters had proportionally fewer pulses (quantized into a fixed number of 16ths of a 100% duty cycle). The pulse width of 40 ms was the assumed minimum on-time for the RCS thrusters [10].

Participating thrusters that were not fired continuously had their firing pulses spread across the pulse train. This would allow the pulse train to be interrupted with a smaller error in the resulting accelerations to the vehicle. Figure 6 shows a schematic of the use of the mixing table as a lookup for proportional thrust commands, which were then converted into a pulse train for each thruster by the time-domain multiplexer.

This TDM implementation was more appropriate for direct pilot control of command duration (corresponding to Direct command mode) in both translational and rotational axes but was perhaps not the best choice for this experiment, which was conducted primarily in Pulse command mode, as described later in section 10.3.

Table 2 shows the changes in velocities and rotation rates (ΔV and $\Delta\omega$) in each axis that was achieved by the TDM mixer solution in response to a full-16-pulse-duration (0.64 s) firing in each axis, as implemented in the simulation software. The majority of off-diagonal terms are near zero with only a small residual cross-contamination in the off-diagonal (uncommanded) axes. This residual error was due to quantization of the scalar proportional jet commands into sixteen discrete numbers of pulses.

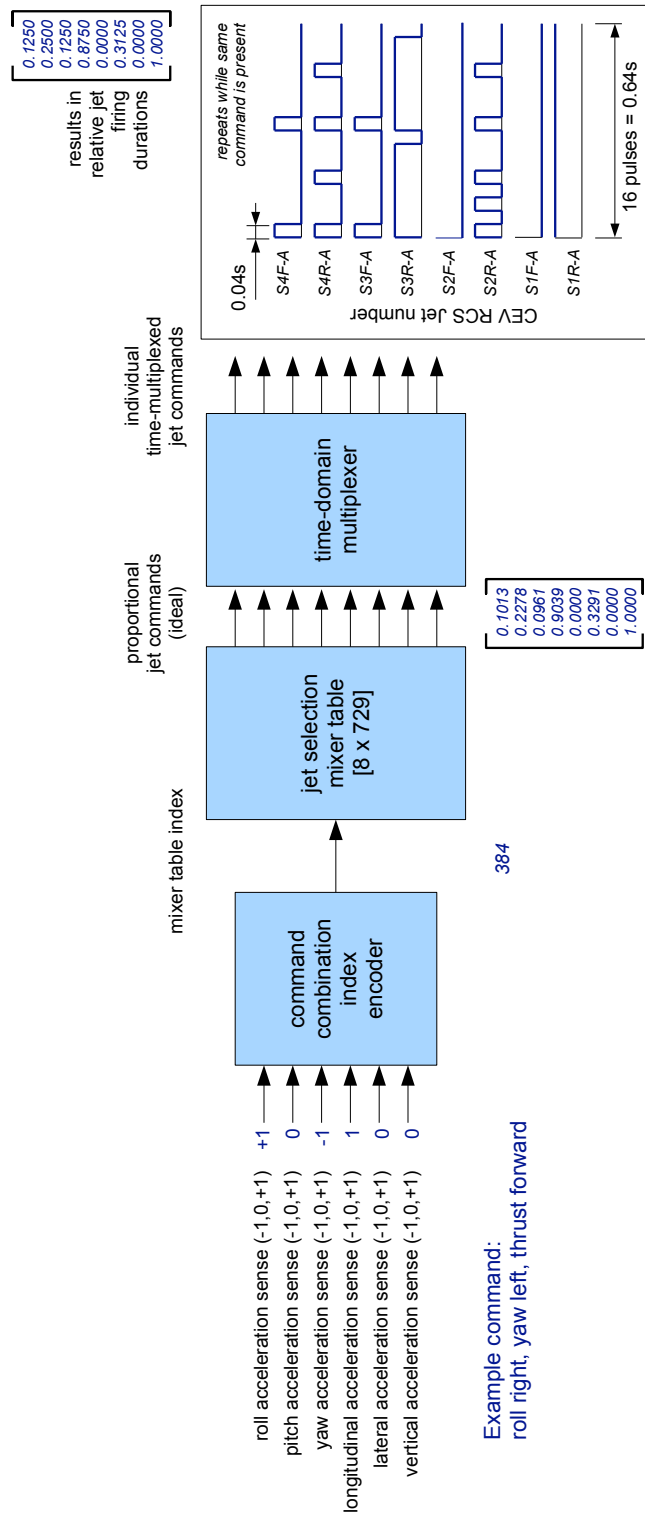


Figure 6: Schematic of time-domain RCS mixer

Table 2: Velocity changes resulting from complete (0.64 s) **TDM RCS** pulse sequences in each axis

Command Input Axis	$\Delta\dot{X}$	$\Delta\dot{Y}$	$\Delta\dot{Z}$	Δp	Δq	Δr
	ft/s			deg/s		
+X	+0.0373	0	0	-0.0002	-0.0007	-0.0032
-X	-0.0373	0	0	+0.0002	+0.0007	+0.0032
+Y	-0.0006	+0.0133	0	+0.0009	0	+0.0074
-Y	-0.0006	-0.0133	0	-0.0009	0	-0.0073
+Z	-0.0006	0	+0.0201	+0.0031	+0.0056	+0.0002
-Z	-0.0006	0	-0.0201	-0.0031	-0.0056	0
$+\phi$	0	0	0	+0.1154	+0.0010	+0.0044
$-\phi$	0	0	0	-0.1154	-0.0010	-0.0043
$+\theta$	0	0	0	+0.0032	+0.2370	+0.0004
$-\theta$	0	0	0	-0.0032	-0.2370	-0.0003
$+\psi$	0	0	0	+0.0135	+0.0003	+0.2033
$-\psi$	0	0	0	-0.0137	-0.0003	-0.2033

Defeating feed-forward. Since the experiment was intended, in part, to determine the relative benefit of a feed-forward decoupling strategy, it was necessary to defeat the beneficial automatic decoupling of the optimized mixing table described above for part of the test matrix. This was accomplished by recalculating the mixer table with the vehicle center-of-mass artificially located at the mean center of the **RCS** locations, resulting in translation-into-rotation coupling being exhibited when used instead of the optimized mixing table.

Table 3 shows the resulting changes in velocities and rotation rates (ΔV and $\Delta\omega$) in each axis that was achieved by the **TDM** mixer solution in response to a full-16-pulse-duration (0.64 s) firing in each axis, with feed-forward defeated, as implemented in the simulation software. The linear velocity changes (ΔV) are slightly higher, since no counter-rotational input is commanded, but the uncommanded (off-diagonal) responses in rotations ($\Delta\omega$) are more pronounced. A lateral translation ($\pm Y$) input results in a large yaw change (Δr), and a vertical translation input ($\pm Z$) results in a large pitch response (Δq) as shown in the table.

6.4.3 Reaction control system model

The **RCS** system was modeled with proper geometry and nominal thrust levels as given in [10]. The thruster dynamics were not modeled; each thruster was assumed to generate nominal thrust (25 lbf) during any 20 ms frame time during which it was selected to be on, and zero thrust when commanded off. Maximum on-time and duty cycle limitations were ignored for this study, but the control system did enforce a minimum on-time of 40 ms.

Some of the evaluated vehicle configurations included the effect of random **RCS** jet thrust variations; for these configurations, a precomputed, uniformly distributed, random 4% variation (± 1 lbf) thrust level was assigned to each thruster. Two sets of thruster variation distributions were used, with roughly half the pilots exposed to each set of variations.

6.5 Displays

Several computer-generated cockpit displays were available to the pilot in addition to the out-the-window, computer-generated, exterior views. These are described in the following

Table 3: Velocity changes resulting from complete (0.64 s) **TDM RCS** pulse sequences in each axis without feed-forward compensation

Command Input Axis	$\Delta\dot{X}$	$\Delta\dot{Y}$	$\Delta\dot{Z}$	Δp	Δq	Δr
	ft/s			deg/s		
+X	+0.0385	0	0	-0.0002	-0.0007	-0.0033
-X	-0.0385	0	0	+0.0002	+0.0007	+0.0034
+Y	0	+0.0198	0	-0.0049	-0.0001	-0.0830
-Y	0	-0.0198	0	+0.0050	+0.0001	+0.0830
+Z	0	0	+0.0330	+0.0071	+0.1548	+0.0004
-Z	0	0	-0.0330	-0.0071	-0.1548	-0.0004
$+\phi$	0	0	0	+0.1190	+0.0010	+0.0046
$-\phi$	0	0	0	-0.1190	-0.0010	-0.0045
$+\theta$	0	0	0	+0.0033	+0.2445	+0.0004
$-\theta$	0	0	0	-0.0033	-0.2445	-0.0003
$+\psi$	0	0	0	+0.0140	+0.0003	+0.2098
$-\psi$	0	0	0	-0.0142	-0.0003	-0.2097

sections. The cockpit displays appeared on two 17-inch diagonal, 5:4 aspect ratio, 1280×1024 Liquid Crystal Display (**LCD**) flat screens, mounted side-by-side in front of the evaluation pilot. The rightmost display was actually centered in front of the pilot, and the second display was beside it to the left of the pilot.

Due to cockpit display geometry limitations, the four heads-down displays were shown on the two separate heads-down LCD screens described above, appearing as a two-by-two matrix of displays whose centerline was offset to the left from the evaluation pilot’s seat, as depicted in figure 7.

6.5.1 Out-the-window display

The exterior view available to the pilot through the simulated **CEV** forward window was generated on a Rockwell-Collins EP 1000 image generator. In addition to a proper depiction of the docking target (either the **ISS** or Apollo **CSM**), the surface of the Earth was projected in the proper orientation against a black background of space.

Due to image generator limitations, however, the whole Earth disk was not visible; instead, rectangular portions of the Earth closest to the evaluation pilot’s orbital location were depicted as the spacecraft orbited. For most docking attempts, especially with the stationary **ISS**, this was not an issue, due to the limited field of view of the **CEV** window. During the rotating target scenarios, however, the Earth depictions could come into view.

No comments were received from evaluation pilots regarding this limitation of the visual system, and it was not felt to be an issue.

6.5.2 Attitude Director Indicator

Figure 8 depicts the Attitude Director Indicator (**ADI**) that was presented to the evaluation pilot in the lower right heads-down display. This **ADI** display was patterned after Shuttle; it included a standard artificial horizon ball as well as flight director bars and rate needle indicators. When **RCS** Discrete Rate mode was selected for a rotational axis, the yellow flight director bar for that axis depicted the attitude error relative to the **DAP** dead-band limits (beyond which the **RCS** would fire to reduce the attitude error). When in **RCS** Pulse

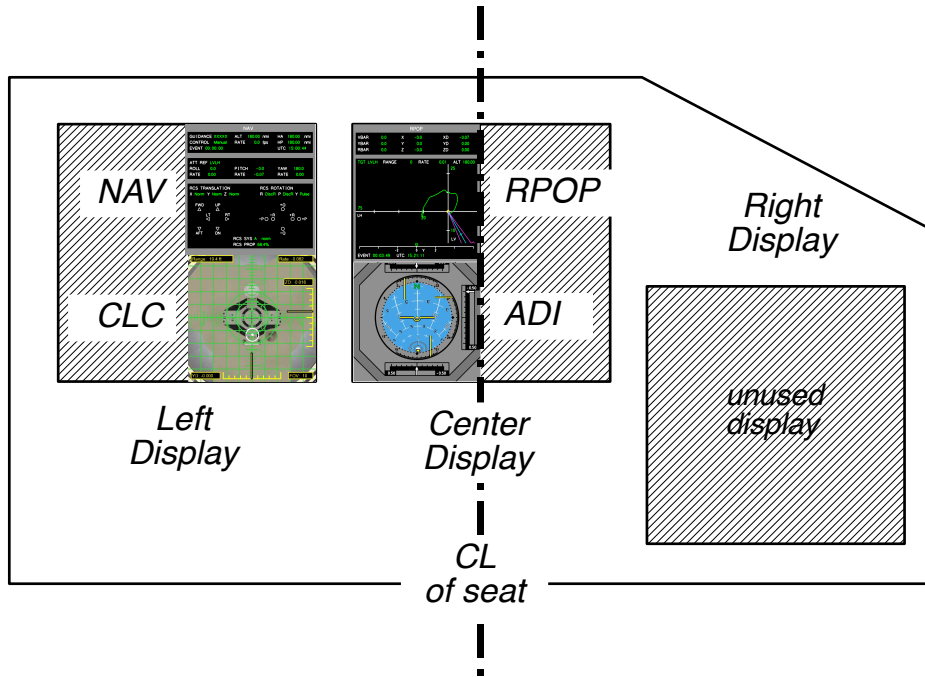


Figure 7: Arrangement of displays on RFD instrument panel

mode for a rotational axis, the corresponding flight director bar served as a vernier attitude indicator, showing ± 5 deg full-scale deflections from the initial attitude. The rate needles showed rates in each of the rotational axes at ± 0.5 deg/s full-scale for all control modes.

6.5.3 Navigation display

Figure 9 depicts the navigation display (NAV) that was presented to the evaluation pilot in the upper left heads-down display. This showed orbital parameters, numerical attitude and rate information, as well as autopilot modes selected for each degree-of-freedom and thruster firing depictions.

6.5.4 Rendezvous and Proximity Operations display

Figure 10 depicts the orbital Rendezvous and Proximity Operations Program display (RPOP) that was presented to the evaluation pilot in the upper right heads-down display. The RPOP depicted the position and past locations of the active spacecraft in a side-view relative to the target in LVLH coordinates, as well as the design approach corridor. Numerical readouts of range and range-rate as well as body-axis linear dock-to-dock position and rates were provided.

6.5.5 Docking Centerline Camera display

The centerline camera (CLC) display that was presented to the evaluation pilot in the lower left heads-down screen is depicted in Figure 11. This display presented a simulated image looking along the centerline of the evaluation pilot's docking port. It included a fixed green overlay that divided the current field-of-view into a ten-by-ten grid. By rotating a discrete

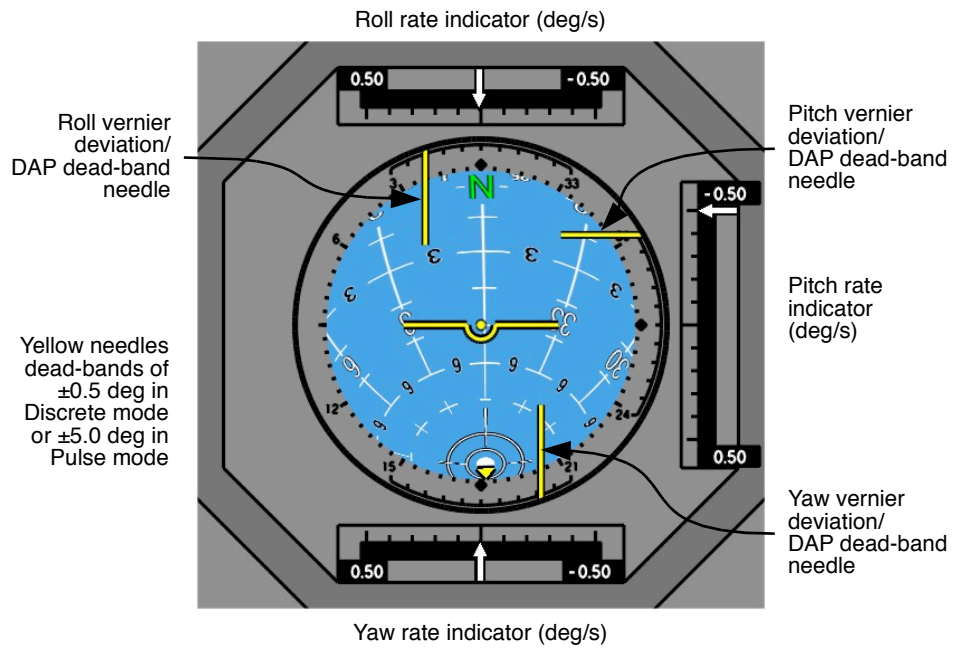


Figure 8: Attitude Director Indicator display

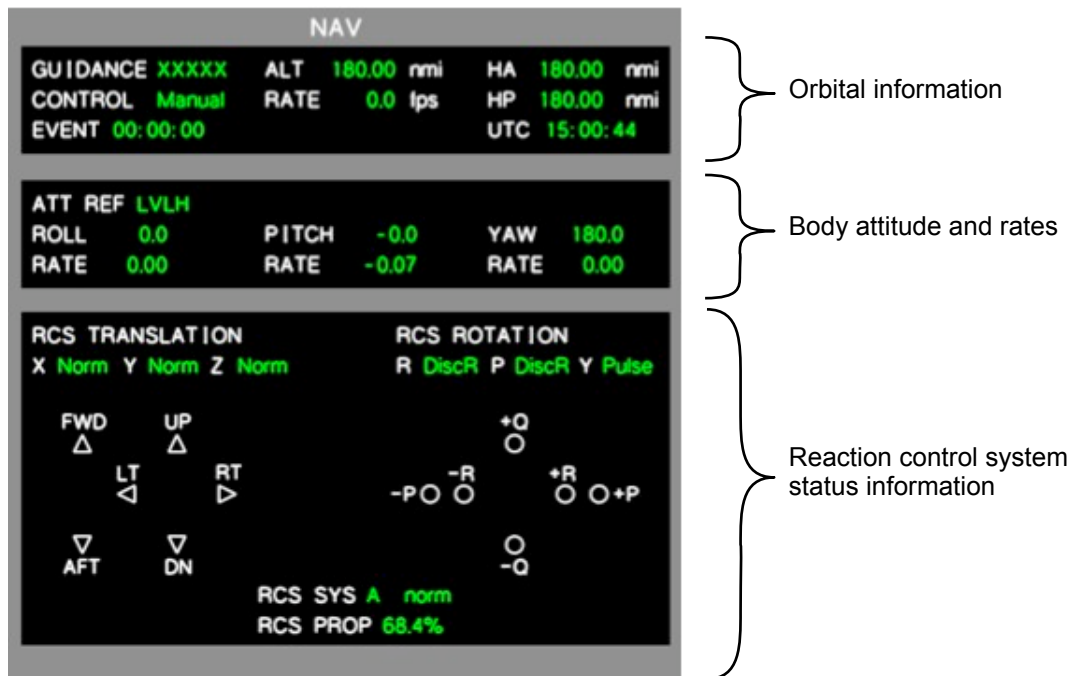


Figure 9: Navigation display

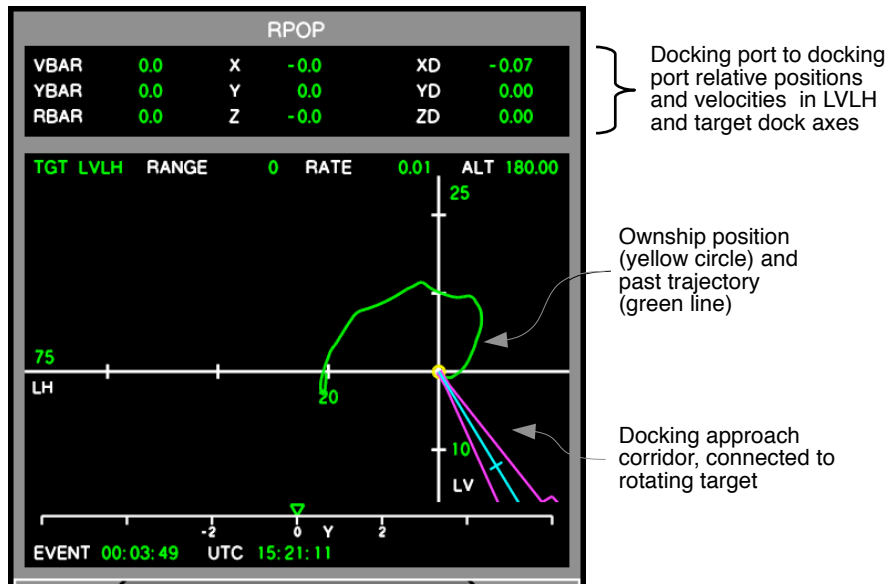


Figure 10: Rendezvous and proximity operations display

selection knob in the center aisle stand to the evaluation pilot's left, he was able to select the camera's field of view from 5 to 80 deg.

This display had a number of optional overlaid elements that were comprised of different symbology sets, as described below.

Minimal symbology. A minimal amount of symbologic information was shown at all times on the centerline camera display in boxes in the corner of the image. These were numerical readouts of range (R , in feet), range-rate (\dot{R} , in feet per second), and field-of-view selection (in degrees), as shown in figure 11.

Docking point predictor. Present in both symbology sets was a computed docking, or impact point, prediction represented by a circle with a dot in the center. This symbol was an attempt to depict where, if no further RCS firings were to take place, the center of the docking port would contact the target, including allowances for orbital mechanics. The location of the predicted docking point was based on the Clohessy-Whiltshire equations [15]. It was normally visible in all data runs (it was turned off prior to being introduced during early training runs) that used either the RCAH or Pulse symbology sets, described next.

RCAH symbology set. When all three rotational axes were in Discrete Rate (RCAH) mode, the RCAH symbology was overlaid with the minimal CLC symbology. This included the impact predictor as well as yellow DAP dead-band indicator needles and scales at the right and bottom of the CLC. These duplicated the pitch and yaw flight director needles on the ADI. In addition, numerical readouts of vertical (\dot{Z}) and lateral (\dot{Y}) dock-to-dock relative velocities were displayed near the appropriate scale, as shown in figure 12.

Pulse symbology set. When any of the rotational axes were in Pulse mode, pulse symbology was shown in addition to the minimal CLC symbology. This symbology included the impact predictor as well as an Attitude Status Indicator (ASI). The ASI attempted to show,

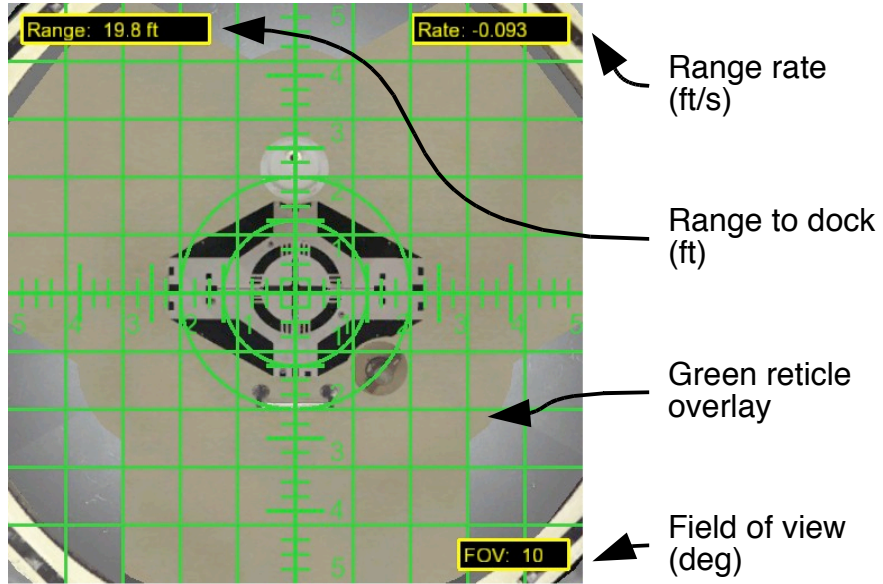


Figure 11: Centerline camera (minimal symbology set)

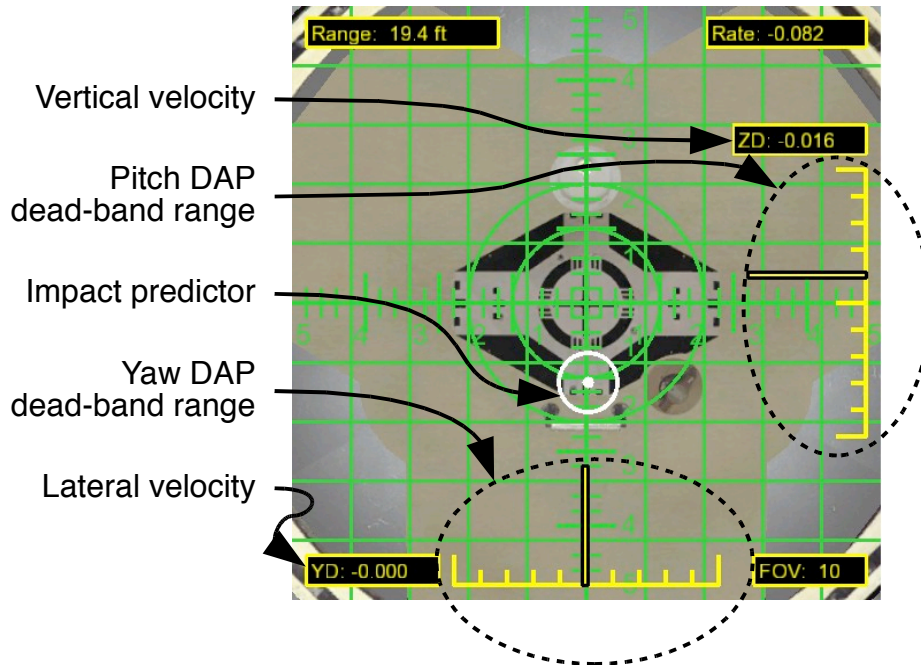


Figure 12: Centerline camera (RCAH symbology set)

in graphical form, ownship attitude error and rate in pitch and yaw axes. This was depicted as a small white square inside a larger segmented white square, as shown in figure 13. The segmented square was fixed in the center of the CLC grid, and the smaller outlined square moved relative to the center of the grid. The larger square represented the limits of desired docking mis-alignment; the smaller square showed the relative error in current alignment in pitch (vertical) and yaw (lateral) axes by its offset from the center of the display, as shown in figure 13.

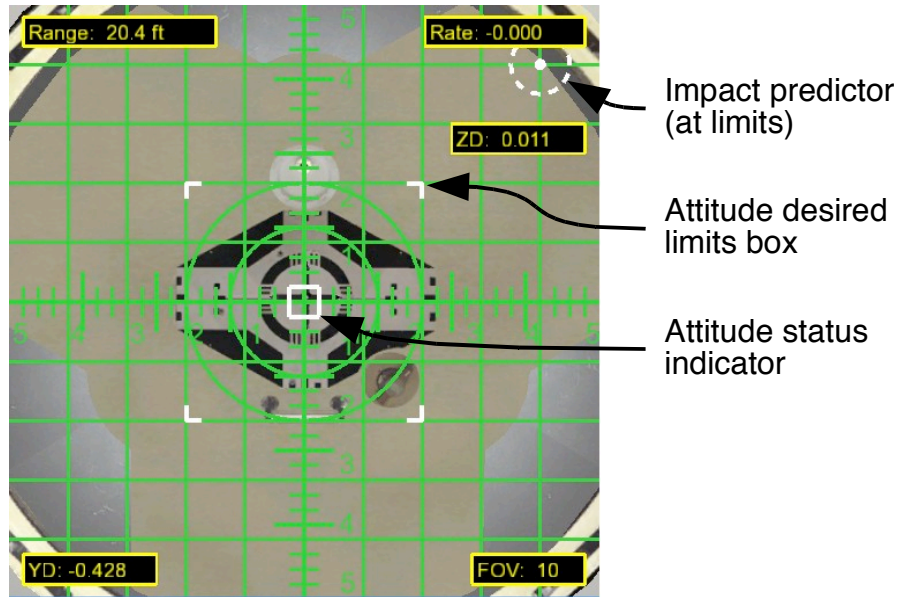


Figure 13: Centerline camera (pulse symbology set)

In addition to depicting attitude error, attitude rate information was shown by two lines drawn as coming out of the smaller square at a converging angle to each other. If the evaluation pilot's vehicle was pitching nose up, the lines grew from the top edge of the smaller square, and vice versa if pitching down; lateral rotation (yaw) rates were shown similarly. Since it was rare for rates to be identically zero, vertical and lateral rotations were normally indicated most of the time. The length of the converging lines was proportional to the rate about the corresponding axis. The point at which the lines intersected represented the limits of desired docking pitch and yaw rates, as shown in figure 14. Figure 14 depicts the situation where the ownship is pitching down at approximately twice the maximum desired rate limit but is within the desired pitch and yaw attitude envelope.

6.5.6 Scorecard display

After each docking run, a scorecard display replaced the NAV display and showed the performance of the run versus the objective performance metrics given in table 4. The purpose of this display was to assist the evaluation pilot in determining whether he had achieved desired, adequate, or less than adequate performance, as required by the Cooper-Harper decision tree post-task. These values were both color-coded and included an adjectival description of the performance ("Desired," "Adequate," or "Not adequate") relative to the desired and adequate performance metrics. An example of the end-of-run scorecard display is shown in figure 15.

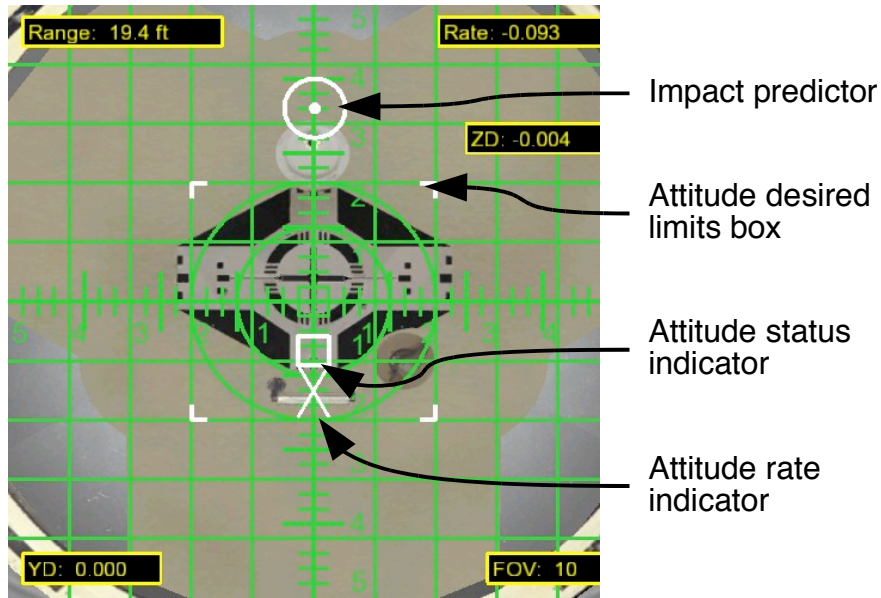


Figure 14: Centerline camera (pulse symbology set), cont'd

DOCKING EVENT 19-JUN-08 13:55Z		CONF I G 2101	
		RUN 00013	
	MIN	MAX	RATING
APPROACH:			
RDOT	-0.06	-0.11	ADEQUATE
DOCKING:			
LINEAR OFFSET		0.53	DES IRED
LINEAR RATE		0.00	DES IRED
RDOT		-0.06	ADEQUATE
PHI		-0.47	DES IRED
PHIDOT		0.00	DES IRED
THETA		-0.48	DES IRED
THETADOT		0.01	DES IRED
PSI		0.39	DES IRED
PSIDOT		0.04	DES IRED
ZDOT		-0.01	DES IRED
YDOT		0.00	DES IRED

Figure 15: End-of-run scorecard display

6.5.7 Digital Autopilot Interface Display and Keyboard

An airline-style **CDU** was used to indicate and change the various **DAP** mode settings, as shown in figure 16. The **CDU** keyboard was not used, but the bezel buttons around the **CDU** display were used to configure the **DAP** modes and gain sets. More information about the **CDU** is given in appendix B.

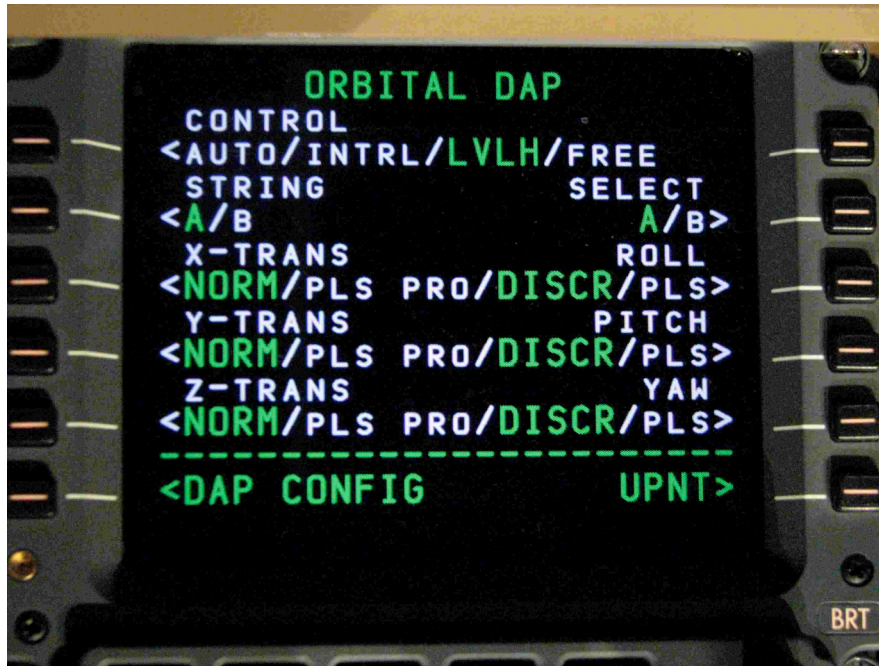


Figure 16: Digital Autopilot Control Display Unit

7 Task Description

The experiment sought pilot opinions and objective metrics in the performance of a manual docking with a target, commencing 20 feet from the target, nominally along the $+\bar{V}$ -vector of the target (so the simulated **CEV** vehicle with the evaluation pilot was in front of, and facing in the retrograde direction of flight of, the target) and initially aligned with the target's docking mechanism. Two main tasks were docking with the **ISS** in which the space station remained stationary (in an **LVLH** sense), and docking with a smaller spacecraft (an image of the Apollo **CSM** was shown) that rotated about a fixed inertial axis. In the primary task of stationary **ISS** docking, a set of vehicle configurations, control law configurations and display symbology sets were evaluated separately. In the secondary task of docking with a rotating target, the main goal was to see how difficult a manual docking would be for the nominal **CEV RCS** thruster geometry and thrust level.

Given the initial distance from the target (20 ft) and the nominal closure rate (0.1 ft/s), a nominal docking to a stationary target took approximately 200 seconds to complete.

Figure 17 shows the initial approach geometry for the primary task.

A set of performance standards for the docking tasks was developed from Constellation program specifications, representing design limitations of the docking interface and artificial experiment-imposed requirements to increase pilot workload. These performance standards

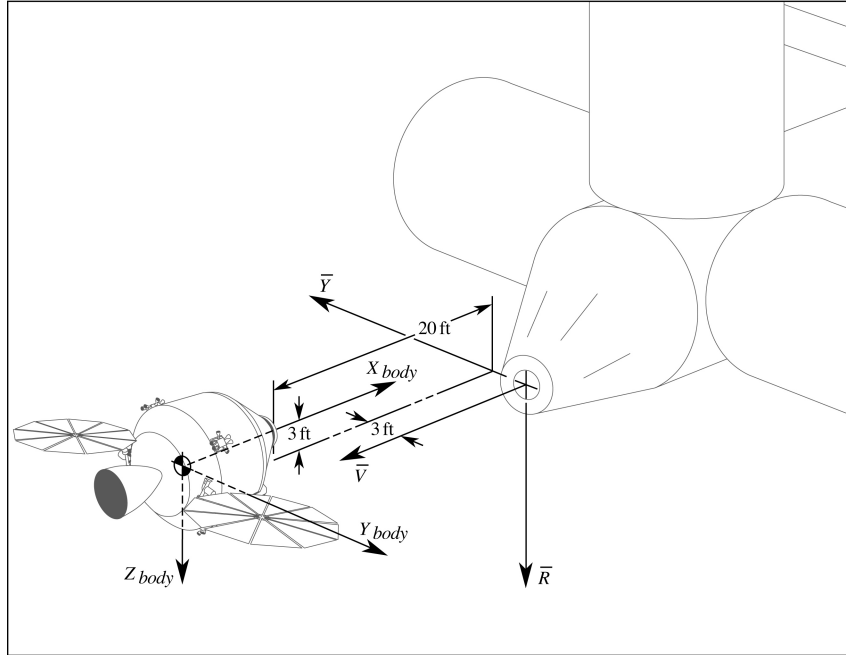


Figure 17: Sketch of CEV docking approach to ISS

are given in table 4 below. The full set of metrics was evaluated at the instant of docking. During the approach to docking, the axial closure rate value was also scored to the same metric as the docking impact rate (nominally 0.1 ft/s).

Table 4: Docking task performance standards

Performance Metric	Units	Desired Bounds	Adequate Bounds
Radial offset	in	1.5	3.2
Absolute value of roll angle	deg	1.5	3.0
Root-mean-square (RMS) value of of pitch and yaw angles	deg	1.5	3.0
Axial closure rate ($-\dot{X}_{body}$)	ft/s	0.075 to 0.125	0.05 to 0.15
Radial drift rate	ft/s	0.075	0.15
Absolute value of roll, pitch or yaw rate	deg/s	0.075	0.15

8 Experiment Protocol

8.1 Evaluation pilots

Table 5 gives biographical information about the nine evaluation pilots who participated in this experiment. Six of the nine were Shuttle-qualified pilot astronauts (five were mission commanders and five had ISS docking experience); three were either US Naval Test Pilot

School graduates and/or NASA research pilots.

8.2 Schedule

Each evaluation pilot was asked to schedule approximately eight hours of time to perform their evaluation of 19 tasks. These evaluations were conducted in approximately 1 hour sessions with at least a 15 minute break between each session, as well as a 1 hour lunch break. In many cases, the pilots started in the afternoon and finished the next morning, providing a significant break between two sessions. In one or two cases, the evaluation pilots were only available for 4 hours and thus were shown a smaller set of tasks.

8.3 Presentation order

The two main tasks of the experiment (stationary [ISS](#) docking and rotating Apollo [CSM](#) docking) were always conducted in the same order: stationary [ISS](#) dockings were completed first, and then the rotating target dockings were attempted.

The primary task, stationary [ISS](#) docking, was performed with 15 vehicle and control system configurations. These tasks were presented in a different random order to each evaluation pilot to minimize learning curve effects.

The four subtasks of the secondary (rotating target) task were always performed in the same order of principal axis rotation followed by slower then faster skewed axis rotations. Some of the subjects saw the yawing target first; others evaluated the pitching target first.

8.4 Briefing

A pilot briefing was held with each evaluation pilot prior to entering the simulation cockpit. During this briefing the simulated vehicle, control system, and displays were described, as well as the main goals of the experiment and the experimental protocol. Operation and modes of the digital autopilot and inceptors and the various docking centerline camera symbology sets were described.

A copy of the pilot briefing guide is contained in [Appendix C](#).

8.5 Training runs

Prior to commencing data evaluation runs, each evaluation pilot was trained in the operation of the inceptors, displays, and digital autopilot configuration changes, as described below. Normally the stationary [ISS](#) docking task training was conducted first, followed by data runs associated with that task; the rotating target training was given just prior to performing evaluations of that secondary task later in the experiment.

8.5.1 Training for task 1 (stationary [ISS](#) docking)

The initial set of training runs for stationary target docking consisted of a straight-in docking from 20 feet out aligned with the $+\bar{V}$ of the [ISS](#), with the feed-forward mixer enabled, translational autopilot in Pulse mode for translations and Discrete Rate ([RCAH](#)) mode for rotations, and docking minimal centerline camera overlay symbology.

The second set of training runs introduced an initial vehicle position that was offset down and right from the $+\bar{V}$ centerline. As in the first run, the feed-forward mixer was on, the translational autopilot was in Pulse mode with Discrete Rate ([RCAH](#)) mode in the rotational autopilot; in addition, the [RCAH](#) symbology set was overlaid on the simulated centerline camera video.

The third set of training runs included the initial vehicle position offset, feed-forward mixer on, but with the autopilot in Pulse mode for both translations and rotations ([RCAH](#)

Table 5: Evaluation pilot biographies

Number	Experience	Training	Currency
1	Multiple shuttle missions as commander; included docking with Mir.	Fully-trained shuttle commander with Mir docking training, but no ISS docking training.	Last mission in 1995 but active general aviation pilot
2	Multiple shuttle missions to ISS.	Fully trained shuttle commander with ISS docking.	Flew docking to ISS recently.
3	Navy test pilot school graduate and instructor, Navy attack pilot. No shuttle experience.	Rendezvous, proximity operations and docking training from previous experiment and several training runs prior to data collection.	No space experience but recent King Air/C-12 flight time.
4	Multiple shuttle missions. Docking with ISS on last two flights.	Fully-qualified shuttle commander with ISS docking experience.	Last flew shuttle 6 years prior but active general aviation pilot.
5	Multiple shuttle flights; all with docking to ISS.	Fully-qualified Shuttle commander.	Assigned to another Shuttle flight in 1 year.
6	Navy fighter pilot; airline co-pilot; NASA research pilot; NASA flight JSC operations pilot.	Shuttle training aircraft instructor pilot; no formal test pilot training	Recent T-38, WB-57, general aviation experience.
7	USAF fighter pilot; MOL crew assignment; shuttle commander (multiple flights). No dockings.	Fully-trained Shuttle commander, USAF test pilot school graduate.	No recent flight experience.
8	US Marine fighter pilot and test pilot; astronaut with multiple missions as Shuttle pilot.	USN test pilot school; fully-trained Shuttle pilot	Active astronaut.
9	US Navy fighter pilot and test pilot.	No space experience. Graduate, USN test pilot school.	No recent flight experience.

off) making this a **6DOF** task; the centerline camera video was overlaid with the Pulse symbology set.

The feed-forward mixer was replaced with a simpler, coupling, mixer for the fourth set of training runs, so the evaluation pilot had to cope with a **6DOF** task with translation inputs coupling into vehicle rotations; symbology remained the same as in the third set of runs.

In the final set of training runs for the stationary docking task, the symbology overlay was the minimal set, yielding a ‘bare’ vehicle whose only automation was Pulse mode control in each axis.

8.5.2 Training for task 2 (rotating target docking)

Prior to conducting docking with a rotating target, each evaluation pilot was allowed to practice docking with an Apollo **CSM** that was pitching nose-up (relative to the evaluation pilot’s vehicle) at a constant 0.4 deg/s rate. The autopilot provided Pulse mode control in lateral and vertical axes but Direct mode in the longitudinal (X_{body}) axis; this change was required to compensate for the relative centripetal acceleration along the target docking centerline due to rotation. The rotational axes were also split: roll and yaw axes were set to Discrete Rate (**RCAH**) mode but the pitch axis was set to Pulse mode, allowing easier adjustment of a steady pitch rate. The Pulse symbology set was overlaid on the docking centerline camera display.

This training run duplicated one of the initial evaluation configurations for this secondary task, so the pilot would normally go straight into data runs when he felt he was ready to evaluate the task.

8.6 Data runs

After the evaluation pilot was training in the operation of the vehicle for docking, he was asked to evaluate the performance of that task using three subjective measures (Cooper-Harper Pilot Rating Scale [16], a Likert scale [17] for each inceptor, and the NASA Task Load Index scale [18]) and to provide summary comments on those ratings and the performance of the task in general. The scorecards associated with each of these metrics are shown slides 34-36 of the pilot briefing guide (appendix C).

To help ensure repeatable assessments, the pilot was allowed one or more practice runs of each configuration, followed by two or more data runs in which objective measures of performance were recorded.

Each run started 20 feet from docking along the $+\bar{V}$ axis of the target with the correct attitude for docking (i.e., the centerlines of the two docking mechanisms were parallel). Task 1 included various offsets from “on-centerline, on-glideslope;” task 2 was performed without an initial offset.

8.6.1 Task 1: Stationary **ISS** docking

Fifteen different vehicle mass, **RCS**, control law, and display symbology configurations were evaluated by nearly all nine evaluation pilots while performing the offset docking task described above. The presentation order of the configurations was randomized ahead of time and each pilot saw the configurations in a different order. The test configurations for Task 1 are given in table 6 below. Some pilots were unable to complete the full matrix of 15 due to schedule constraints.

Each set of runs was conducted with a combination of three-foot lateral and three-foot vertical offset from “on-centerline, on-glideslope” alignment. The same sequence was followed each time: the practice run (or runs) was started from a lower-left offset, then the upper-left and lower-right offsets were performed for data. Any fourth or subsequent data run was started from the upper-right offset (if requested by the evaluation pilot).

Table 6: Test configurations for docking with a stationary ISS target (Task 1)

Test Number	Rot. Mode	Ang. DB (deg)	Rate DB (deg/s)	Feed-forward	Thrust var.	CM var. (in)	Symbology set
1	6DOF	–	–				none
2	6DOF	–	–	✓			none
3	6DOF	–	–				Pulse
4	6DOF	–	–	✓			Pulse
5	RCAH	0.50	0.04				none
6	RCAH	0.50	0.04	✓			none
7	RCAH	0.50	0.04				RCAH
8	RCAH	0.50	0.04	✓			RCAH
9	RCAH	0.50	0.04	✓	✓		none
10	RCAH	0.50	0.04	✓		6 (+Y)	none
11	RCAH	0.50	0.04	✓		6 (+Z)	none
12	RCAH	0.50	0.01				none
13	RCAH	1.00	0.04	✓			none
14	RCAH	0.50	0.04	✓		12 (–Y)	none
15	RCAH	0.50	0.04	✓		12 (–Z)	none

8.6.2 Task 2: Rotating target docking

To evaluate the feasibility of performing manual dockings with a rotating target, four different motions of a smaller spacecraft target were simulated. Each pilot saw similar sequences of rotating targets, arranged in rough order of increasing difficulty. In each case, the target was visually presented as an Apollo CSM with a modern docking ring and target, as shown in figure 18.

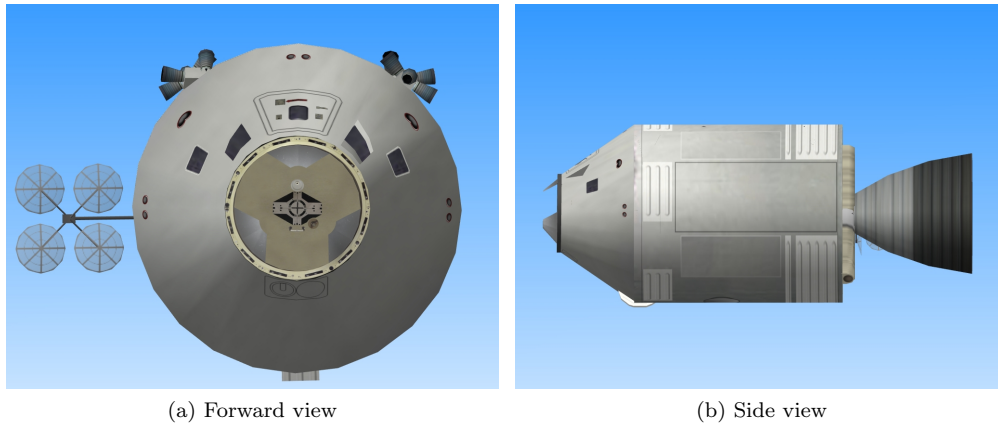


Figure 18: The modified Apollo Command/Service Module used as a rotating docking target

In each case, the run commenced with the evaluation pilot’s vehicle located 20 feet from dock with the two spacecraft nose-to-nose; unless otherwise stated, both vehicles were initially pitching at 0.06 deg/s to maintain local vertical. The docking ports were initially aligned with no lateral or vertical offset. The evaluation pilot was informed of the rotation

rate of the target; this information was felt to likely be provided in a real-world situation. Unlike the [ISS](#) docking scenario, the initial closure rate with the target was set to zero.

As in the stationary [ISS](#) docking scenario, each pilot was requested to perform at least two data runs after one or more practice runs, if they felt the task to be feasible.

The target rotation scenarios were a constant 0.4 deg/s yaw rotation (test 16), 0.4 deg/s pitch rotation (test 17), a combined pitch/yaw rotation totaling 0.4 deg/s (root-sum-square of pitch and yaw rotations, test 18), and a faster 0.4 deg/s in both pitch and yaw (a combined 0.566 deg/s [RMS](#) rotational rate, test 19). Not all pilots evaluated all four Task 2 docking scenarios.

For these dockings attempts with a rotating target, the control system was configured according to pilot preference, but in general the Y and Z translational axes were configured for Pulse mode and the X translational axis was configured for Direct mode (allowing continuous firing in X as long as the translational hand controller was out of detent). The rotational axes were normally configured for Discrete Rate ([RCAH](#)) mode in the roll axis and [RCS](#) Pulse mode in pitch and yaw; in the pitching-only target scenario the yaw axis was also normally in Discrete Rate ([RCAH](#)) mode.

Table 7 summarizes these motions; note that the pitching target scenario (test 17) was sometimes presented to the evaluation pilot before the yawing target scenario (test 16) to try to gauge training effects.

The symbology set used for all rotating targets was the [RCAH](#) set.

Table 7: Test configurations for docking with a rotating target (Task 2)

Test Number	Target Motion	Rate deg/s	X Mode	Y Mode	Z Mode	Roll Mode	Pitch Mode	Yaw Mode
16	Yawing	0.4	Direct	Pulse	Pulse	RCAH	Pulse	Pulse
17	Pitching	0.4	Direct	Pulse	Pulse	RCAH	Pulse	RCAH
18	Pitch/Yaw	0.4	Direct	Pulse	Pulse	RCAH	Pulse	Pulse
19	Pitch/Yaw	0.566	Direct	Pulse	Pulse	RCAH	Pulse	Pulse

8.7 Scoring

The same metrics were compared in all scenarios to determine desired, adequate, or inadequate task performance, as shown previously in table 4, at the instant of docking, as well as closure rate (\dot{R}) during the docking approach. For the rotating target scenarios it was impossible for the evaluation pilot to maintain \dot{R} within tolerance due to the initial relative rotation of the target vs. the stationary [CEV](#); thus for the approach the \dot{R} metric was not enforced in the secondary task evaluations. The closure rate at docking was required to be within tolerance, however.

Also for the rotating target scenarios, due to singularities near vertical [LVLH](#) pitch attitude, relative angular rates at docking were also discounted as these were sometimes numerically large in the [LVLH](#) frame used to perform the calculation and were not enforced.

At the end of each successful docking attempt, a scorecard display similar to that shown in figure 15 was presented to the pilot and observer to assist in performing the Cooper-Harper rating determination.

9 Experiment Results

The results of this experiment, obtained during 62 hours of simulation occupancy, are given below.

9.1 Task 1 - Stationary ISS docking

For this task, 15 configurations were evaluated in 245 runs by most of the nine evaluation pilots in the course of 116 separate task evaluations. Due to time constraints, some configurations received fewer evaluations than others.

The primary metrics evaluated are shown in the following two tables (8 and 9); more complete metrics can be found in Appendix A.

The Cooper-Harper rating assigned by pilots to each of the test configurations after performing a docking with the stationary ISS are given in table 8.

Table 8: Cooper-Harper ratings assigned to each configuration for the stationary ISS docking task

Test	Configuration name	Evaluation Pilot								
		1	2	3	4	5	6	7	8	9
1	6DOF CEV	7	4	5	5	8	6	6	4	3
2	6DOF CEV + feed-forward (FF)	5	4	1	5	8	5	6	4.5	4.5
3	6DOF CEV + symbols	3	4	4	4	6	3	7	4.5	4
4	6DOF CEV + FF + symbols	3	4	4	4	7	4	4.5	4.5	4.5
5	CEV - FF	4	3	4	5	-	4	5	2.5	4
6	CEV (baseline)	3	3	2	4	2	2	5	3	3
7	CEV - FF + symbols	4	3	3	5	3	3	4	3	4
8	CEV + symbols	4	3	3	4	2	3	3	2.5	3
9	CEV + 4% random thrust	3	3	2	5	-	2	5	2.5	4
10	CEV + 6" lateral CM offset	3.5	3	3	4	-	2	5	2.5	3
11	CEV + 6" vertical CM offset	4	2	3	4	-	4	5	3	4
12	CEV - FF + smaller rate DB	3	2	2	2	5	3	3	2	3
13	CEV + larger attitude DB	-	-	2	-	-	4	4	-	3
14	CEV + 12" lateral CM offset	-	-	2	-	-	3	4	-	4
15	CEV + 12" vertical CM offset	-	-	2	-	-	3	3	-	3

The average fuel consumed on during evaluation docking attempts, by pilot, for each of the test configurations evaluated against docking with the stationary ISS are given in table 9.

A summary table giving the range and median Cooper-Harper Rating (CHR) opinions assigned to and RCS fuel consumed for each configuration are given in table 10.

As discussed below in section 10.3, pilot opinions of the handling qualities of these configurations were inadvertently contaminated by the TDM mixer due to a significant amount of pilot attention spent in managing closure rate (\dot{R}). The bulk of the analysis is therefore given in terms of comparing the change of each pilot's opinion between configurations, rather than absolute CHR values.

Table 9: Average fuel consumption (lbm) for each configuration for the stationary ISS docking task

Test	Configuration name	Evaluation Pilot								
		1	2	3	4	5	6	7	8	9
1	6DOF CEV	6.15	4.32	6.85	4.82	8.18	11.92	6.51	6.05	10.75
2	6DOF CEV + FF	6.67	5.52	7.33	4.29	7.38	15.04	5.25	7.04	12.94
3	6DOF CEV + symbols	6.17	5.41	6.37	4.22	6.86	9.61	6.29	5.52	14.78
4	6DOF CEV + FF + symbols	4.95	4.93	8.83	4.02	6.00	12.15	5.21	8.26	11.78
5	CEV – FF	7.07	4.43	8.71	4.72	-	6.27	3.63	6.73	10.45
6	CEV (baseline)	5.40	3.88	6.12	4.85	3.86	5.24	4.00	6.00	8.39
7	CEV – FF + symbols	6.53	4.04	6.51	3.31	4.90	8.65	4.61	5.57	9.41
8	CEV + symbols	6.89	3.51	5.41	4.27	2.98	6.96	3.76	7.15	6.67
9	CEV + 4% random thrust	5.87	3.75	6.09	5.22	-	6.11	3.92	8.65	7.32
10	CEV + 6" lateral CM offset	6.72	3.84	5.86	4.84	-	7.58	3.15	6.20	9.48
11	CEV + 6" vertical CM offset	6.53	4.36	6.37	5.75	-	8.21	4.60	6.06	9.14
12	CEV – FF + smaller rate DB	6.90	6.81	6.17	5.62	7.17	9.31	6.05	6.48	9.35
13	CEV + larger attitude DB	-	-	5.16	-	-	10.86	3.73	-	6.92
14	CEV + 12" lateral CM offset	-	-	6.23	-	-	7.04	4.00	-	9.83
15	CEV + 12" vertical CM offset	-	-	6.94	-	-	7.83	3.63	-	8.43

Table 10: Summary of results from evaluations of various vehicle configurations docking with a stationary ISS

Test Number	Configuration Name	No. of Pilots	Min CHR	Median CHR	Max CHR	Avg. fuel used (lbm)
1	6DOF CEV	9	3	5	8	7.28
2	6DOF CEV + FF	9	1	5	8	7.94
3	6DOF CEV + symbols	9	3	4	7	7.25
4	6DOF CEV + FF + symbols	9	3	4	7	7.35
5	CEV – FF	8	2.5	4	5	6.50
6	CEV (baseline)	9	2	3	5	5.48
7	CEV – FF + symbols	9	3	3	5	5.95
8	CEV + symbols	9	2	3	4	5.29
9	CEV + 4% random thrust	8	2	3	5	5.86
10	CEV + 6" lateral CM offset	9	2	3	5	5.96
11	CEV + 6" vertical CM offset	8	2	4	5	6.38
12	CEV – FF + smaller rate DB	9	2	3	5	7.10
13	CEV + larger attitude DB	4	2	3.5	5	6.67
14	CEV + 12" lateral CM offset	4	2	3.5	4	6.77
15	CEV + 12" vertical CM offset	4	2	3	3	6.71

9.2 Task 2 - Rotating target docking

For this task, a total of 41 dockings were attempted by as many as seven evaluation pilots in 23 separate task evaluations. These were all conducted with essentially the same baseline **CEV** with the feed-forward **TDM** mixer, pulse symbology, **RCAH** autopilot, nominal **RCS** thrust levels and nominal center of mass (**CM**) location, but one or more axes of **RCAH** was turned off (depending on target motion) as shown earlier in table 7. Due to schedule constraints of some participants, some scenarios received more evaluations than others.

As shown in table 7, the Y and Z translation axes were controlled through **RCS** Pulse mode, but the X axis was controlled with **RCS** Direct mode. This allowed the evaluation pilot to change their \dot{X}_{body} translation rate more rapidly than in Pulse; whenever the **THC** inceptor was out of detent in the X axis, the **RCS** system fired continuously in the X_{body} axis. This rotating task was configured in this manner since closure rate (generally along the X_{body} axis) continuously decayed due to the rotating nature of the target motion, through relative centripetal acceleration.

The Cooper-Harper ratings assigned by each evaluation pilot to the task of docking the baseline **CEV** with a rotating target, at a variety of target rotational motions, are given in table 11. The contamination of \dot{X}_{body} by the **TDM** feed-forward mixer (see section 10.3) may have affected the overall **CHR** for these tasks (but to a much lower extent than the stationary tasks, due to the larger effect of centripetal acceleration); however, the given **CHRs** may still not be representative of expected **CEV** performance.

Table 11: Cooper-Harper ratings assigned to the docking with a rotating target scenario, by pilot

Test	Target Motion	Rate	Evaluation Pilot						
			2	3	4	6	7	8	9
16	Yawing	0.4 deg/s	6	7	6	-	7	4.5	4.5
17	Pitching	0.4 deg/s	3	6	5	3	3	4.5	3
18	Pitch/Yaw	0.4 deg/s	5	7	6	-	7	4.5	5
19	Pitch/Yaw	0.566 deg/s	-	7	7	-	-	4.5	5

The average fuel consumed during docking attempts by each evaluation pilot for each of the rotating target scenarios are given in table 12. These values may be somewhat inflated due to additional \dot{X}_{body} thrust inputs required by the **TDM** mixer “braking effect.”

Table 12: Average fuel consumption (lbm) for each docking with a rotating target scenario

Test	Target Motion	Rate	Evaluation Pilot						
			2	3	4	6	7	8	9
16	Yawing	0.4 deg/s	37.30	49.77	19.70	-	30.68	39.91	35.43
17	Pitching	0.4 deg/s	15.95	28.20	16.25	25.77	15.16	16.54	18.01
18	Pitch/Yaw	0.4 deg/s	30.54	34.35	34.56	-	92.56	33.49	63.43
19	Pitch/Yaw	0.566 deg/s	-	42.81	45.96	-	-	41.60	47.81

A summary table giving the range and median Cooper-Harper opinions assigned to and **RCS** fuel consumed for each type of target motion during the rotating target docking task

are given in table 13.

Table 13: Summary of results from evaluations of docking with a rotating target

Test Number	Target Motion	Rate deg/s	No. of Pilots	Min CHR	Median CHR	Max CHR	Avg. fuel used (lbm)
16	Yawing	0.4	6	4.5	6	7	35.5
17	Pitching	0.4	7	3	3	6	19.4
18	Pitch/Yaw	0.4	6	4.5	5.5	7	50.9
19	Pitch/Yaw	0.566	4	4.5	6	7	44.5

10 Discussion of Results

Due to difficulties introduced by the time-domain-multiplexing mixer (described in section 10.3 below), comparison of per-pilot opinions and performance were felt to be a more appropriate comparison of the benefits or impact of various configuration changes rather than absolute values of pilot opinions or objective measures. Thus, it is probably not appropriate to discuss a mean CHR for the nominal CEV versus a degraded 6DOF CEV.

Evaluation pilot 8 brought a colleague, another experienced astronaut, with him to the simulation cab and thus had some assistance in performing some of the tasks; the guest astronaut called out range rate on certain tasks. This assistance probably affected the subsequent task ratings provided by pilot 8.

10.1 Task 1 - Stationary ISS docking

Effectively two CEV versions were tested; one with some functioning autopilot, whose baseline was represented by test configuration 6, hereafter referred to as the “nominal” CEV; and a “bare-bones” CEV capsule with little or no feedback control system operating, which might represent a reversionary mode of the future CEV control system, hereafter referred to as “6DOF” CEV. This latter baseline was evaluated as test configuration 1.

The analysis compares the per-pilot performance, fuel use and subjective ratings between either baseline and one of its variants in docking with the stationary ISS as described below.

A complete set of plots is found in appendix A; they are referred to herein by ‘figure Axy ’ where x is the figure number and y is the subplot thereon.

10.1.1 Comparison of variants vs. the nominal CEV configuration baseline

The nominal CEV configuration was assumed to have feed-forward compensation and an RCAH autopilot, but without additional symbology on the CLC display. This was represented by test configuration 6. Configurations 5 and 7 through 15 represented variants of this baseline nominal CEV vehicle, including adding symbology to the CLC display, control system changes, RCS thruster force variations, and offsets of the vehicle center of mass.

In each section below, the discussion compares the nominal CEV configuration against the test configuration. The plots in Appendix A have lines tying metrical results generated by the same evaluation pilot for the two configurations (baseline and variant) being compared.

Effect of additional display symbology. As shown in figure A1, the effect of adding the RCAH symbology set (described in section 6.5.5) to the centerline camera display (test configuration 8) gave mixed results. In figure A1a, handling qualities rating improved (lowered) for two pilots, degraded (increased) for two pilots, and remained the same for five pilots. Fuel consumed during the docking maneuver decreased for all but three of the nine evaluation pilots as shown in figure A1b. Perhaps the most consistent metric was the decrease in pre-dock coasting time, shown in figure A1c. Pre-dock coasting time was the amount of time between the final pilot input and moment of docking contact; this duration actually decreased for all but one pilot, indicating possibly more control activity to sweeten the alignment with the docking target.

In terms of performance, figures A1e through A1g show that linear and angular offsets did not appreciably change with the RCAH symbology set on or off.

When comparing subjective measures, no clear preference was shown in any of the task load indices (plots h-l) by the set of nine evaluation pilots, which is consistent with the lack of change in median Cooper-Harper ratings.

Pilot comments regarding the symbology indicate some problem in lateral alignment of the impact predictor:

Pilot 3 reported “oscillating around the center” in the lateral axis and stated:

I just couldn't quite get the lateral placement of the projected impact point where I wanted it. It was going left and right of center and finally I just accepted it until I got to a deviation and then corrected back. Just slightly annoying but controllable.

He gave a mental task load of 25 (out of 100), mostly dealing with “the seeming dichotomy between having to aim the impact point low to keep the camera focused on the centerline or the center of the aiming cross.”

Pilot 4 mentioned “doing . . . a lot of monitoring of dead-bands” and “having to watch where you were in the [DAP] dead-bands when you finally had it lined up.”

Pilot 8 spoke specifically to the symbology, saying:

I'll just mention the predictor and the other symbology changes, which were primarily the digital \dot{Y} and \dot{Z} and the attitude error needles on the centerline camera [figure 12]. I think the predictor was probably the least useful out of all of them. It does show you a relative trend of where you're going but it almost gets to a point of cluttering as you get everything a little closer to one of the parameters. So, I might shed that in favor of a one-to-one attitude symbol which would give me a little more useful information. The \dot{Z} and \dot{Y} [readout] was useful. The attitude needles were useful.

The main difficulty cited appears to be with the residual motion of the predicted impact point when the ownship had small rotational rates. The equations driving the predictor gave the location of the docking ring center, which was located about 10 ft forward of the center of mass. Thus, any rotational rate would show a significant vertical or lateral motion of the predicted impact point, even if the center of mass was translating directly toward the center of the target docking ring.

Taken together, the RCAH symbology set provided no improvement in the manual docking task for the baseline CEV with a functioning digital autopilot providing rate-command, attitude hold capability with feed-forward mixing.

Effect of thruster variations. Figure A2 shows the effect of applying a 4% thrust variation (± 1 lbf) randomly to each of the eight RCS thrusters (test configuration 9), compared with the baseline CEV. Two different sets of variations were evaluated by two groups of

four evaluation pilots - even-numbered pilots saw one variation set, and odd-numbered pilots saw a second set of 4% thrust variations. (Pilot 5 did not evaluate either variant.) The variations remained fixed for each set of runs for a given pilot.

In performance terms, slightly more (0.38 lbm) RCS propellant (figure A2b) was consumed, with an average of three additional pilot inputs (figure A2d) being made during the docking maneuver; slightly less (0.99 s) pre-dock coasting time was observed on average. (figure A2c). However, alignment (figure A2f), centering (figure A2e) and motion at dock (figure A2g) were improved for the cases with thruster variation. Closure rate (figure A2h) was basically unchanged.

In terms of pilot subjective opinion, one pilot went from CHR Level One to Level Two (pilot 9 in figure A2a); task load opinions were basically unaffected (figures A2i through A2l).

Pilot 1 called this “a pretty good system.” Pilot 2 noted no observable difference between this and the configuration he saw immediately prior, the baseline system with symbols (test configuration 8). Pilot 3 noted that the error needles on the ADI display were moving faster, due to the larger coupling across axes, caused by the unmodeled thruster variations, which he initially found distracting. Pilot 4 may have noticed the variation; he reported “this bouncing off the dead-bands in attitude is more annoying in this configuration in digital autopilot low-authority setting (B-DAP) especially . . . there’s a lot more scatter in attitude.” But pilot 6 called it “one of the best” configurations (this was the ninth configuration he evaluated in docking with the stationary ISS). Pilot 8 said it “wanders a little bit within the dead-band.”

This indicates a 4% thruster variation, representing the CEV-specified limits for the thruster variability, would have a small but imperceptible effect on manual dockings for a baseline CEV with a functioning digital autopilot providing rate-command, attitude hold capability with feed-forward mixing. Larger variations would no doubt lead to a different conclusion.

Effect of smaller rate dead-band. As shown in figure A3, the baseline CEV with feed-forward mixing (test configuration 6) was compared to one with a control system with no feed-forward mixing, but with a tighter attitude rate dead-band (0.01 deg/s versus the baseline 0.04 deg/s), represented by test configuration 12.

A penalty was paid in terms of RCS fuel use (figure A3b) which increased an average of 1.8 lbm (a 33% increase). However, the number of pilot inputs decreased markedly (figure A3d), as did angular alignment at dock (figure A3f) and motion across the dock face (figure A3g). Other performance metrics were not significantly affected.

In terms of pilot opinions, Cooper-Harper ratings improved with only one pilot lowering his opinion by a Level; two pilots improved their opinions from Level Two to Level One (figure A3a). Mental and temporal demand and frustration decreased slightly (figures A3i through A3k) but overall effort was judged constant (figure A3l).

Pilot 2 noted the more frequent RCS thruster firing (cued by the aural cueing system):

It was controllable. It [had] adequate performance with a tolerable workload. It was satisfactory without improvement. I’ll give this one an handling qualities rating [CHR] of 2. It seemed slightly improved. It seemed to [have] even less dead-banding; it almost wasn’t a factor. To say that, I’m assuming that that thing we heard [was] the almost continuous RCS, I’m going to call that a sim artifact and just pretend that wasn’t there. Because that certainly is distracting.

Pilot 3 said, “About the only thing that keeps it from being [rated] a [CHR] 1 is the requirement to constantly monitor your [closure] rate which does not have a whole lot of visual cues other than the display in the upper right hand corner of the camera field of view”

and gave it a 2. He also said “the pilot is able to precisely control and maintain position and closure.”

The difficulty cited in maintaining closure rate is discussed below in section 10.3.

Although feed-forward was turned off in this configuration, pilot 4 said “it looked like . . . feed-forward was active . . . very acceptable” and gave this configuration a CHR 2 and graded the performance a perfect 100. (The pilots were briefed before each configuration whether feed-forward would be on or not.)

However, pilot 5 found the excessive dead-band firings and ADI attitude error needle movement distracting:

So, we’ll go down to control coupling. I saw the ADI working and all the needles working hard, and I could tell there were some inaccuracies in the real world picture because it had some attitude excursions but in the end it got there. If you stay out the loop a little bit and let it do its thing you’re going to be okay. I’m going to go neutral on that control coupling. I didn’t think it was very good, because if it was really good, I wouldn’t even have to see those needles moving.

The excessive needle motion was caused by a re-scaling of the error needle limits to indicate the smaller DAP dead-band; thus the motion of the ADI needles was amplified due to the more sensitive scale.

As discussed later in section 10.3, the TDM mixer introduced artifacts in the \dot{X}_{body} closure rate from lateral translation firings. This was true even for this configuration; pilot 6 noted that the vehicle was “still decelerating with translational inputs” and gave this configuration a CHR 3 due to minimal pilot compensation of having to provide forward ($+X_{body}$) inputs to maintain the desired 0.1 ft/s closure rate.

Pilot 8 noted a reduction of “dead-banding” but an increase, especially in digital autopilot high-authority setting (A-DAP), of coupling into range rate (\dot{X}_{body}); pilot 9 echoed these comments as well.

In general, tightening the allowable rate error dead-band in the digital autopilot’s RCAH control logic gave one of the more significant improvements, despite having the feed-forward mixer feature disabled, at the expense of additional RCS propellant use.

Effect of larger attitude dead-band. Configuration 13 differed from the baseline CEV by a doubling of the attitude dead-band of the RCAH autopilot function. Results for most metrics are shown in figure A4.

Only a small number (4) of pilots evaluated this configuration and results are mixed. Except for pilot 6, fuel used decreased (figure A4b), probably due to fewer attitude control RCS firings, but also due to fewer pilot inceptor inputs (figure A4d). As expected, docking alignment worsened with the increased attitude dead-band (figure A4f) but remained within the 1.5 deg desired bounds, while position showed no clear improvement.

Pilot 6 noted that configuration 13 “wallowed a little bit, it was difficult to precisely hold it in position” with a sluggish RCAH response to attitude errors.

Pilot 9 also mentioned “bobbling around just a little bit.”

Since no clear improvement in CHR (figure A4a) or perceived effort (figure A4l) was shown, this variation may not have been large enough to have significance, but it was noticeable to half the pilots who saw it. Thus, an increase in attitude dead-band in an attempt to conserve fuel while remaining within the desired task performance docking alignment error of ± 1.5 deg may not be advisable.

Effect of center of mass offset. The next set of comparisons with the baseline CEV configuration (test 6) involve center-of-mass offset conditions. The feed-forward mixer was designed to decouple translational inputs from rotational accelerations for a given design

center-of-mass location. Unless the spacecraft contains on-board logic to determine the actual center-of-mass in-flight, having an offset in the actual center-of-mass from the design location will cause the translation-to-rotation coupling to appear to some degree. The RCAH function would suppress to this coupling outside of DAP dead-band limits, but not mask it completely.

Four related configurations were evaluated to determine how much effect such offsets would have on the pilots' perception of the vehicle in performing the docking with stationary ISS task.

Eight pilots evaluated a configuration (test 10) that included a six-inch lateral offset of the center-of-mass. Results of various metrics are shown in figure A5. This offset should have exhibited both yaw-from-longitudinal-input and roll-from-vertical-input coupling, as well as heave motion (\dot{Z}) from roll inputs and \dot{X} from yaw inputs.

While most metrics showed no clear trend, fuel use (figure A5b) increased (as was the case for all center-of-mass offset configurations) by about a half pound of propellant and docking alignment actually improved a fraction of a degree (figure A5f), as did relative motion across the docking plane at contact (figure A5g).

Pilot comments also showed mixed results; no pilot was able to discern the root cause of the difference (although all had been briefed that center-of-mass offsets would be evaluated) but one came very close.

Pilot 1 said he was aware of coupling “but it was very minimal.”

Pilot 3 spoke directly about control coupling and ADI motions, saying:

Control coupling was very acceptable, I'll give it a 6 [on a Likert scale where 1 was “very unacceptable” and 7 was “very acceptable”]. [The task] didn't seem to require a whole lot of anticipation looking at the vertical pitch, roll and yaw deviations on the ADI. They didn't seem to generate large rates based on the translation control inputs, and they were very predictable as to when they were going to make an input into the controllers.

Pilot 4 also illuminated his experience:

Most of [the coupling is] handled, the rates are under control, it's the dead-band. So the rates are pretty good, it's the rotational offset that you can't control because you're just watching it.

Pilot 6 fortuitously saw this configuration directly after evaluating the baseline (test configuration 6), just due to random selection of configurations; he said they were “very, very similar” and that:

The only difference I noticed was there seemed to be some coupling when I made my translational inputs in the [\dot{X}_{body}] axis. As I would make inputs to go either slower or faster it seemed to have some kind of cross coupling involved in there. It also seemed to have a little bit more coupling involved when I made either Y corrections or Z corrections. But not bad at all and it was very easy to get very good performance ... I thought there was some coupling. I would say it was neutral, a 4. It really wasn't that detrimental but it seemed to be a little more prevalent to me than the previous [baseline, unknown to him] configuration ... Overall it seemed very, very similar to the previous one. The only subtle change I saw, and it was so subtle that it could have been just the way I was controlling it, but it seemed to have a little bit more coupling. There seemed to be some interesting things going on when I made the X -axis or the range corrections. That's all I could detect.

Pilot 8 also noted “it would be nicer if there was no coupling at all” so he did detect some coupling; whether this was due to the [TDM](#) mixer contamination or the center-of-mass offset is unclear, but he then discussed the motion of the target on the centerline camera so a rotational coupling, rather than \dot{X} caused by the [TDM](#) mixer “braking effect,” is suggested.

The same eight pilots evaluated a configuration (configuration 11) that included a six-inch vertical offset of the center-of-mass. Results of various metrics are shown in figure [A6](#). This offset should have exhibited both pitch-from-longitudinal-input and roll-from-lateral-input coupling and, to a lesser extent, \dot{X} from pitch inputs and \dot{Y} from roll inputs.

Again, as with the six-inch lateral offset, fuel use (figure [A6b](#)) increased, while docking alignment and relative motion decreased (figures [A6f](#) and [A6g](#)). Pilot input count (figure [A6d](#)) increased and pre-dock coasting period (figure [A6c](#)) decreased, indicating additional pilot effort being expended; this seems to have been borne out by slight increases in pilot perception of mental effort, temporal demand, frustration, and overall effort (figures [A6i](#) through [A6l](#)).

Pilots 1 and 2 noticed no more than the normal amount of coupling.

Pilot 3 picked up on the coupling into roll axis:

There’s always a flurry of activity once the roll command attitude fires in at least the vertical axis and the yaw axis. I don’t know that I noticed the roll axis firing.

He also commented that he didn’t see any vertical input coupling into pitch, roll or yaw.

Pilot 6 noticed “a lot of drifting or wallowing in close when you’re making your fine corrections” and noted “nuisance pitch corrections coming in too late from the [RCAH](#).” He called it “demanding in close” and graded this configuration a [CHR 4](#) (Level Two) versus his baseline configuration [CHR 2](#) (Level One).

Pilot 8 noted “the attitude [control] is still just a little sloppy.”

The other pilots seemed sufficiently distracted by the braking effect of the [TDM](#) mixer problem that they didn’t gripe the less obvious coupling from having a center-of-mass offset.

A smaller number of pilots (four) evaluated configuration 14, which included a twelve-inch lateral offset of the spacecraft center-of-mass from the design point (originally located along the vehicle X_{body} axis). The comparison of metrics for this configuration with the results of the baseline (configuration 6) are shown in figure [A7](#).

No clear trend is obvious in the metrical pairings, aside from an increased amount of [RCS](#) propellant (figure [A7b](#)); pilot 9 downgraded this configuration to [CHR](#) Level Two versus Level One for the baseline configuration (figure [A7a](#)).

Pilot 3 did note that “the needles were moving more” but liked this configuration, calling himself “very confident” instead of frustrated; this was the same way he described the baseline.

Pilot 6 noted “wallowing” again in close with some attitude correction “lag” and more apparent “coupling.” He cited a “lack of predictability of the translational kind of wandering there inside of two feet or so.”

Pilot 7 noted “you do wander around” in rotation and that you would “pound yourself to death” trying to get an exact alignment at docking.

Pilot 9 summed up his frustrations, but exactly which cause he was citing is unclear:

Control coupling is the issue. I’m giving it the [Likert] rating of $3\frac{1}{2}$ [towards the “unacceptable” side of neutral]. The issue is the frequency and magnitude of coupling between the rotational axis and the translational axis. So in other words, it was caused by rotational dead-bands, but the response is seen in the translational axes. It’s all three of them, it’s lateral, vertical, and [longitudinal].

The same four pilots evaluated a configuration with a twelve-inch vertical center-of-mass offset. Comparison of metrics with the baseline [CEV](#) are shown in figure [A8](#).

In terms of metrical comparisons, one pilot (7) joined the other pilots in rating this configuration [CHR](#) Level One which was an improvement over his Level Two rating for the baseline [CEV](#) (figure [A8a](#)). Fuel use (figure [A8b](#)) increased, and docking alignment (figure [A8f](#)) and lateral rate (figure [A8g](#)) were improved over the baseline, which is again a surprising result.

Pilot 3 found it “a little bit harder to control pitch” and saw the same “flurry of activity” in the controller associated with an [RCAH](#) roll correction, and that lateral inputs, both left and right, “seem to generate a slight nose-down pitch.” [The reason for this is not entirely obvious.]

The center-of-mass offset may also account for pilot 6’s comment that “your sim gets a little bit out of phase with the corrections made by the attitude [RCAH](#) inputs.” He also raised his task-load index ([TLX](#)) frustration level from 20 (from the baseline configuration) to 40 (for the 12” vertical offset) [on a scale of 0 to 100] due to unpredictability:

It appeared . . . that there was something that was making the slight loss of predictability in the attitude corrections, which would then cause the attitude just to fire at inopportune times.

In general, the effect of having the actual center-of-mass of the spacecraft as much as a foot away laterally or vertically from the design position had only minimal effect on pilot rating or task load; fuel use was increased, however, due to additional [RCS](#) activity to compensate for the resulting additional coupling.

Effect of loss of feed-forward compensation. This variant (test 5), in which the feed-forward mixer was inactive (but [RCAH](#) autopilot function was still engaged) was more clear-cut than most of the other comparisons, as shown in figure [A9](#). Cooper-Harper rating was degraded with only one of the eight evaluation pilots improving their opinion (figure [A9a](#)), and three pilots moving from Level One to Level Two in their ratings. Fuel use (figure [A9b](#)) increased by an average of 1 lbm (about an 18% increase). The pilots were more active in control (figure [A9d](#)) with less coast time prior to dock (figure [A9c](#)) while docking performance perhaps became a bit more scattered (figures [A9e](#) through [A9h](#)). With few exceptions, pilots perceived an increase in task load, including mental demand, temporal demand, frustration, and overall effort (figures [A9i](#) through [A9l](#)).

Pilot 1 said it was like flying with “rubber bands,” that he didn’t feel like he had sufficient control, especially in “low” [DAP](#) gain settings: “. . . it’s still moving in the wrong direction and I’m whacking away at the [THC](#). . .”

Pilot 4 mentioned “coupling in close is really bad.”

Pilot 6 gave it “the lowest [rating he] could give it with having met desired performance across the board” and that this configuration also had a tendency to “wallow” with a tendency for a very low frequency pilot-induced oscillation ([PIO](#)) with a lot of overshoots on attitude.

Pilot 7 talked about “playing the dead-bands,” i.e., trying to time inputs so that any attitude correction by the [RCAH](#) would occur in the proper direction just prior to dock.

The results seem to indicate that a feed-forward mixer, even one with a less-than perfect implementation in this test, is an improvement over having no feed-forward mixing coupling compensation.

Effect of loss of feed-forward compensation but with symbology. The final comparison with baseline [CEV](#) was similar to the previous one, in which the feed-forward mixer

was disabled, but with the **RCAH** symbology set (section 6.5.5) turned on (test configuration 7).

The comparison plots for several metrics are shown in figure A10.

In general the additional symbology didn't seem to help much, for reasons discussed in section 10.1.1. Cooper-Harper ratings degraded (figure A10a), fuel use increased (figure A10b), pre-docking coast time decreased (figure A10c), pilot input count increased (figure A10d), most performance metrics worsened (figures A10e through A10h), and virtually all pilots saw their workload and frustration increase (figures A10i through A10l).

Pilot 1 noted a lot of effort in interpreting the information, but did say the \dot{Y} and \dot{Z} readouts were helpful.

Pilot 3 stated “the symbology on the camera display basically negates the necessity to use the ADI at all. Having the needles there is a really nice feature” but said “the impact predictor [is] essentially useless other than as a vector on the initial part of the approach in A-DAP.”

Pilot 7 said the docking predictor “helped” as did the “guidance” by which it may be inferred the attitude needles on the centerline camera display.

Pilot 8, however, said he didn't think “the symbology really helps all that much; it's kind of nice to see. I'm still kind of in favor of just a pure center latitude symbol as opposed to a predictor.”

In general, the **RCAH** symbology set was not as helpful as hoped, mostly due to complaints about the impact predictor's motion.

10.1.2 Comparison of variants vs. a reversionary 6DOF CEV configuration

Another set of variants were based on a **CEV** with minimal control compensation, which might represent a reversionary mode of the control system with no active feedback control system. For these configurations, the pilot had direct control over all six degrees of freedom (three rotational and three translational axes), in a manner similar to that reported in [9]; herein called the **6DOF CEV**. However, in each of these variants, some minimal control capability did provide Pulse command mode such that **RCS** firings were limited in duration for each movement of an inceptor out of detent to provide a fixed approximate ΔV or $\Delta\omega$ increment. This might be accomplished via simple timing circuits without accelerometer feedback. Again, two Pulse gain sets were available, an “A” and a “B” gain set, given in table 1.

The baseline for these comparisons was represented by test configuration 1, a basic **CEV** without an **RCAH** autopilot, no feed-forward mixing or symbology. Variants included test configurations 2 through 4: adding a feed-forward mixer table, adding Pulse mode symbology (described in section 6.5.5) but without the feed-forward mixer, and a configuration with both a feed-forward mixer and Pulse mode symbology. The paragraphs below discuss the effect of each combination of these two pilot aides in performing a docking with a stationary **ISS**.

Effect of adding feed-forward compensation. The first comparison for the **6DOF CEV** configuration gives the effect of adding feed-forward mixing table to reduce coupling of translational commands into rotation coupling (due to the center of mass being non-coplanar with the **RCS** jets). Figure A11 compares the resulting metrics of test configuration 2 with the **6DOF CEV** baseline configuration, test configuration 1.

Some performance improvements resulted, but pilot opinions reflecting this improvement are not compelling. Cooper-Harper ratings stayed approximately the same (figure A11a) with one pilot (pilot 3) going from **CHR** 5 to 1; in general, though, pilot opinions remained about the same. Fuel use went up slightly, on average, as shown in figure A11b. Pre-dock

coast period (figure A11c) shows no clear improvement, aside from pilot 1. Pilot inputs did decrease slightly but two pilots (2 and 9) bucked that trend (figure A11d).

Performance metrics showed some improvement: offset (figure A11e) improved slightly but alignment actual worsened (figure A11f) (increasing by 0.1 deg average error). Residual lateral rate (figure A11g) improved significantly but the average range rate at dock (figure A11h) wandered away from the nominal 0.1 ft/s target.

The pilots' perception of their task load decreased slightly, in average, but contra-examples were present in figures A11i through A11l.

Pilot 1 didn't see a problem in maintaining closure rate, despite the braking effect of the TDM mixer used in Pulse mode, instead citing a deficiency in "the translation ability, particularly in [the vertical axis]." This reflects the reduction of control authority by adding the feed-forward mixer, particularly in the Z axis, as shown by comparing tables 2 and 3.

Pilot 2, however, did complain about the "significant cross-coupling between Y and Z [lateral and vertical] translations and change in closure [rate]." This is the TDM mixer braking effect discussed later. He also suggested having a smaller scale on the ADI attitude error needles.

Pilot 3 liked the feed-forward, calling it "predictable" and said the feed-forward "keeps your displacements and rates close to zero" and let him cross-check range rate; but he did say he had to constantly cross-check range rate. He did note having made several pitch corrections in the wrong direction but in general made very few inputs in the RHC. He saw "very little . . . coupling."

An oft-heard complaint about the gain sets used in Pulse mode was summarized by pilot 4:

Rotational control is way too sensitive in A-DAP. So even in A-DAP translation I'll switch to B-DAP to put a rotation control in, or just wait. That just waiting is a bad thing because you can allow the problem to get too far out of bed and then you have to work too hard close in. So it's almost like you need "B" rotation in A-DAP translation and you need something smaller than "B" in B-DAP . . . I guess that would be considered control harmony compared to an airplane, the translational control harmony is not very good.

Pilot 4 also does a nice job of summarizing the frustration he and several others felt about the TDM mixer braking effect:

The control coupling, the feed-forward is helping with the control coupling, but there's still this strange B-DAP closure versus translation coupling that just gets away from you. The rotation coupling is not bad; it's just you're having to do all six degrees of freedom. So I kind of give that just a slightly unacceptable rating. . . It's just a lot of work to do all six axes. But the actual "put a translation and [get] cross coupling in roll" is not very bad, but that plus the translation to closure rate together is a little bit annoying.

Pilot 5 didn't like this (or any other 6DOF configuration), rating each 6DOF configuration except one a CHR Level Three; of the feed-forward mixer configuration he said "it was just too hard, too many axes, too hard, no fun" but didn't really provide insight into what specific aspect he found objectionable.

Pilot 6 also griped about the Pulse mode settings:

In the A-DAP [translation control power is] fine. In the B-DAP you have insufficient control power, you have to over-control it to get it to move, and then you cannot stop it once it starts moving. So not only is the sensitivity poor, but there is a feeling of a lack of control power. You can't stop drift rates once

they start. You've got a whole lot of propellant going in there. The ability to precisely control and maintain position and closure is very poor.

Pilot 6 seemed to pinpoint his main concern, having to do with the “B” gain set:

... the main thing was the lack of predictability in **B-DAP**. It appeared that in **B-DAP** either there was a thruster misrigging or mismatch or it was very poor coordination. It was a high degree of coupling, so something changed when you went from **A-DAP** to **B-DAP**. You would also not be able to feel like you could move the nose around. You could translate it. It would be very, very long transport delays or lags or something that didn't cause you to put in too large a correction and it would way over-control. So a pretty lousy configuration all the way around.

He may have been speaking of the braking effect introduced by the feed-forward mixer interaction with the Pulse mode controller described later.

Pilot 7 cited the inability to precisely maintain position and closure due to “cross-coupling;” he seemed to be experiencing the braking effect as well.

Pilot 8 disagreed with pilot 4: “**A-DAP** was just too coarse, but the **B-DAP** was fine” for rotational control. In translation, he thought both settings were “good.” But he did note that coupling into closure rate was more noticeable in **B-DAP**.

Pilot 9 said workload for the feed-forward on case was too high and he had to shed some of it, giving it a **CHR** of 4.5 “because desired performance requires more than moderate compensation for me, and yet adequate performance requires less than considerable” compensation. He rated the non-feed-forward configuration, which he evaluated next, as a “solid” **CHR** 3, and said the difference was the lack of braking effect introduced by the feed-forward mixer (he called it the “effect of feed-forward on \dot{R} ”). Pilot 9 also suggested having a finer rotational control (“**C-DAP**”) setting would be helpful.

In general, adding the feed-forward mixer showed slight improvements for flying qualities but was not a clear winner, probably due to the inadvertent introduction of the braking effect (discussed in section 10.3).

Effect of adding symbology without feed-forward compensation. As shown in figure A12, the addition of the Pulse symbology set (described in section 6.5.5) in test configuration 3 to the bare **6DOF CEV** configuration of test configuration 1 yielded some improvement in pilot perception of the task and small improvements in most performance metrics.

Cooper-Harper ratings improved slightly, going from having one Level One without symbology to two Level One ratings with symbology; simultaneously, two Level Three ratings were reduced to one Level Three rating with the addition of symbology (the remaining six pilots maintained their Level Two ratings) as shown in figure A12a.

Fuel use (figure A12b) decreased a small amount, as did the number of pilot inceptor movements (figure A12d). Docking offset and alignment were not significantly improved, however, but residual motion across the docking face was somewhat better (figure A12g).

Pilot perceptions of task load also improved for the four **TLX** measures shown in figures A12i through A12l.

Regarding the symbology itself, pilot 1 said it increased his mental demand (but he had given the minimal-symbology case the same **TLX** score (80) for mental demand, five configurations earlier):

There's more information and more lines on the screen, some of which begins to blur out the camera view. I mean I start looking around for a different sort of controller that has video game kind of differences, in that there's so many

things moving around on the screen. I think I made at least one error in that, and it wouldn't be the only time but, trying to operate all the whiskers and look forward balls that's what pushes the mental demand up there.

Pilot 3 made some insightful comments regarding the Pulse symbology set, which included the [ASI](#) box-and-whiskers and the orbital-droop-corrected impact predictor:

The symbology, specifically the predicted impact point, doesn't seem to be working for me. It's slewed to the axis system and at times it seems to be giving me different information than what the camera's giving me, even though the attitude information is zeroed out. I think it's accurate laterally but the vertical I almost feel like it's giving me false cues in that the alignment is drifting up but it's telling me my predicted path is low. So, it seems to be giving me conflicting information, and I find myself looking through it or looking for a declutter option for the predicted impact point. I think at the beginning of the run, at 20 feet, it's good, it lets me know what direction I'm moving in. But then when I get in close I'd like to be able to declutter the predicted impact point or have it just give me a shorter velocity vector [than] where my ultimate velocity vector is [going to be] ... Inside of about 10 feet I'd like to be able to get rid of the predicted impact marker. The square with the whiskers on it I think is valuable information. I think the whiskers... it would be nice if they were tied to the sensitivity of the translational hand controller so I can zero them out, but I don't know if that's an option or not. It's kind of frustrating when the most sensitive input I can make on the translational hand controller can't zero those out. I don't think that's any different than the symbology on the [ADI](#), but those seem to be step inputs on the whiskers where the [ADI](#) yellow deviation markers are verniers, so that may be what's driving that.

He also said:

I feel like I'm having to work harder to look through the symbology. Where if I could just ignore the symbology and go back to what I was doing with the translational controller which is setting the grid to the alignment marks and just flying that. That might actually be easier.

Pilots 4 and 5 indicated the symbology helped. Pilot 6 didn't comment much on the symbology but did note this was one of the most fun configurations he had flown (this was the eighth configuration for him).

Neither pilots 7 or 8 commented on the symbology specifically. Pilot 9 said "there are a lot of symbols and a lot of things to control at one time" and thought there might be a performance "cliff:"

I haven't seen the cliff yet, but maybe if you pounded on my head with a ball-peen hammer while you were doing this, or gave me a fuel emergency, or something else that really increased the temporal demand, you might find a cliff here.

In general, symbology was a mixed blessing. It seemed to help performance, but did not significantly improve workload, for several reasons. The impact marker, which included compensation for orbital effects, tended to counter what the motion of the target on the centerline camera was doing; the impact predictor would often indicate that docking would occur below where the trend in the camera was, even if the centerline of the camera was above and moving farther away from the target.

Several test runs were made during checkout to confirm the predictor was operating correctly. In every case, the impact point occurred where the predictor indicated, especially in the vertical axis (the lateral axis was not as precise due to the effect of rotation as discussed in the paragraph headed by “Effect of additional display symbology” in section 10.1.1 above.

Effect of adding both feed-forward compensation and display symbology. The final 6DOF comparison was between the basic CEV with no feed-forward compensation and no additional symbology (configuration 1) with a configuration having both the feed-forward mixer and the Pulse symbology set (test configuration 4). Metrical comparisons are shown in figure A13.

Here, a clear improvement in Cooper-Harper ratings is evident from figure A13, with all but two pilots giving improved ratings (although one pilot crossed the CHR Level One to Level Two border). Although fuel usage showed a slight increase (figure A13b), inceptor use decreased (figure A13d), and docking parameters (figures A13e through A13h) mostly improved.

The four task load indices depicted also decreased slightly (figures A13i through A13l) except for pilots 8 and 9, who felt an increased workload.

Pilot 1 again cited a lot of mental processing required, giving both configurations an 80 (out of 100) in mental demand. Even though he saw configuration 4 as his fifteenth configuration, he thought it would have been good to “be a little bit more trained on it.”

Pilot 2 said “once you get used to the square [ASI] it does simplify the scan, [it] does make a slight improvement in rotational control” but said he wasn’t “convinced that the small [impact] predictor really takes into account attitude and pitch error and rate” and thus he didn’t use it for “fine control” but did use it for coarse correction toward the target.

Pilot 3 noted “the whiskers [on the ASI] give me good indication of the direction of movement from the centerline target, giving me adequate cues as to which way it’s drifting and how to correct . . . almost as well as [RCAH].”

Pilot 4 said he thought the B-DAP rotational command pulse ($0.04 \text{ deg/s } \Delta\omega$) was still too big; he noted “your display and the feed-forward helps a whole bunch” (he had just flown test configuration 3 with just symbology and no feed-forward) to reduce coupling.

Pilot 7 said the biggest problem was how Y and Z translational corrections affected \dot{X} , again, the unintentional braking effect of the TDM mixer implementation (discussed in section 10.3 below).

Pilot 8 expressed a desire for finer rotational control for the Pulse mode.

Pilot 9 appreciated the “workload alleviation” from having feed-forward RCS mixing to reduce coupling, but the braking effect made the task more difficult; he also would have liked a smaller rotational control input than he could achieve with B-DAP.

Overall, adding both feed-forward and symbology (specifically the ASI and impact predictor) improved the flying qualities of this task.

10.1.3 Comparing reversionary 6DOF CEV to the baseline CEV

A final comparison was made between the reversionary open-loop CEV with the so-called baseline CEV with minimal symbology but with feed-forward compensation and with the RCAH autopilot operating. The per-pilot metrical comparisons are shown in figure A14. Inclusion of the RCAH autopilot obviated the need to manipulate the RHC inceptor, making this a single-handed (i.e., THC-only) task.

As is evident in the metrics, addition of feed-forward compensation had a significant effect on most performance metrics and pilot numerical opinions. Cooper-Harper ratings improved significantly (figure A14a), despite the inadvertent braking effect discussed in section 10.3. Two pilots, in fact, changed their opinions from CHR Level Three to One (pilots 1 and 5).

Only one pilot (pilot 9) seemed to be indifferent to the change, and retained his CHR 3 for both configurations.

Fuel use (figure A14b) decreased, pre-dock coast time (figure A14c) increased, pilot input count (figure A14d) decreased, docking offset (figure A14e) and alignment (figure A14f) tightened up, as did residual motion across the docking face (figure A14g) and docking impact velocity (figure A14h). All pilots (except pilot 9) perceived a reduction in mental demand (figure A14i), temporal demand (figure A14j), frustration (figure A14k) and effort (figure A14l).

In summary, adding even a somewhat defective feed-forward compensation to reduce coupling and a rate-command, attitude-hold autopilot to the vehicle brought a Level Two/Three configuration into the Level One/Two area.

10.2 Task 2 - Rotating target docking

Only one CEV vehicle configuration (the CEV baseline configuration described in section 9.2) was evaluated against a rotating target. The motion of the docking target vehicle, an Apollo CSM with an updated docking mechanism (figure 18), was varied from a constant inertial yaw (test 16), constant pitch (test 17), and combined pitch and yaw at two rates: 0.4 deg/s total (test 18) and 0.566 deg/s (test 19). The CEV design requirement CV0126 [19] called for the ability to dock “with Lunar Surface Access Module (LSAM)... with inertial rate less than 0.4 deg/s per axis” but it was not clear if this included multiple axes of rotation, or was total rotation about an arbitrary axis.

Target roll rotation was initially zero in the LVLH axis, but due to the rotation of the LVLH frame relative to the inertial frame, some roll and pitch rates appeared in the LVLH frame; this meant the evaluation pilots needed to command some LVLH roll and pitch through the RCS for their ownship in order to dock within the specified roll error parameters (see table 4) for the tests involving a target with a yaw rate component (tests 16, 18 and 19).

For the rotating-target docking tasks, the requirement to hold range rate within tolerance during approach phase was waived (since the initial geometry quickly degraded \dot{R} as the target rotated away from the non-rotating ownship) but was enforced at the moment of docking.

Pilot comments that illuminate the Cooper-Harper ratings given in table 11 are discussed below.

10.2.1 Test 16 - Yawing target

For this task, the RCAH autopilot was engaged only in the roll axis with the pitch and yaw axes in Direct mode, meaning the pilot had direct control of both pitch and yaw rate, while the autopilot would attempt to hold roll attitude constant relative to LVLH.

The X translation RCS mode was set to Direct while Y and Z were set to Pulse mode.

The pilots were briefed on the actual yaw rotation rate of the target, since it is considered likely that this rate could be determined by observation and timing. A helpful tactic recommended to the evaluation pilots was to match the yaw rate of the target (using the NAV display yaw rate readout) through the RHC and then concentrate on translating their simulated CEV to line up with the docking target visually, making small inputs around the target yaw rate.

Complicating docking with the yawing target was that, due to the rotation of the LVLH frame and the design of the ownship’s RCAH autopilot to hold constant pitch and roll attitudes in an LVLH, instead of inertial, frame, matching the target’s inertial yaw rate required making small pitch and roll corrections.

Pilots 2, 3, and 4 saw this task before the simpler pitching target task.

Pilot 2 said this task revealed “very objectionable but tolerable deficiencies” in the control system and assigned a CHR of 6. He said it was hard to match the yaw rate and again cited closure rate being affected by attitude jet firing (but this braking was probably mostly due to centripetal acceleration). He noted his mental, temporal and overall effort as high, a 90 on a scale of 0-100.

Pilot 3 was unable to obtain adequate performance and thus rated it a CHR 7. From two feet in, “it [required] continual control inputs in every possible axis just trying to stabilize” the docking target in the centerline camera.

Pilot 4 was able to obtain adequate performance but with extensive compensation and rated it a CHR 6. He rated his effort as a 90 out of 100.

Pilot 7 indicated he’d like more translational command capability and rated this scenario a CHR 6 due to extensive pilot compensation; he also indicated a relative-attitude-based ADI would be better than an LVLH-based one.

Pilot 8 also noted the decay of \dot{R} but was unable to determine if it was due to the TDM mixer “braking effect” or “just the environment you’re operating in and the task you’re trying to perform.” A colleague astronaut helped him perform this task by calling out range rate; perhaps because of this pilot 8 was able to get desired performance but indicated it took more than moderate compensation to do so; he thus placed this configuration in the Cooper-Harper “gap” between CHR 4 and CHR 5 by rating this a CHR 4.5 .

Pilot 9 gave it a 4.5 CHR as well, citing the workload; he didn’t feel control was an issue, and cited the \dot{R} coupling as a “physics issue,” not a control issue.

10.2.2 Test 17 - Pitching target

Of the two single-axis target motion scenarios, the pitching-only configuration (test 17) was considered simpler. Three of the pilots (pilots 2, 3, and 4) saw this configuration after the yawing target (test 16); pilots 7, 8 and 9 saw this configuration before the yawing task. This was the only rotating target scenario evaluated by pilot 6.

For this task, the RCAH autopilot was engaged in both roll and yaw, leaving just the pitch axis in Direct mode. The X translation RCS mode was again set to Direct while Y and Z were left in Pulse mode. Thus, the evaluation pilot had direct control of pitch rate, while the autopilot would attempt to hold yaw and roll attitudes at their initial values.

The pilots were briefed on the actual pitch rotation rate of the target, since it is considered likely that this rate could be determined by observation and timing. Thus, the tactic briefed to and used by by most pilots was to match the pitch rate of the target (using the NAV display pitch rate readout) and then concentrate on translating their ownship to line up with the docking target visually. Small variations in pitch rate were required to dock within the desired relative pitch error bounds, but this was relatively easy to accomplish with the Direct control of pitch.

A limitation of the RCAH logic in roll and yaw was, if the target were not captured by the time the ownship pitched past vertical, the RCAH would try to reorient to ‘wings-level’ zero LVLH roll angle and yaw backwards in the original LVLH heading; the few times this occurred the pilots were asked to briefly move the RHC out of detent and release which re-initialized the RCAH target LVLH roll and yaw attitudes to match the current values.

Seven evaluation pilots performed a successful docking with the Apollo CSM target that was pitching at this constant 0.4 deg/s LVLH rate. As shown in table 13, a median Cooper-Harper rating of 5 and an average fuel burn of 20.9 lbs were documented for this scenario.

Pilot 2 noted some “braking effect” due to the TDM mixer as described in section 10.3, but gave it a CHR of 3. Pilot 3 rated it at CHR 6, primarily due to only adequate performance in obtaining desired closure rate at docking, citing poor visual cues for angular displacement and closure rate. Pilot 7 called it a tough task but got desired performance

and rated it a CHR 3. Pilot 8 called it difficult but very do-able but lost track of closure rate; he gave it CHR 4.5. Pilot 9 said it took minimal compensation and gave it a CHR 3, despite noting a braking effect (which was no doubt partly due to centripetal acceleration).

10.2.3 Test 18 - Pitching & yawing target at 0.4 deg/s total rate

The six pilots that evaluated the slower combined pitch and yaw target motion case evaluated this task after evaluating both yaw- and pitch-only target motion cases.

While pilot 2 was able to obtain adequate performance, pilot 3 was not and rated this task an CHR 7, citing an “almost exponentially” excessive workload while closing with the target (but controllability was “not in question”). He noted that his approach “stagnated” several times, meaning his closure rate dropped to zero (or perhaps reversed); this is due primarily to centripetal acceleration. He suggested more cues to assist in situation awareness would be good.

Pilot 4 said this task was “really hard” due to workload and gave it a CHR 6. He noted it had a “frantic” pace and rated temporal demand at 90 out of 100.

Pilot 7 gave a CHR of 7, but pilot 8 gave this “tough but do-able” task a CHR of 4.5 (which he consistently did for all four rotating target docking tasks). Pilot 9 agreed, with a CHR of 5 despite having adequate performance. He summed up the situation as follows:

... there’s so much going on that you don’t have enough situational awareness to use fine control. You’re making corrections, it’s almost like when things are centered you don’t know what the heck to do. If you’re not making a correction, you’re not really sure where you are. If you’re making a correction and it’s coming in now I know where I am. What happened the last time is we were off but we were correcting, and I knew we were inside the desired range and correcting back to center, and that’s the time to punch it and try to hit it before it goes out the other way, so you don’t have to make a correction. So this isn’t a control issue, it’s an information issue and a workload issue.

10.2.4 Test 19 - Pitching & yawing target at 0.566 deg/s total rate

This configuration was similar to the previous one except the relative target motion was higher, with a larger centripetal “braking” effect on \dot{R} . Only four pilots evaluated this maneuver with about the same result as test 18; most judged it to have too high a workload with sometimes less than adequate performance.

Pilot 4 commented:

What you probably need to do, is you need to be able to type into the system to match the rates and just hit a button and engage it, and it flies the rates and then you just translate. Trying to do it all manually is just too hard.

Pilot 8 noted that this sort of docking was not part of Shuttle training; the closest experience he had was training to capture a rotating free-flying payload which was easier since the alignment didn’t have to be as precise (just close enough to use the robot arm to grapple the payload).

Pilot 9 suggested this would be an interesting task to do with real motion, thinking the pilot’s inner ear would probably be “going nuts.”

10.3 TDM mixer contamination

As described in section 6.4.2, the approach taken to design combinations of multiple fixed-thrust RCS jets to provide translational motion decoupled from rotational motion was to

generate a repeating pulse train of sixteen 40 ms pulses. This pulse train attempted to spread out the firing of the jets with lower required thrust, as depicted in figure 6. The goal was to provide a continuous decoupled acceleration capability for manual control of translation commands; some residual coupling was inevitable due to choice of a 40 ms pulse quantization level shown in table 2.

As development of the experimental matrix progressed, it was decided to adopt Pulse mode in the translational axes instead of Direct mode; it was decided that Pulse mode was a more realistic choice and would be more familiar in operation to the several Shuttle-qualified evaluation pilots.

When autopilot gain set “A” was selected by the pilot, each movement of the translational hand controller out of detent commanded 0.01 ft/s ΔV in that axis. Given the acceleration authority of the decoupled RCS jet combinations, the total firing duration to achieve this amount of ΔV was 0.45 s in the lateral axis and 0.33 s in the vertical axis, resulting in completion of the first 11 or 8 pulses of a full (16×40 ms, or 0.64 s) pulse sequence, respectively.

Even worse, when autopilot gain set “B” was selected, each motion of the translational hand controller out of detent commanded just 0.002 ft/s ΔV . The RCS firing duration to achieve this amount of ΔV was just 0.09 s in the lateral axis (resulting in two 0.04 s pulse widths) and 0.065 s in the vertical axis (rounded up to two pulses as well).

As a result of firing incomplete pulse trains for each \dot{Y} or \dot{Z} command, the partial firing train did not include sufficient balance between $+X$ and $-X$ acceleration components. This resulted in a decay of the closure velocity (along the X_{body} axis), and required the evaluation pilot to put in $+X$ pulse commands on a frequent basis to avoid violating the desired range-rate limits during both the approach and docking metrics. Pilots sometimes referred to this as a “braking” effect. This effect was particularly evident in B-DAP gains as shown in table 15 below where the uncommanded response in $\Delta\dot{X}$ from an input in $\pm Y$ was fully two-thirds as large as the (commanded) response in $\Delta\dot{Y}$ (and always acted in the negative X_{body} direction).

Tables 14 and 15 shows the resulting contamination or cross-talk from Y and Z axis commands into the other axes with “A” and “B” gains selected.

Table 14: Velocity changes resulting from an incomplete TDM RCS pulse sequences: “A” gain set (0.01 ft/s ΔV)

Command Input Axis	No. of 40 ms pulses	$\Delta\dot{X}$	$\Delta\dot{Y}$	$\Delta\dot{Z}$	Δp	Δq	Δr
		ft/s			deg/s		
+Y	11	-0.0018	+0.0102	-0.0005	-0.0001	-0.0060	-0.0065
-Y	11	-0.0018	-0.0102	-0.0005	+0.0001	-0.0060	+0.0065
+Z	8	-0.0006	-0.0003	+0.0098	-0.0004	-0.0037	+0.0045
-Z	8	-0.0006	-0.0003	-0.0098	+0.0003	+0.0037	+0.0045

Translation commands made in the X axis were not affected, since ΔV commands in that axis were accomplished by continuous firing of a balanced sets of four thrusters, resulting in no time-domain mixing and very little coupling into rotations.

Most of the evaluation pilots noted this additional workload, and downgraded their pilot ratings as a result. For this reason, the absolute CHRs and TLX values were adversely affected and should not be considered representative of the CEV control system, which has a better approach to time-domain multiplexing with much finer control over firing durations; unfortunately that control system was not available for this experiment.

Table 15: Velocity changes resulting from an incomplete **TDM RCS** pulse sequences: “B” gain set (0.002 ft/s ΔV)

Command Input Axis	No. of 40 ms pulses	$\Delta\dot{X}$	$\Delta\dot{Y}$	$\Delta\dot{Z}$	Δp	Δq	Δr
		ft/s			deg/s		
+Y	2	-0.0012	+0.0018	0	0	0	-0.0011
-Y	2	-0.0012	-0.0018	0	0	0	+0.0011
+Z	2	-0.0012	0	+0.0031	+0.0005	+0.0068	+0.0001
-Z	2	-0.0012	0	-0.0031	-0.0005	-0.0068	+0.0001

11 Conclusions

Pilot ratings were contaminated by excessive workload caused by an unintended \dot{X} decay from the **TDM** mixer implementation. The **TDM** mixer worked fairly well in Direct translational mode but caused this \dot{X} “braking effect” when used with Pulse translation mode, a test configuration change made based on comments by the final checkout pilot but not completely checked prior to the first evaluation pilot. As a result, the direct prediction of Cooper-Harper pilot ratings for a production vehicle could not be made from this experiment. However, the relative value of various control, display, mass properties and **RCS** variations may be inferred, as given below.

11.1 Task 1 - Stationary **ISS** docking

For this task, having the **RCAH** symbology made little handling qualities improvement possibly due to lack of compensation for residual angular motion of the **CEV**.

A 4% thrust variation, applied randomly to each **RCS** thruster, had only slightly perceptible but no significant effect for the two thruster variation sets evaluated.

Reducing angular rate dead-band by a factor of four in the **RCAH** controller showed promise; the need for a pre-calculated feed-forward mixer may thus be obviated at the expense of additional **RCS** propellant. In this experiment, the last 20 feet of docking task consumed 33% more **RCS** fuel.

Enlarging the attitude dead-band by a factor of two in the **RCAH** controller had no significant effect on handling qualities.

Lateral and vertical offsets of the spacecraft center of mass location of as much as 12 inches had only minor effect on handling qualities, but did show up in fuel consumed (up by about 10%).

The effect of feed-forward compensation was significant, despite the contamination of the “braking effect.” Median **CHR** degraded from Level One, with feed-forward enabled, to Level Two without feed-forward compensation. On the downside, fuel use increased about 18%.

Some improvement was seen when the Pulse mode symbology (and the inclusion of the innovative **ASI** indicator) was added to the six-degree-of-freedom, no attitude-hold, reversionary control system **CEV**.

When both feed-forward and Pulse mode symbology was added to the six-degree-of-freedom vehicle, a clear improvement in handling qualities was seen, as much as a full **CHR** rating point, with only minimal increase in propellant consumption. Expecting to have both operable displays and feed-forward mixing without attitude hold would be an unusual circumstance, however.

A full Cooper-Harper Level improvement was seen between the unaugmented [CEV](#) and a baseline [CEV](#) with feed-forward and an operable [RCAH](#) in the stationary target docking task.

11.2 Task 2 - Rotating target docking

These initial evaluations of docking a baseline [CEV](#) with a rotating target indicate this is a difficult task. Only in the most fortuitous circumstances could one expect the target to be exhibiting rotation only about the Y_{bar} axis (pure pitch), which was still judged to be a Level One/Two task. With any inertial yawing component (roll component was not evaluated) the task became solid Level Two/Three despite some automation (e.g. symbology and rate-command, [LVLH](#) attitude hold autopilot). Interestingly, increasing the target rotational rate by 40% had only a minimal increase of perceived workload.

Some additional control compensation or machine-vision automation may be required to make docking with an uncooperative target Level Two or better.

12 References

References

1. H. G. Hatch, Jr.; Riley, D. R.; and Cobb, J.B.: Simulating Gemini-Agena Docking. *Astronautics and Aeronautics*, volume 2(11):pp. 74–81, November 1964.
2. Jaquet, B. M. and Riley, D. R.: An Evaluation of Gemini Hand Controllers and Instruments for Docking. Technical Report NASA TM X-1066, 1965.
3. E. R. Long, Jr.; Pennington, J. E.; and Deal, P. L.: Remote Pilot-Controlled Docking With Television. Technical Report NASA TN D-3044, October 1965.
4. Pennington, J. E.; H. G. Hatch, Jr.; Long, E. R.; and Cobb, J. B.: Visual Aspects of a Full-Size Pilot-Controlled Simulation of the Gemini-Agena Docking. Technical Report NASA TN D-2632, 1965.
5. Riley, D. R.; Jaquet, B. M.; Bardusch, R. E.; and Deal, P. L.: A Study of Gemini-Agena Docking Using a Fixed-Base Simulator Employing a Closed-Circuit Television System. Technical Report NASA TN D-3112, 1965.
6. Riley, D. R.; Jaquet, B. M.; Pennington, J. E.; and Brissenden, R. F.: Comparison of Results of Two Simulations Employing Full-Size Visual Cues For Pilot-Controlled Gemini-Agena Docking. Technical Report NASA TN D-3687, 1966.
7. Riley, D. R.; Jaquet, B. M.; and Cobb, J. B.: Effect of Target Angular Oscillations on Pilot-Controlled Gemini-Agena Docking. Technical Report NASA TN D-3403, 1966.
8. Anon.: System Requirements for the Orion System. Technical Report NASA CxP 72000, Rev. A, June 2007.
9. Bailey, Randall E.; Jackson, E. Bruce; Goodrich, Kenneth H.; Ragsdale, W. A.; Neuhaus, Jason; and Barnes, Jim: Initial Investigation of Reaction Control System Design on Spacecraft Handling Qualities for Earth Orbit Docking. In *AIAA Atmospheric Flight Mechanics Conference*, AIAA Paper 2008-6553, Honolulu, Hawaii, August 2008.
10. Anon.: Orion Vehicle Simulation Data Book, Issue 1, Revision A. Technical Report CEV-MA-07-003, January 2008.
11. Leslie, R.; Geyer, D.; Cunningham, K.; Madden, M.; Kenny, P.; and Glaab, P.: LaSRS++: An Object-Oriented Framework for Real-Time Simulation of Aircraft. AIAA Paper 98-4529, August 1998.
12. Smith, R. M.: A Description of the Cockpit Motion Facility and the Research Flight Deck Simulator. In *AIAA Guidance and Control Conference*, AIAA Paper 2000-4174, Denver, Colorado, August 2000.
13. Cheng, Betty H. C. and Auernheimer, Brent: Applying Formal Methods and Object-Oriented Analysis to existing Flight Software. In *Proc. of 18th Annual NASA Software Engineering Workshop*, pp. 274–278, December 1993.
14. Mueller, Eric; Bilimoria, Karl; and Frost, Chad: Handling Qualities Evaluation for Spacecraft Docking in Low Earth Orbit. AIAA Paper 2008-6832, August 2008.
15. Wie, Bong: *Space Vehicle Dynamics and Control*. Reston: American Institute of Aeronautics and Astronautics, 1998, ISBN 1-56347-261-9.

16. Cooper, G. E. and R. P. Harper, Jr.: Use of Pilot Rating in the Evaluation of Aircraft Handling Qualities. Technical Report NASA TN D-5153, April 1969.
17. Likert, Rensis: A Technique for the Measurement of Attitudes. *Archives of Psychology*, volume 140:pp. 1–55, 1932.
18. Hart, S. G. and Staveland, L. E.: Development of NASA-TLX (Task Load Index): Results of Empirical and Theoretical Research. In P. A. Hancock and N. Meshkati, eds., *Human Mental Workload*, pp. 129–183, Amsterdam: North-Holland, 1988.
19. Anon.: Constellation Program System Requirements for the Orion System. Technical Report NASA CxP 72000, Revision A, August 2007.
20. Anon.: NSTS Shuttle Reference Manual. <http://science.ksc.nasa.gov/shuttle/technology/sts-newsref/sts-hrc.html>, 1988.
21. Kirchwey, Christopher R. and Saket, Lester L.: Stability of the Shuttle On-Orbit Flight Control System for a Class of Flexible Payloads. AIAA paper 83-2178, 1983.

Appendix A

Metrical Data Plots

This appendix contains comparisons of pilot opinions and performance metrics for a baseline configuration versus some configuration variation relative to that baseline configuration. Individual pilot values are connected by a line, allowing for per-pilot comparison as well as general trends between the baseline and variant configurations.

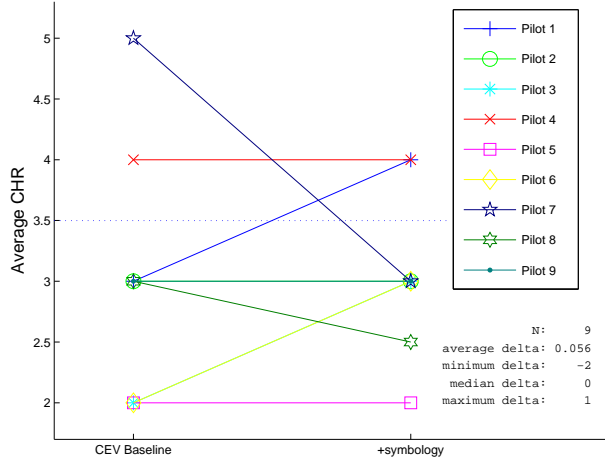
The plots are all in the same order:

- (a) Cooper-Harper pilot opinion rating ([CHR](#))
- (b) Fuel consumed during docking maneuver, lbm
- (c) Number of seconds between final pilot input and docking
- (d) Number of discrete pilot inputs during maneuver
- (e) Docking-ring-to-docking-ring centers offset, in docking plane, inches
- (f) Docking axis misalignment, degrees
- (g) Relative velocity across docking plane at moment of docking, ft/s
- (h) Rate of closure at moment of docking, ft/s
- (i) Pilot's opinion of mental task load ([TLX](#)), 0-100, where 0 is low and 100 is high
- (j) Pilot's opinion of temporal demand, 0-100, where 0 is low and 100 is high
- (k) Pilot's opinion of amount of frustration, 0-100, where 0 is low and 100 is high
- (l) Pilot's opinion of overall effort required, 0-100, where 0 is low and 100 is high

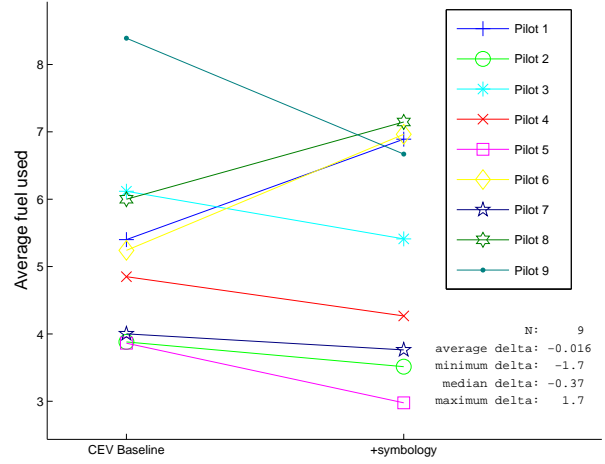
Figures A1 through A10 compare variants against a nominal [CEV](#) baseline configuration. Figures A11 through A14 compare variants against a reversionary control, six-degree-of-freedom, [CEV](#).

In sub-figure (a) of each figure (the Cooper-Harper pilot rating), a dotted line is drawn at CHR 3.5 to distinguish between Level 1 (CHR 1-3) and Level 2 (CHR 4-6) ratings; a dashed line is drawn at CHR 6.5, when appropriate, to distinguish between Level 2 and Level 3 (CHR 7+) ratings.

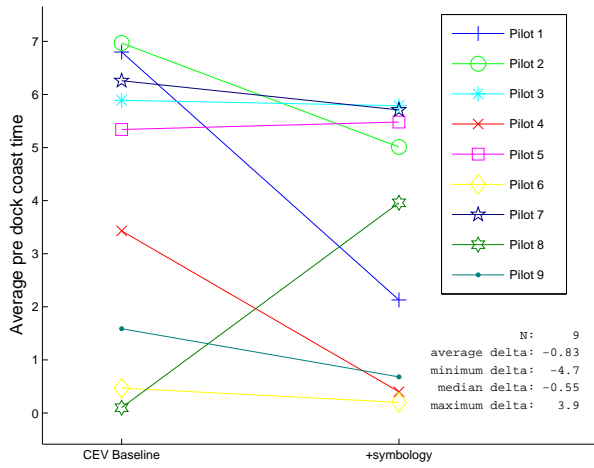
In other sub-figures (e, f, g and h), where appropriate, a dotted line shows the limit of desired performance and a dashed line shows the limit of adequate performance found in table 4. If no line appears, all the results were within desired performance bounds.



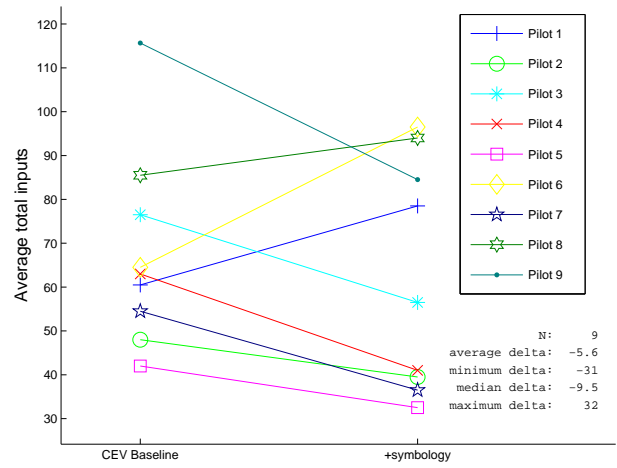
(a) Cooper-Harper rating



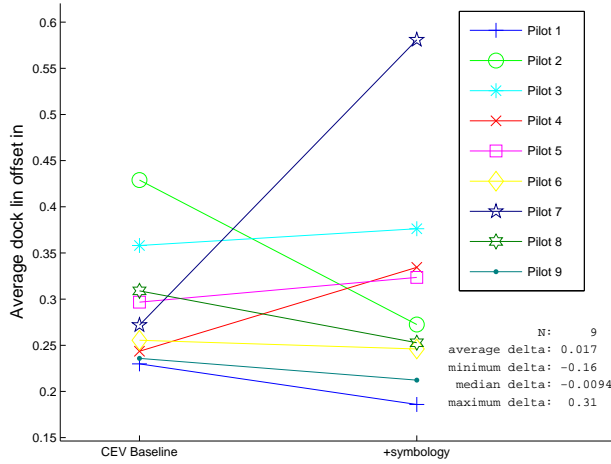
(b) Fuel use, lbm



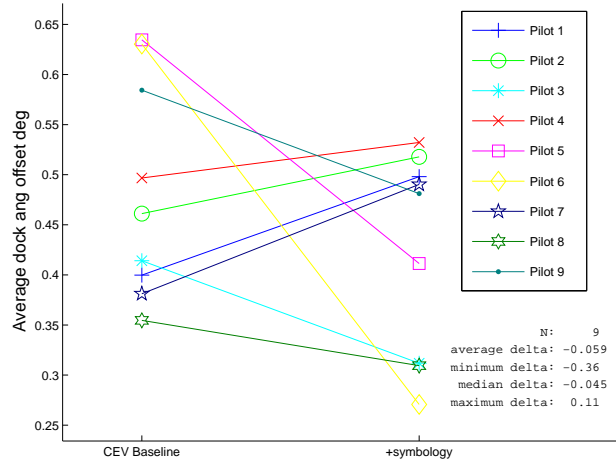
(c) Pre-dock coast time, s



(d) Number of pilot control inputs

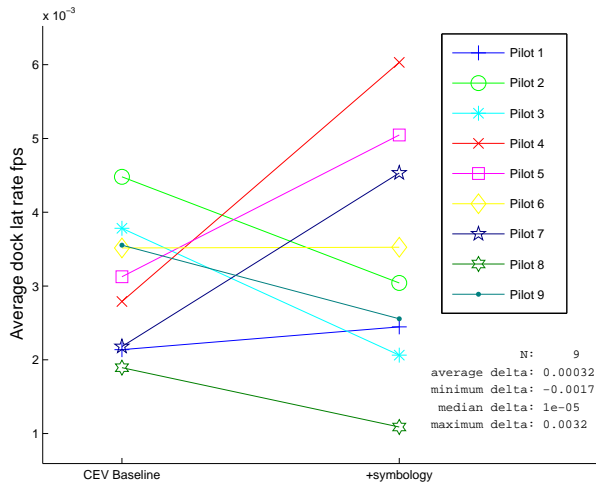


(e) Docking offset, in

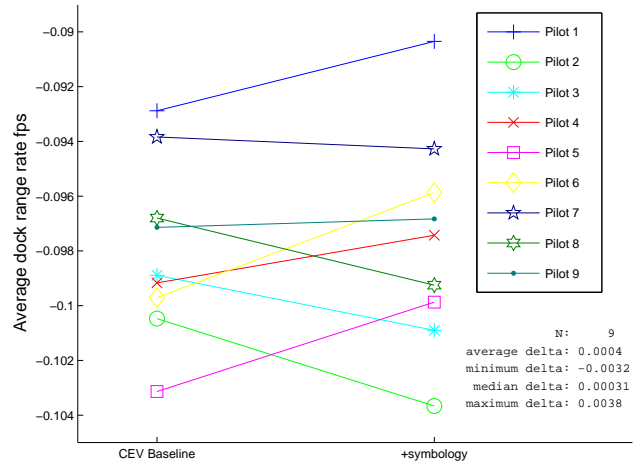


(f) Docking alignment, deg

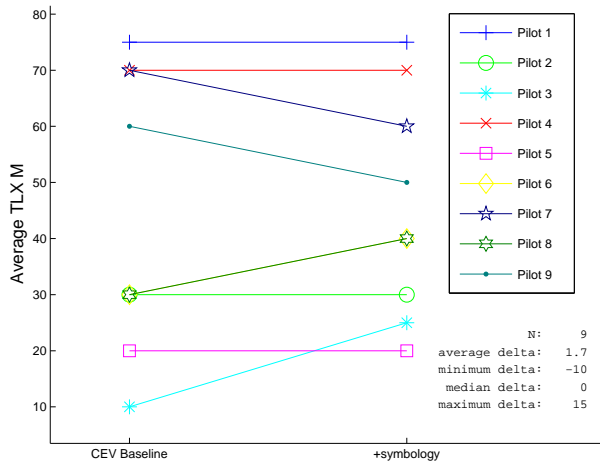
Figure A1: Effect of additional display symbology on baseline CEV



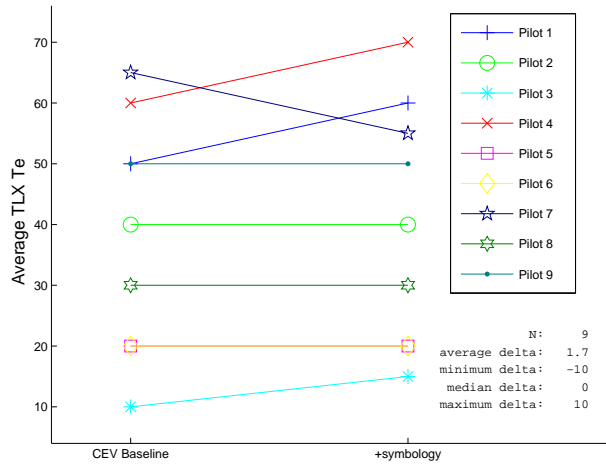
(g) Motion across dock face at dock, ft/s



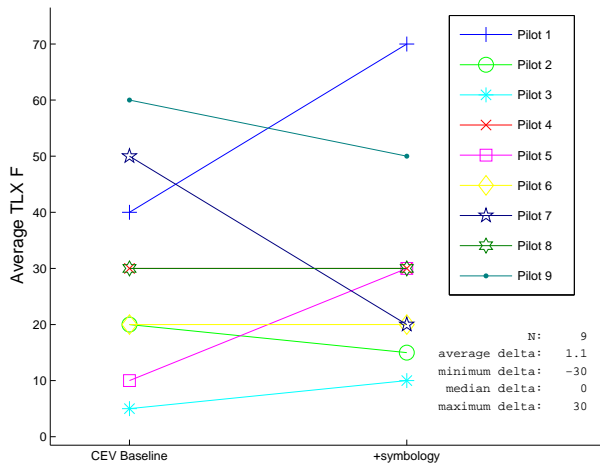
(h) Range rate at dock, ft/s



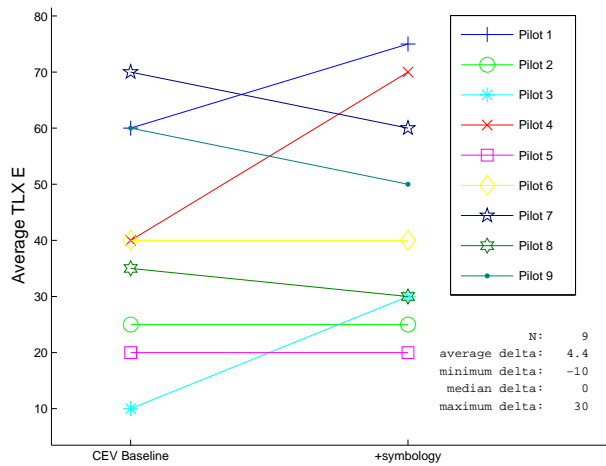
(i) Mental task load



(j) Temporal task load

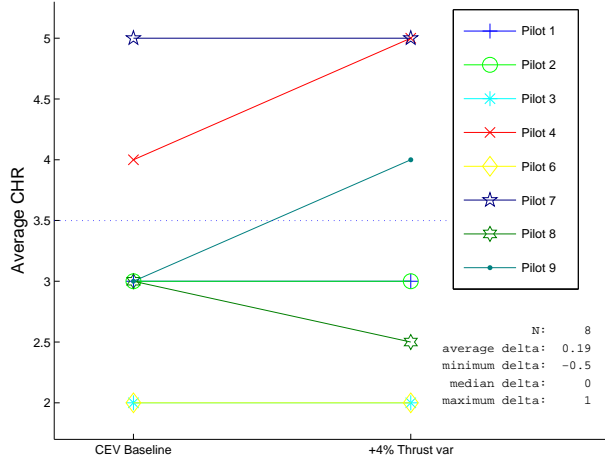


(k) Frustration

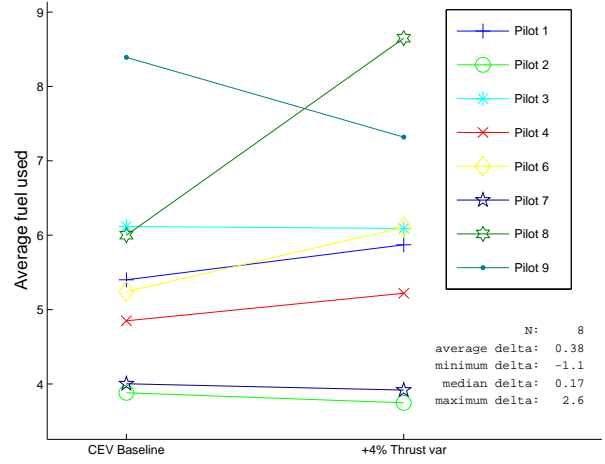


(l) Effort

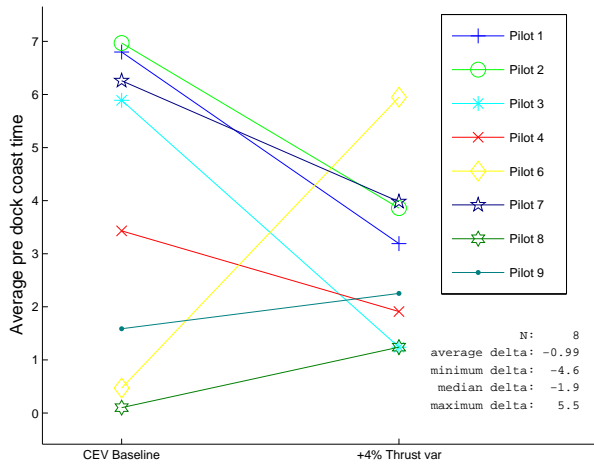
Figure A1: Effect of additional display symbology on baseline CEV (concluded).



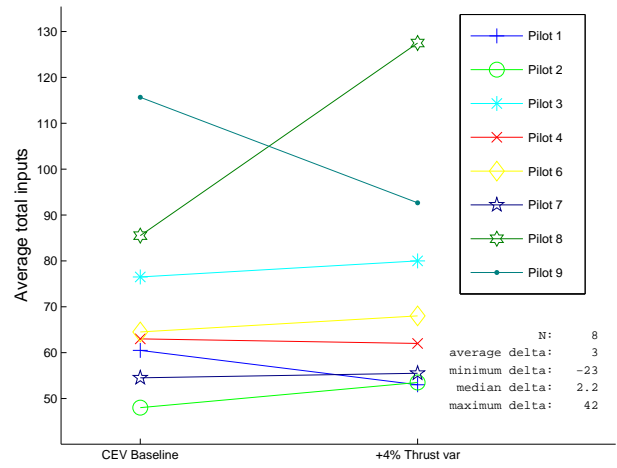
(a) Cooper-Harper rating



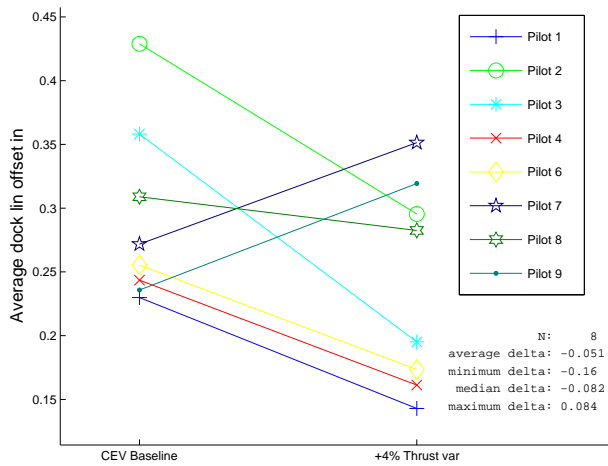
(b) Fuel use, lbm



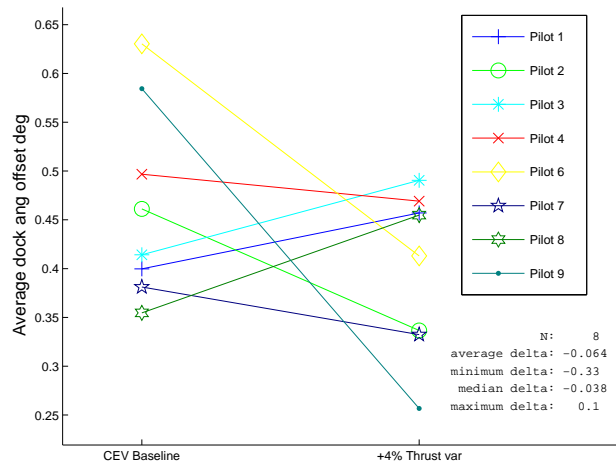
(c) Pre-dock coast time, s



(d) Number of pilot control inputs

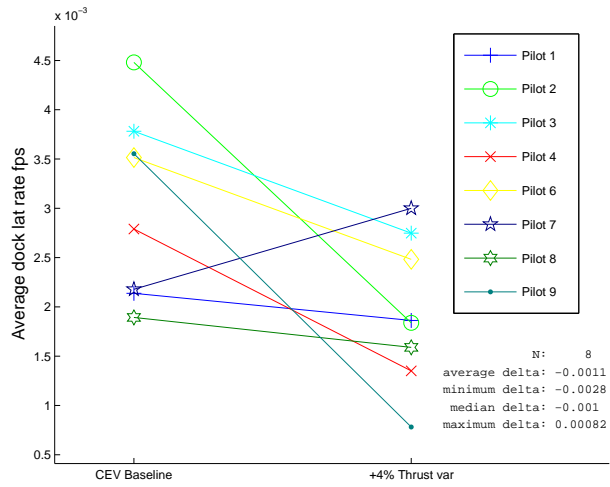


(e) Docking offset, in

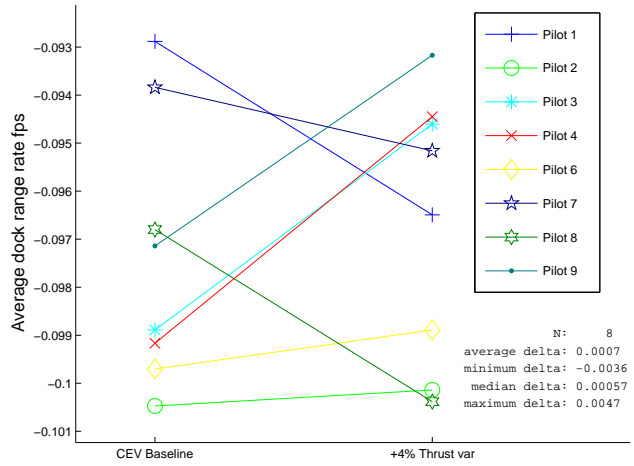


(f) Docking alignment, deg

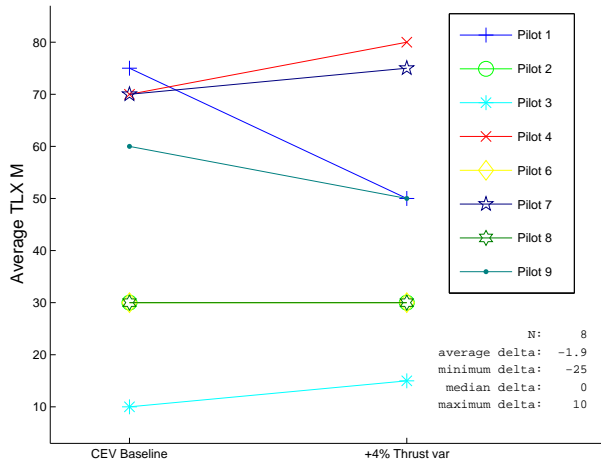
Figure A2: Effect of 4% random thrust variation on baseline CEV



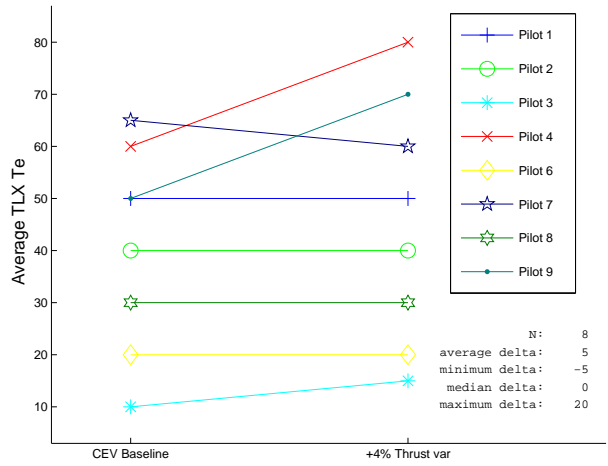
(g) Motion across dock face at dock, ft/s



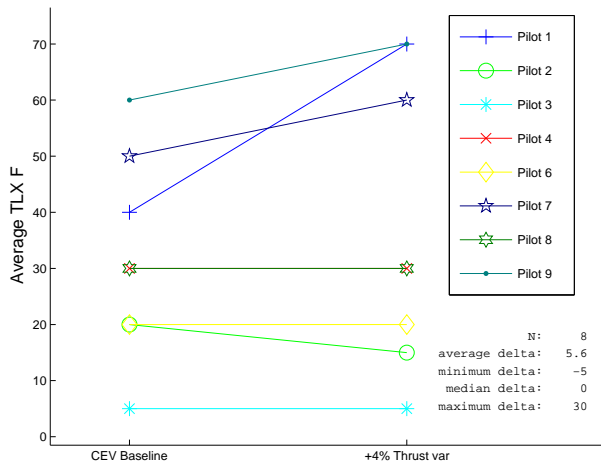
(h) Range rate at dock, ft/s



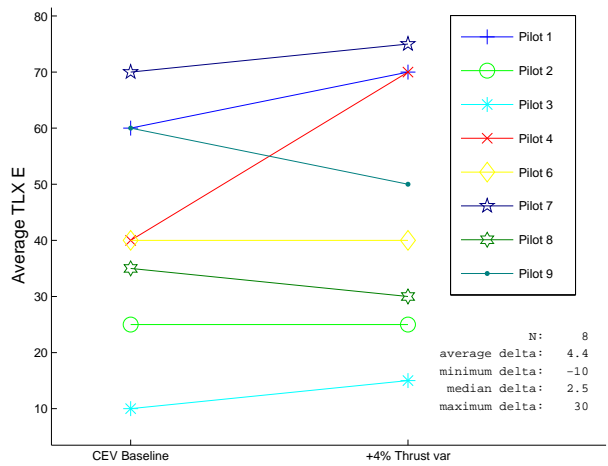
(i) Mental task load



(j) Temporal task load

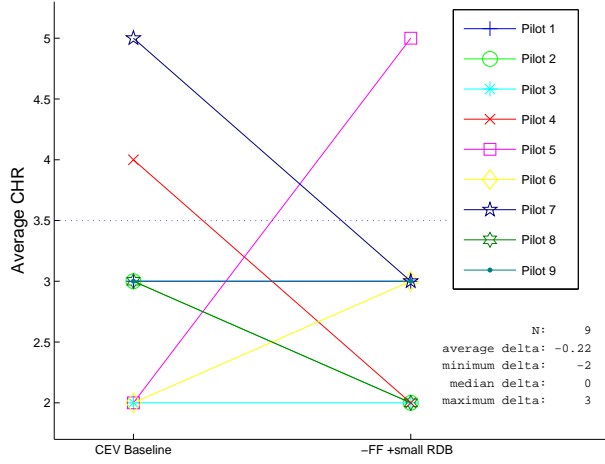


(k) Frustration

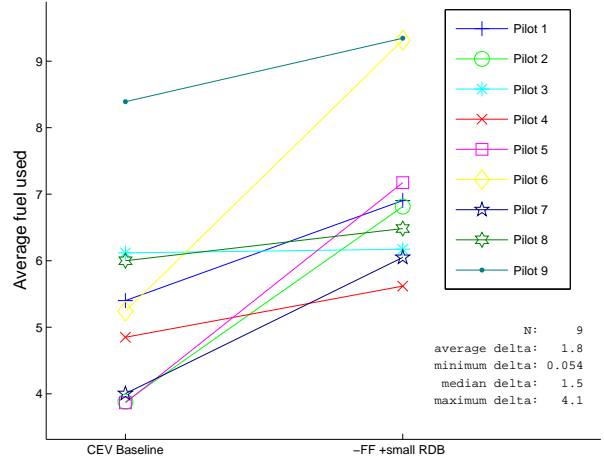


(l) Effort

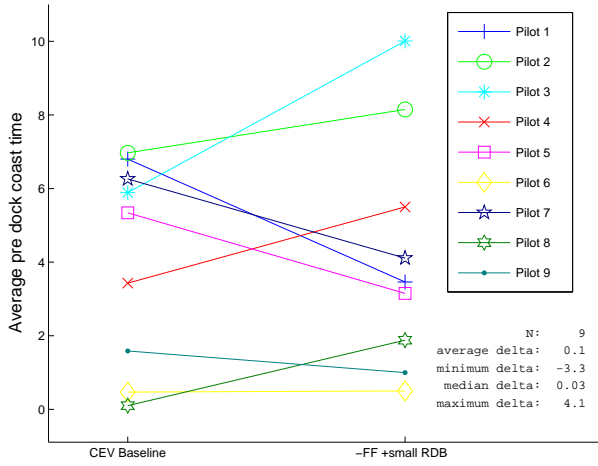
Figure A2: Effect of 4% random thrust variation on baseline CEV (concluded)



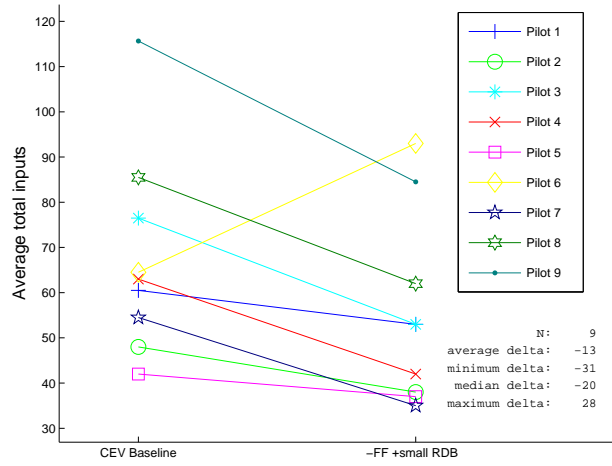
(a) Cooper-Harper rating



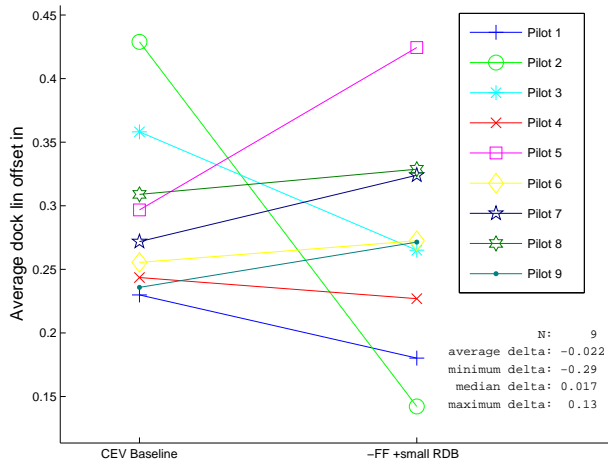
(b) Fuel use, lbm



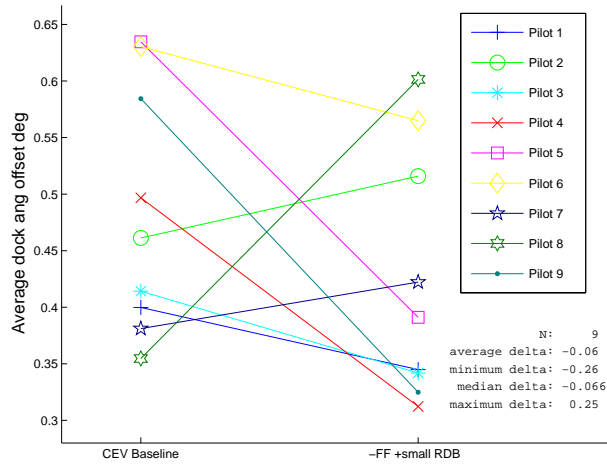
(c) Pre-dock coast time, s



(d) Number of pilot control inputs

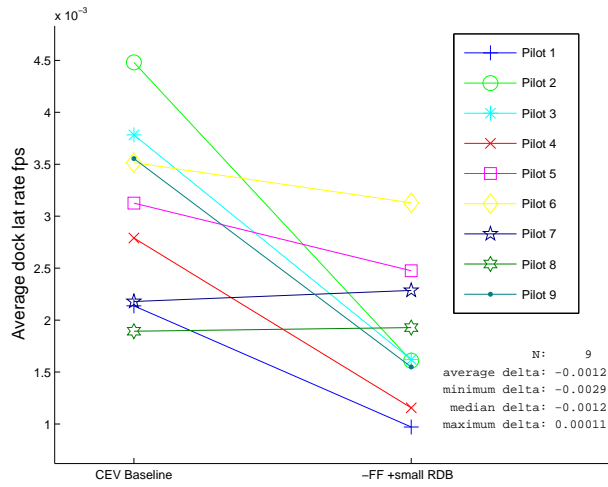


(e) Docking offset, in

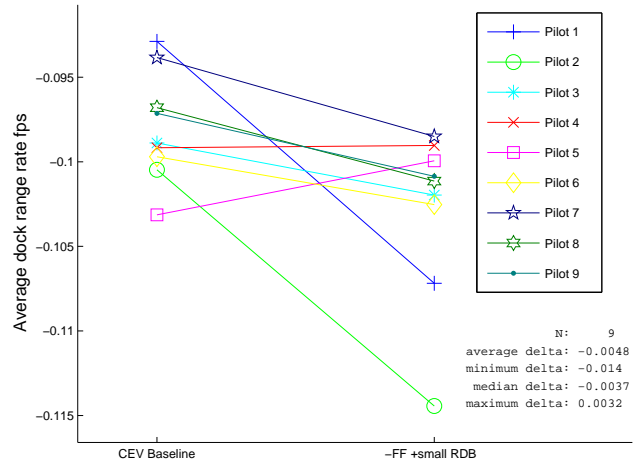


(f) Docking alignment, deg

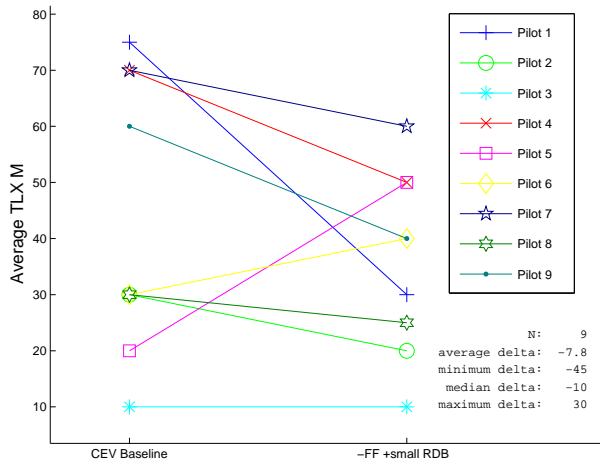
Figure A3: Effect of smaller rate deadband and feed-forward mixer off vs. baseline CEV



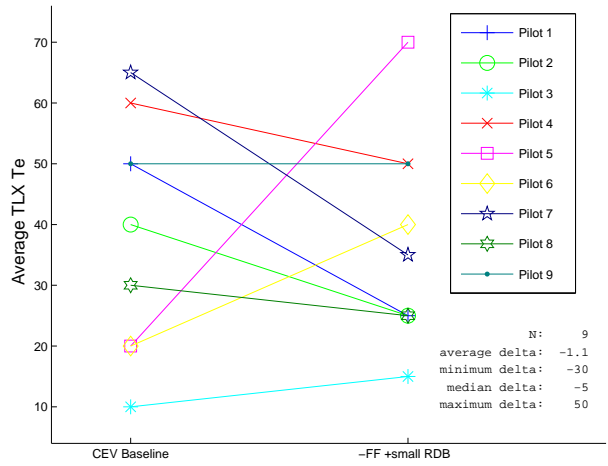
(g) Motion across dock face at dock, ft/s



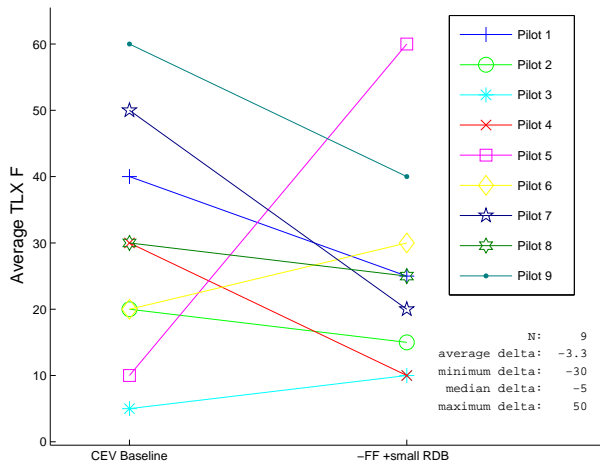
(h) Range rate at dock, ft/s



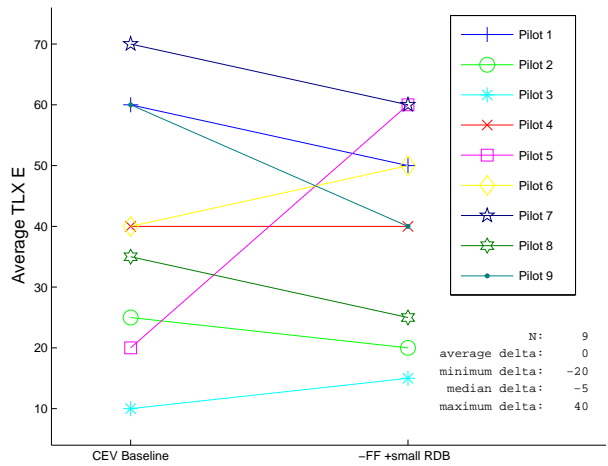
(i) Mental task load



(j) Temporal task load

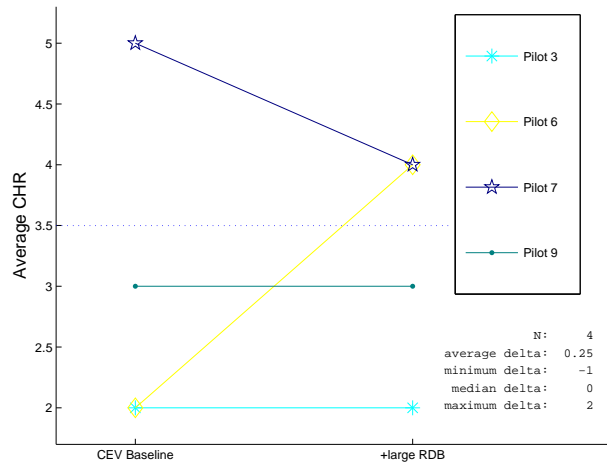


(k) Frustration

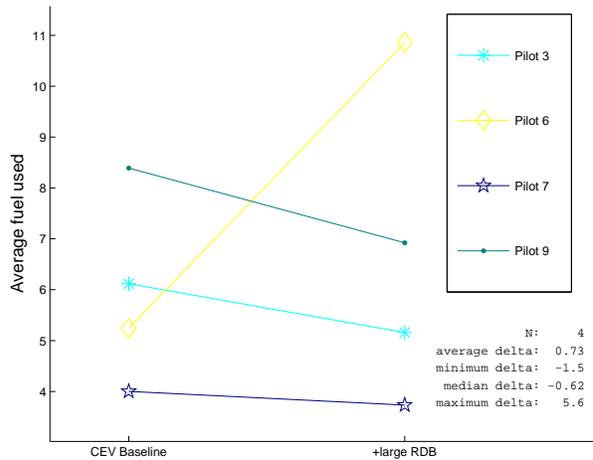


(l) Effort

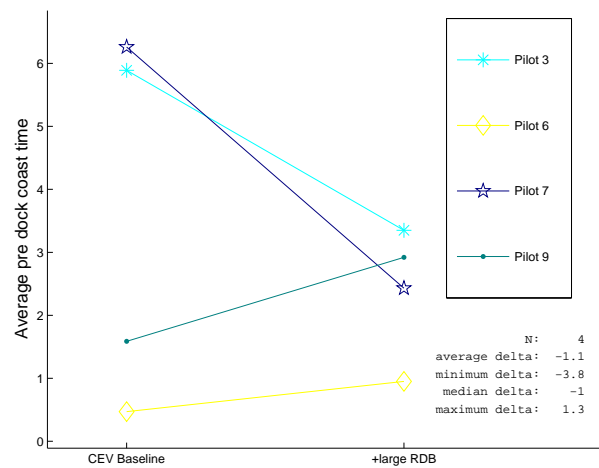
Figure A3: Effect of smaller rate deadband and feed-forward mixer off vs. baseline CEV (concluded)



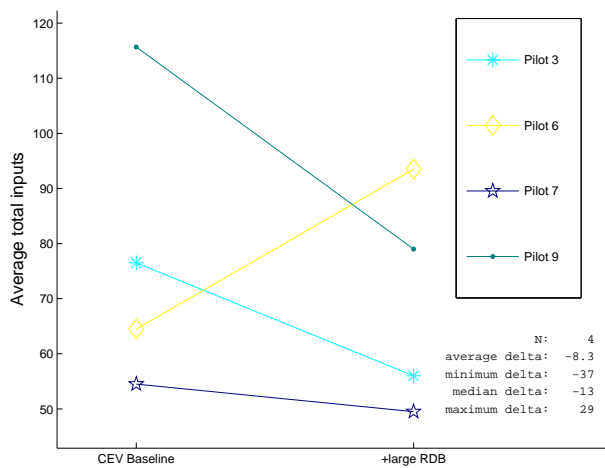
(a) Cooper-Harper rating



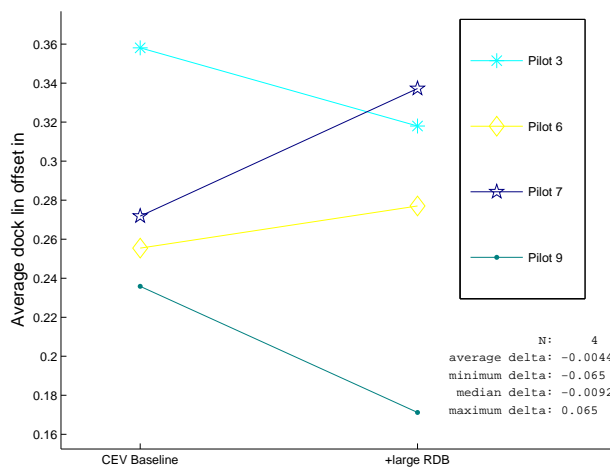
(b) Fuel use, lbm



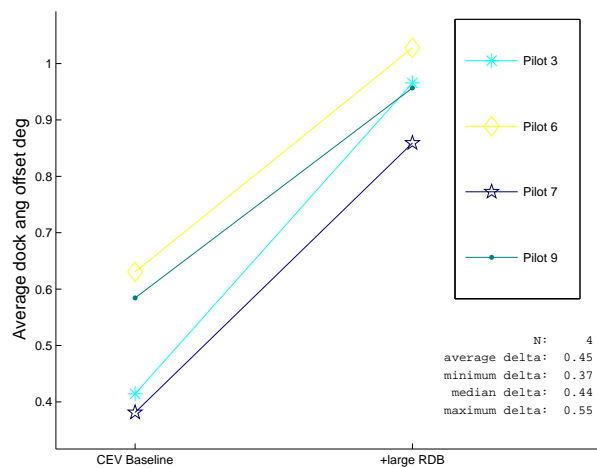
(c) Pre-dock coast time, s



(d) Number of pilot control inputs

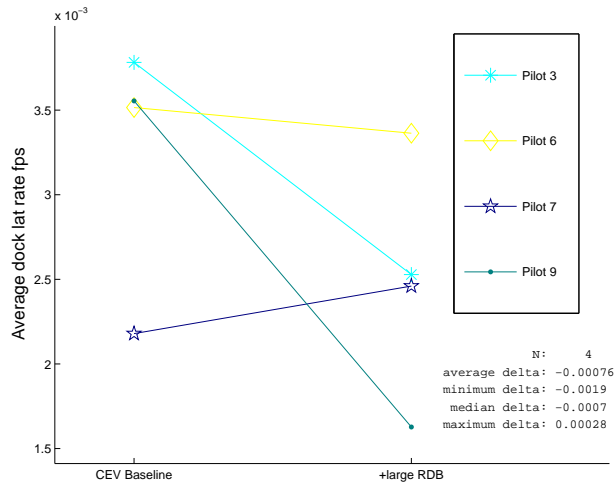


(e) Docking offset, in

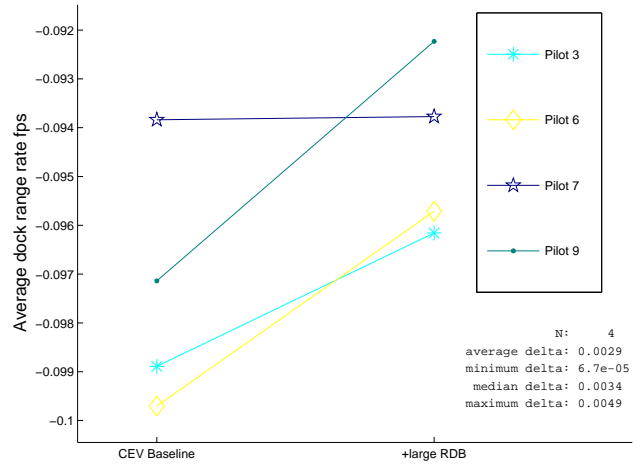


(f) Docking alignment, deg

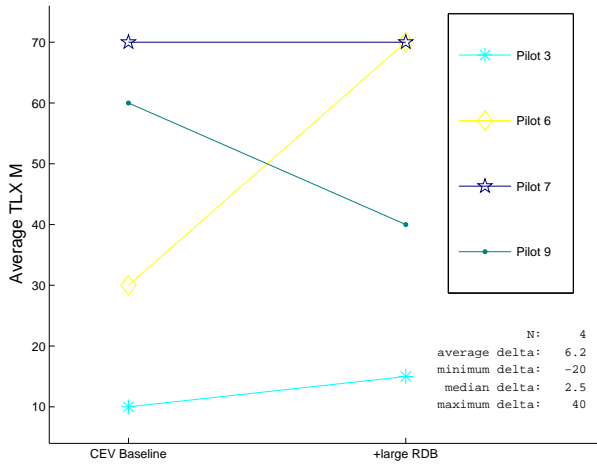
Figure A4: Effect of larger attitude deadband vs. baseline CEV



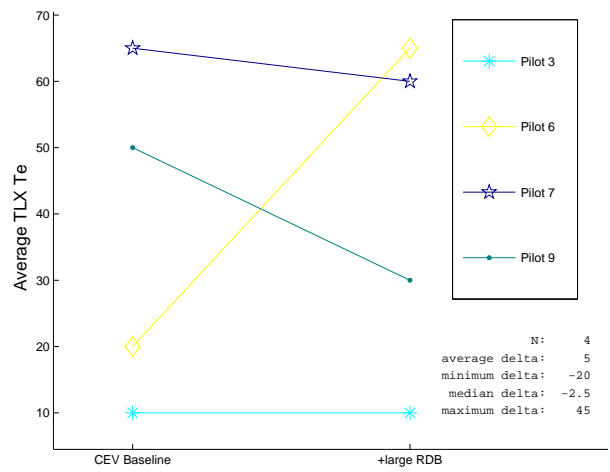
(g) Motion across dock face at dock, ft/s



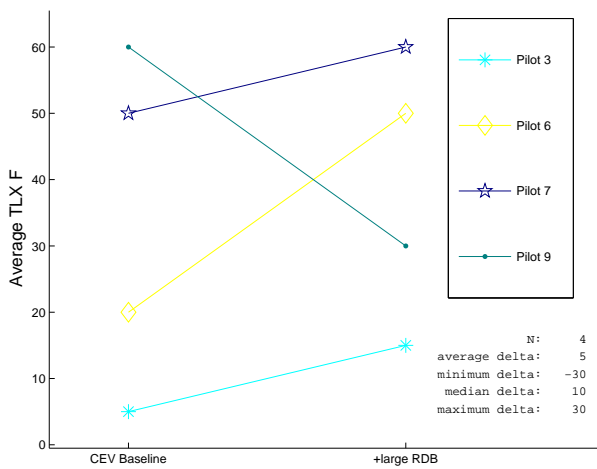
(h) Range rate at dock, ft/s



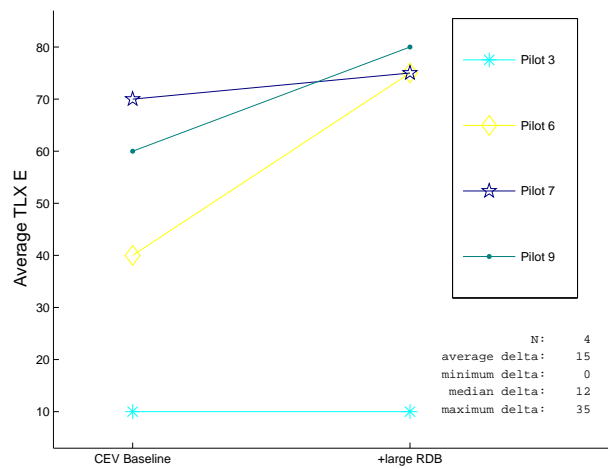
(i) Mental task load



(j) Temporal task load

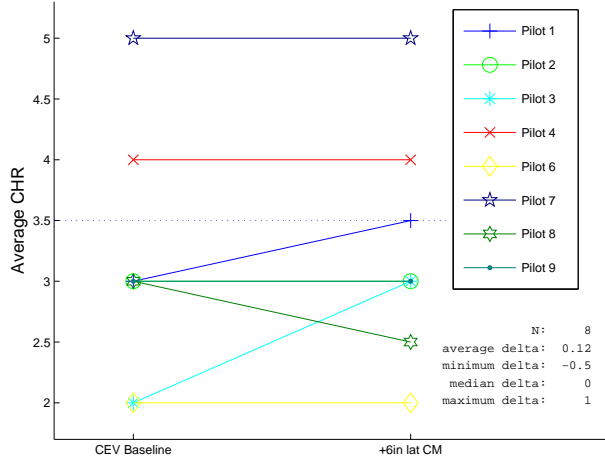


(k) Frustration

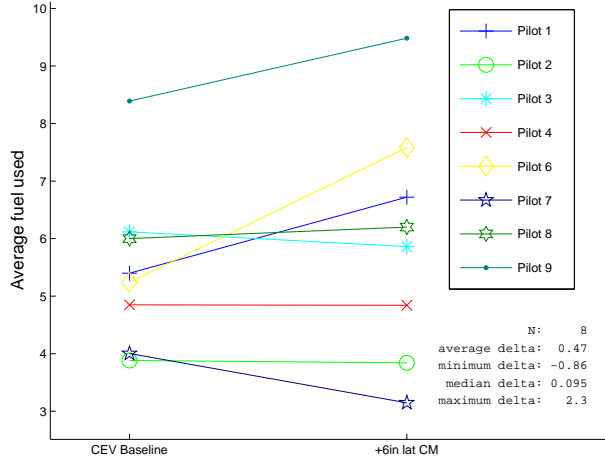


(l) Effort

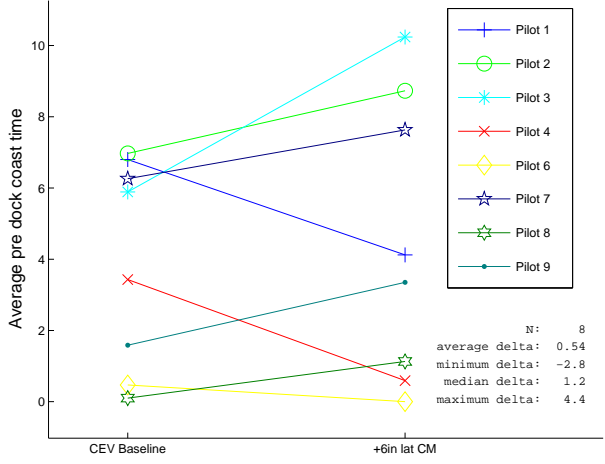
Figure A4: Effect of larger attitude dead-band vs. baseline CEV (concluded)



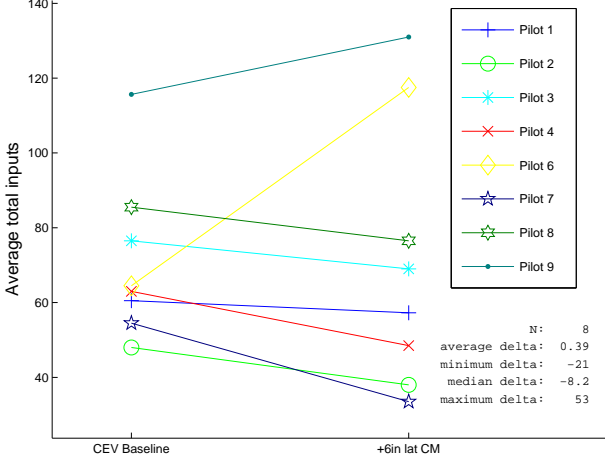
(a) Cooper-Harper rating



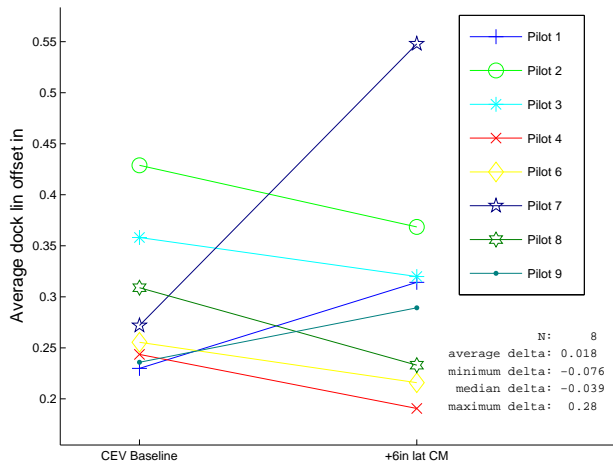
(b) Fuel use, lbm



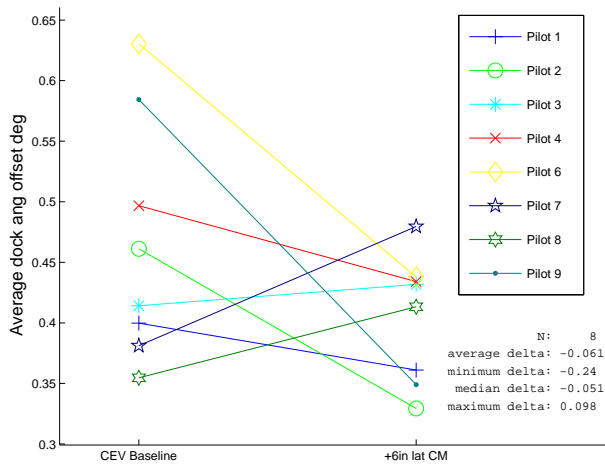
(c) Pre-dock coast time, s



(d) Number of pilot control inputs

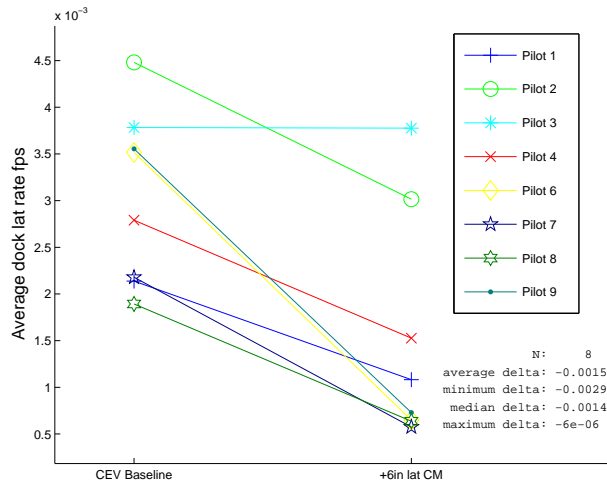


(e) Docking offset, in

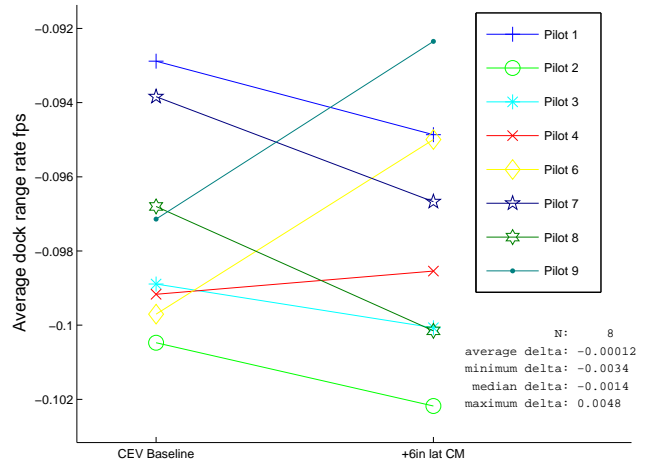


(f) Docking alignment, deg

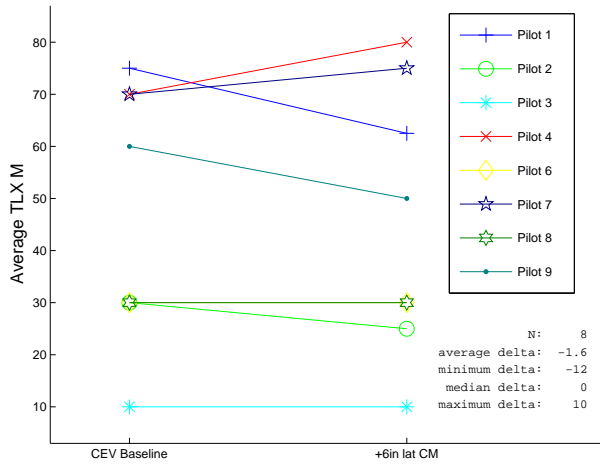
Figure A5: Effect of six-inch lateral CM offset on baseline CEV



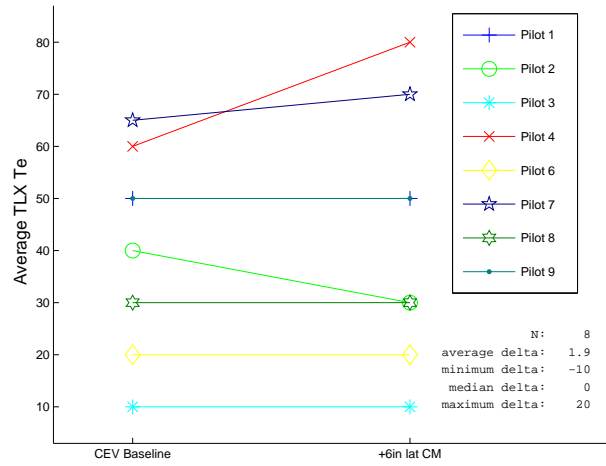
(g) Motion across dock face at dock, ft/s



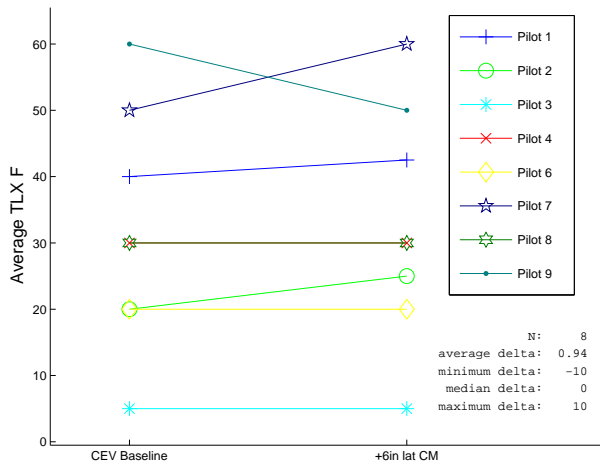
(h) Range rate at dock, ft/s



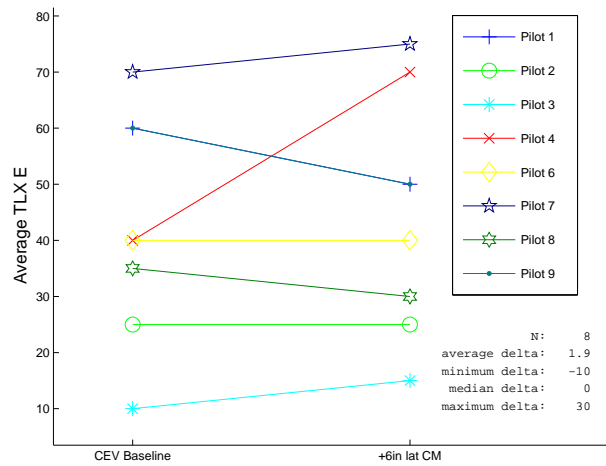
(i) Mental task load



(j) Temporal task load

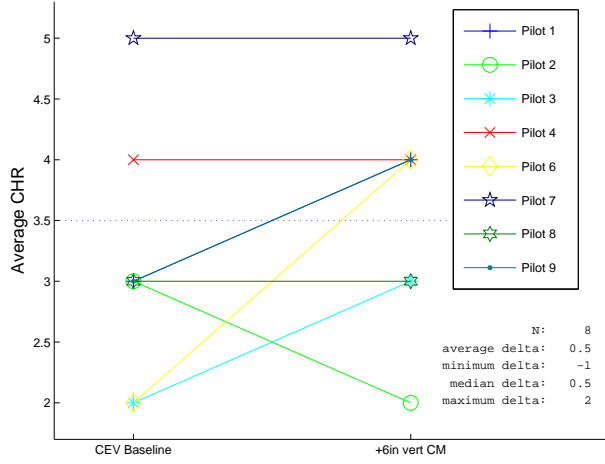


(k) Frustration

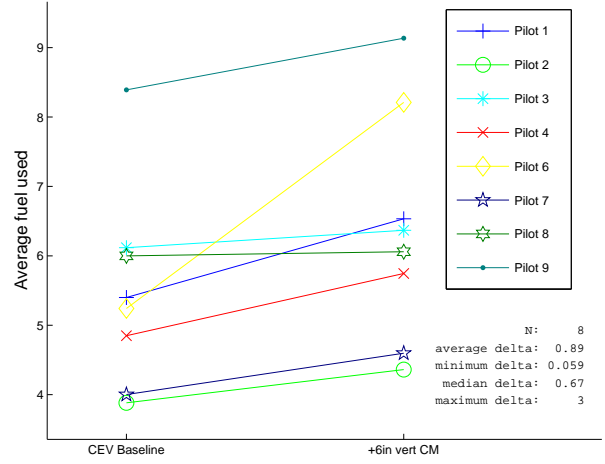


(l) Effort

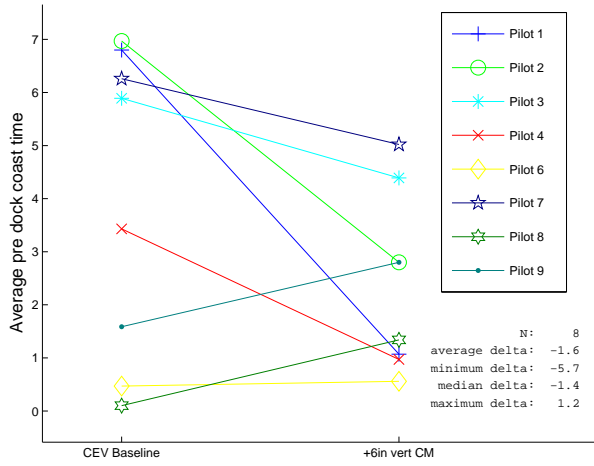
Figure A5: Effect of six-inch lateral CM offset on baseline CEV (concluded)



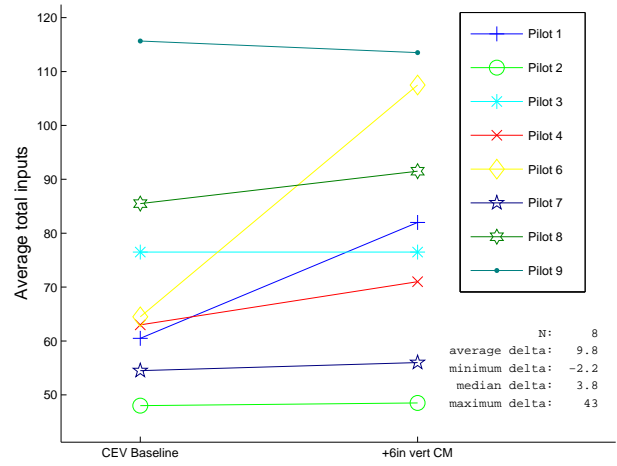
(a) Cooper-Harper rating



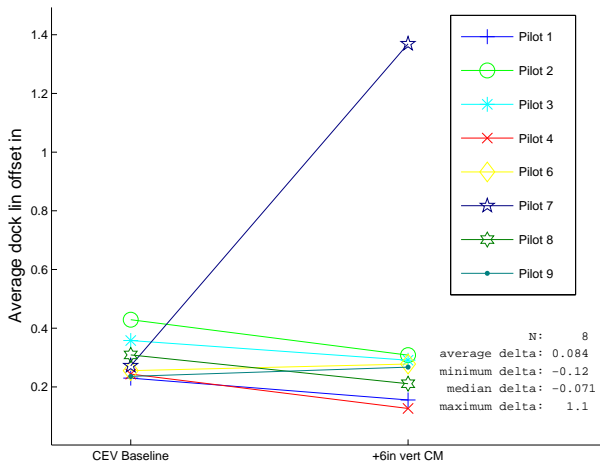
(b) Fuel use, lbm



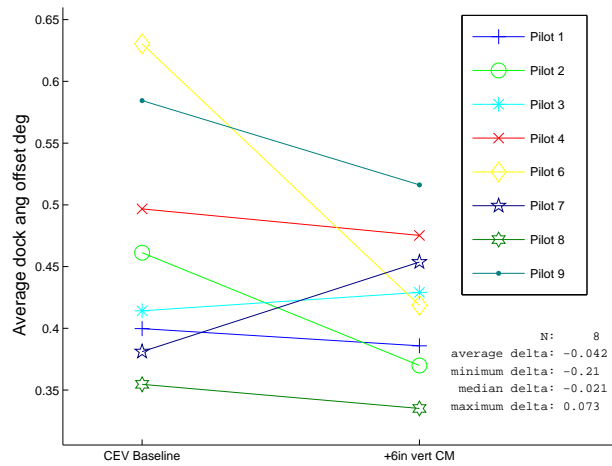
(c) Pre-dock coast time, s



(d) Number of pilot control inputs

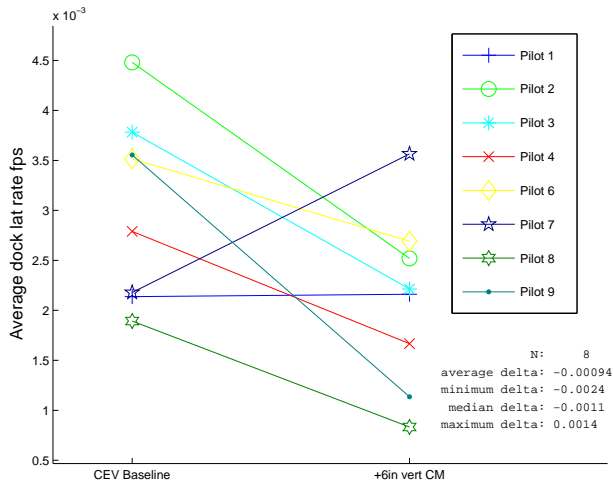


(e) Docking offset, in

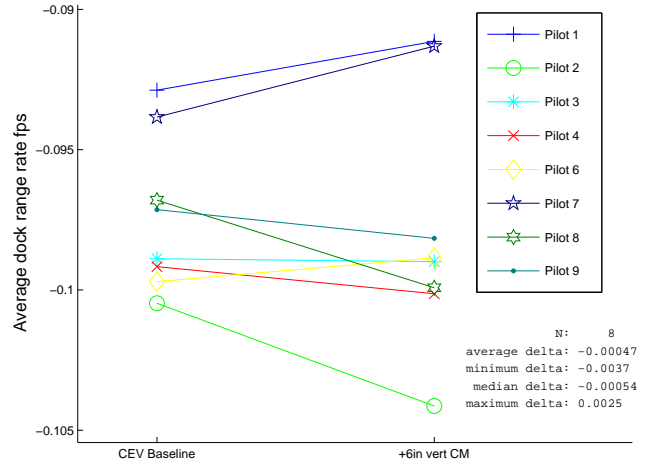


(f) Docking alignment, deg

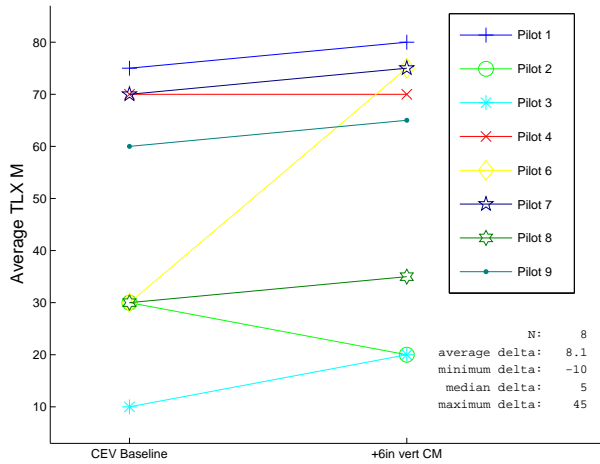
Figure A6: Effect of six-inch vertical CM offset on baseline CEV



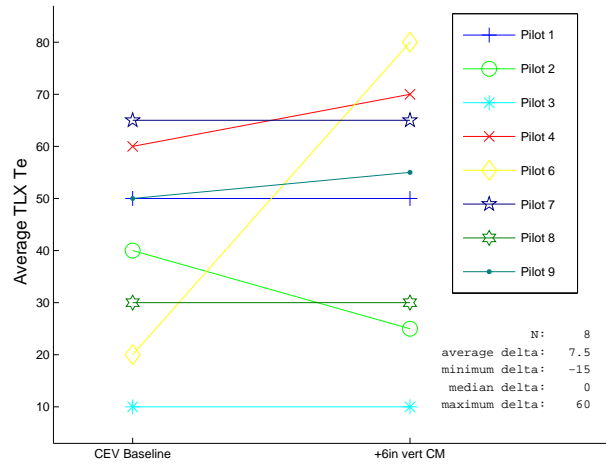
(g) Motion across dock face at dock, ft/s



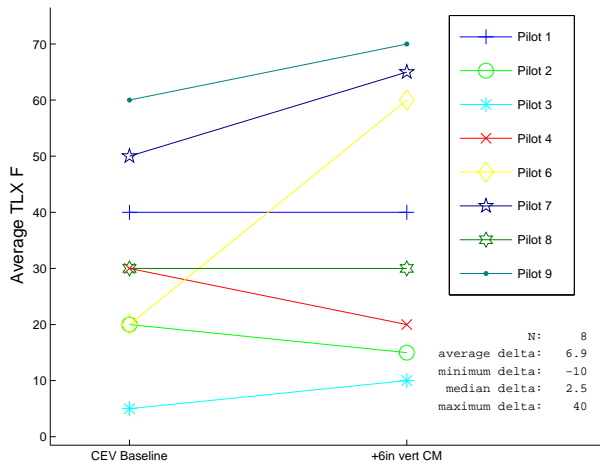
(h) Range rate at dock, ft/s



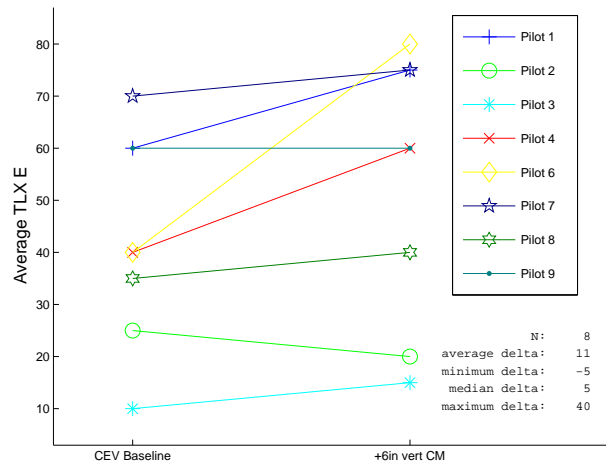
(i) Mental task load



(j) Temporal task load

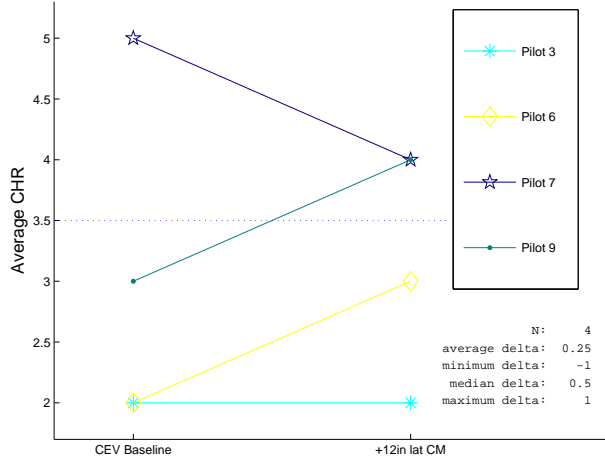


(k) Frustration

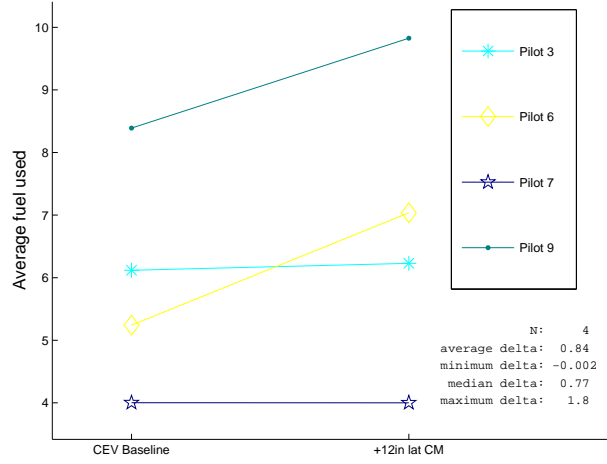


(l) Effort

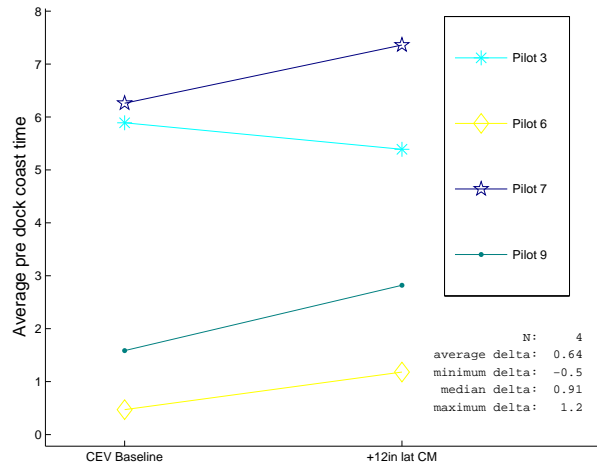
Figure A6: Effect of six-inch vertical CM offset on baseline CEV (concluded)



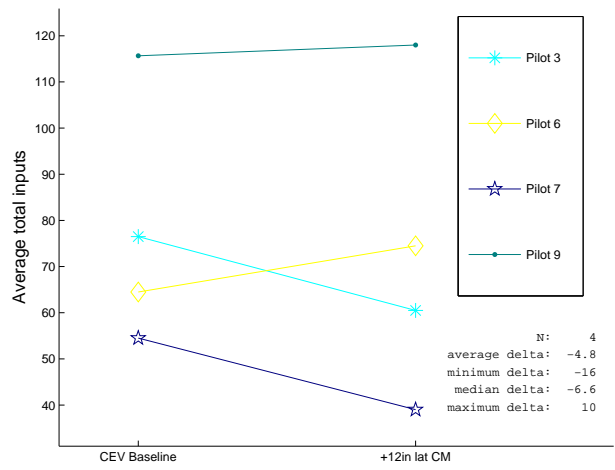
(a) Cooper-Harper rating



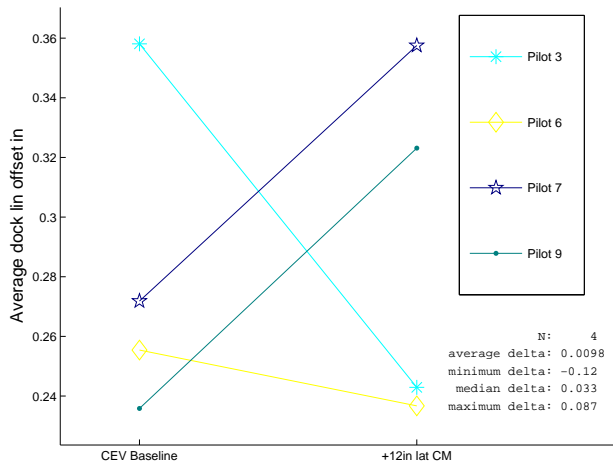
(b) Fuel use, lbm



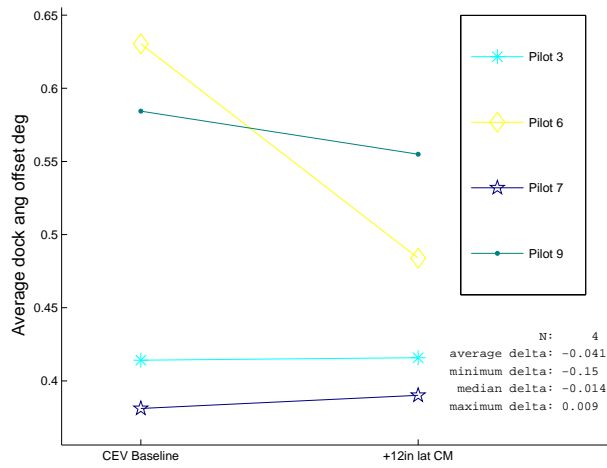
(c) Pre-dock coast time, s



(d) Number of pilot control inputs

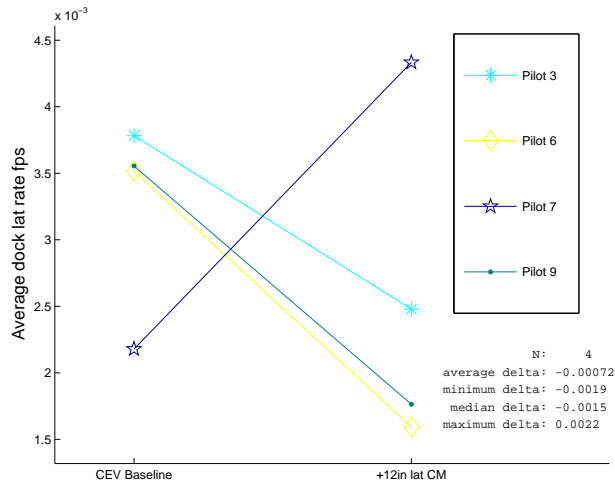


(e) Docking offset, in

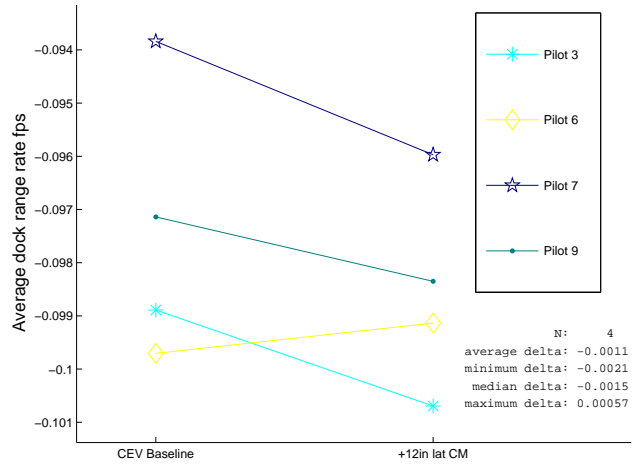


(f) Docking alignment, deg

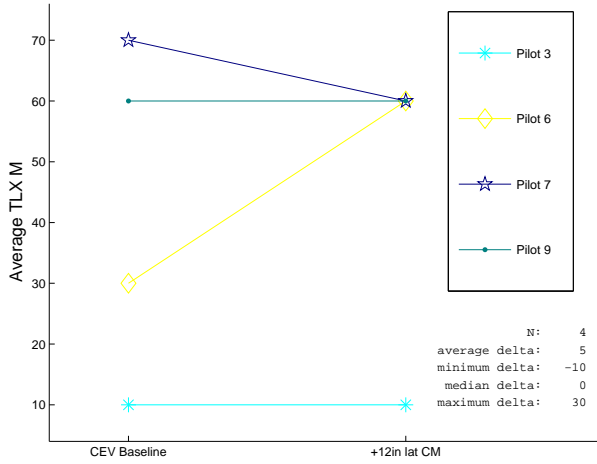
Figure A7: Effect of 12-inch lateral CM offset on baseline CEV



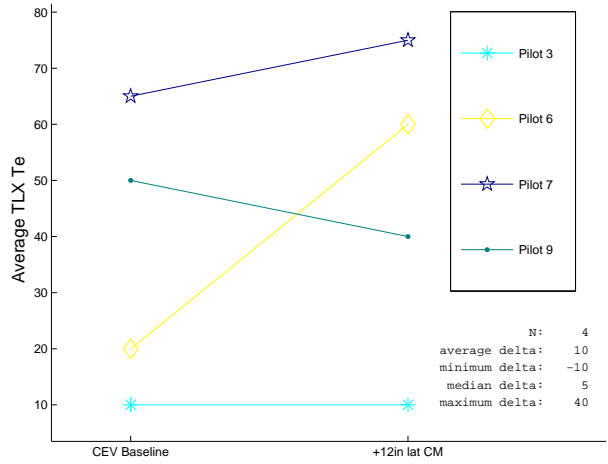
(g) Motion across dock face at dock, ft/s



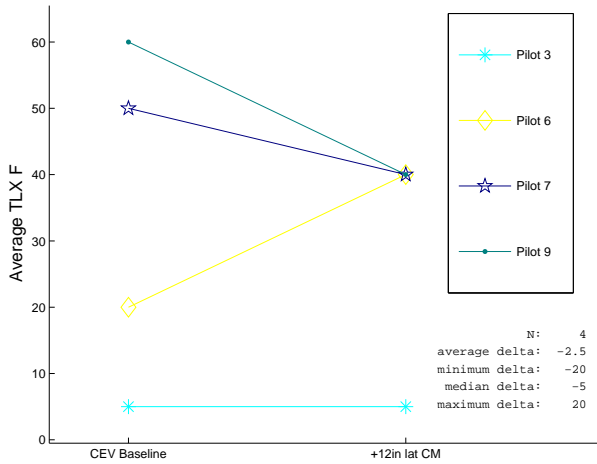
(h) Range rate at dock, ft/s



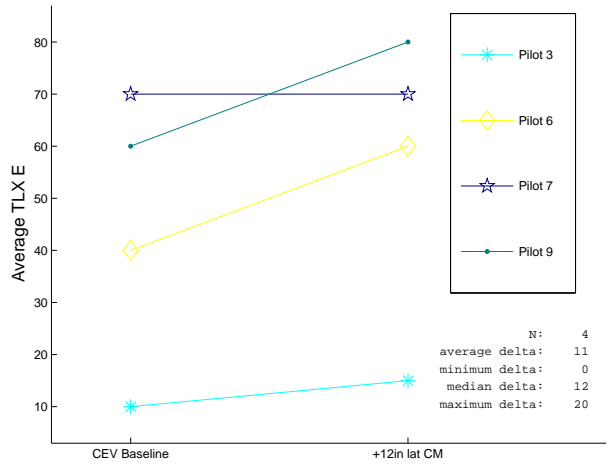
(i) Mental task load



(j) Temporal task load

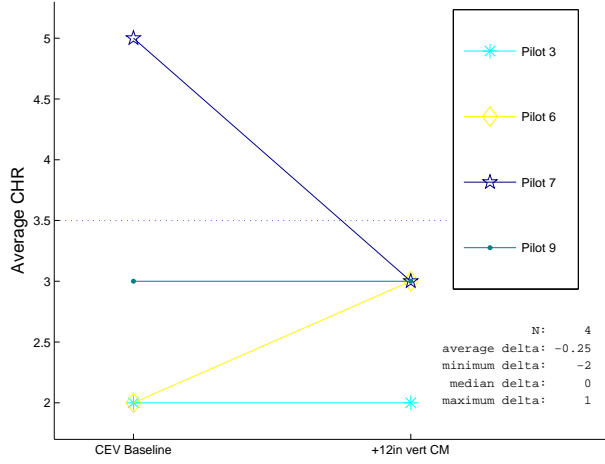


(k) Frustration

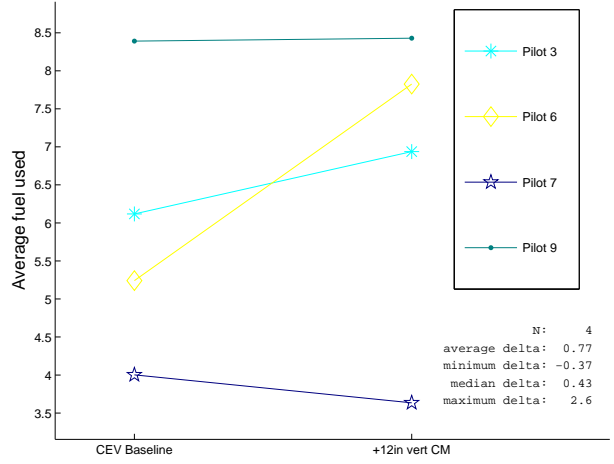


(l) Effort

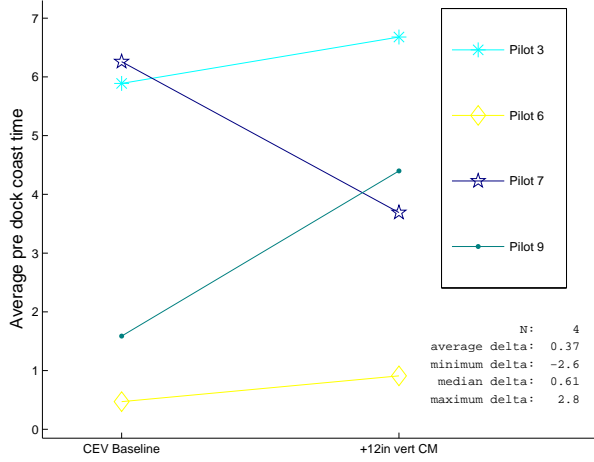
Figure A7: Effect of 12-inch lateral CM offset on baseline CEV (concluded)



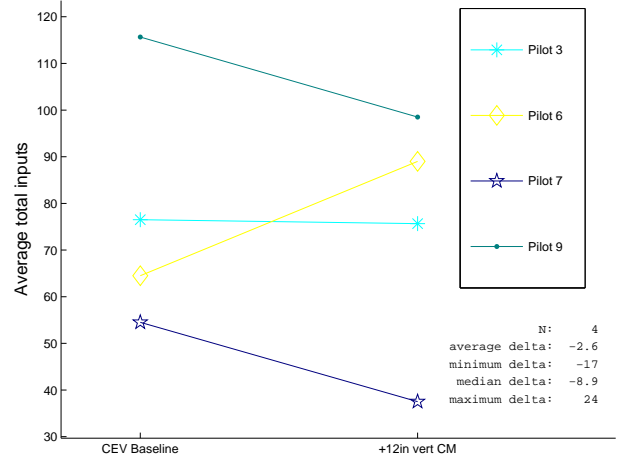
(a) Cooper-Harper rating



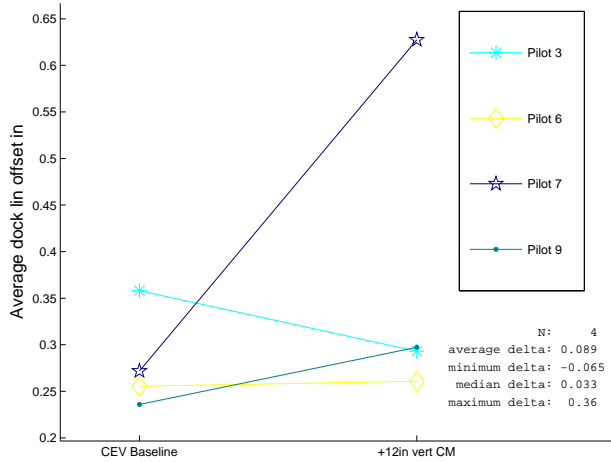
(b) Fuel use, lbm



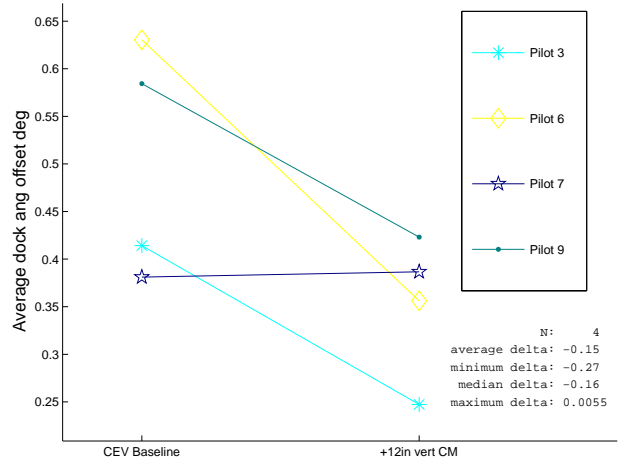
(c) Pre-dock coast time, s



(d) Number of pilot control inputs

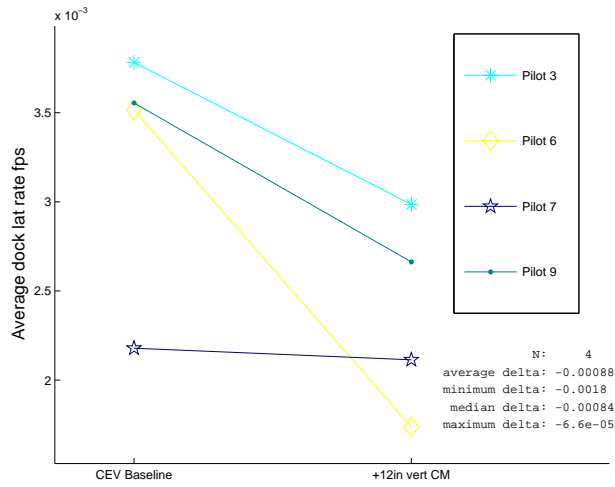


(e) Docking offset, in

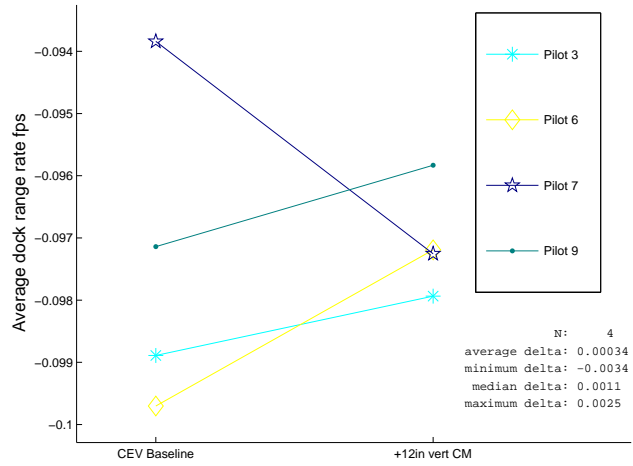


(f) Docking alignment, deg

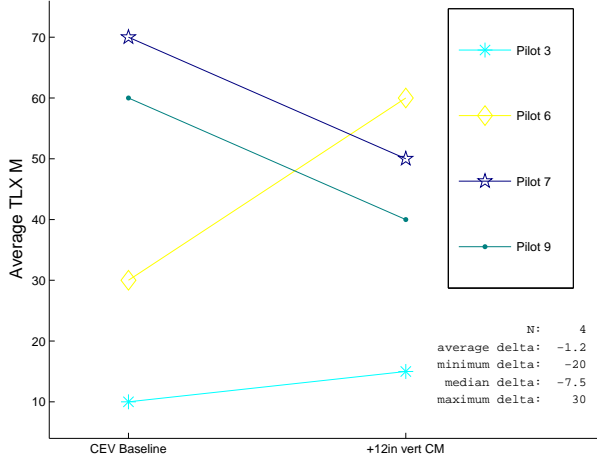
Figure A8: Effect of 12-inch vertical CM offset on baseline CEV



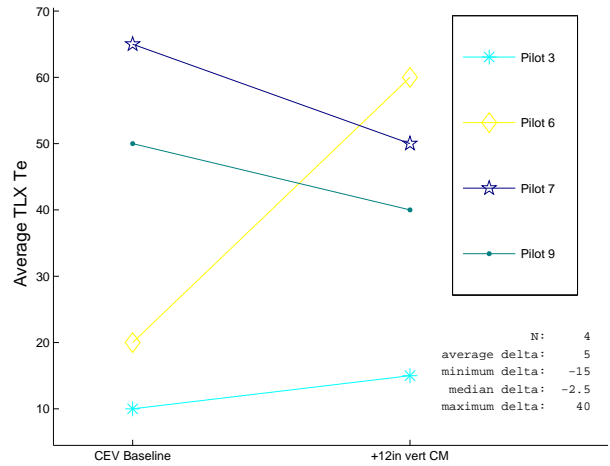
(g) Motion across dock face at dock, ft/s



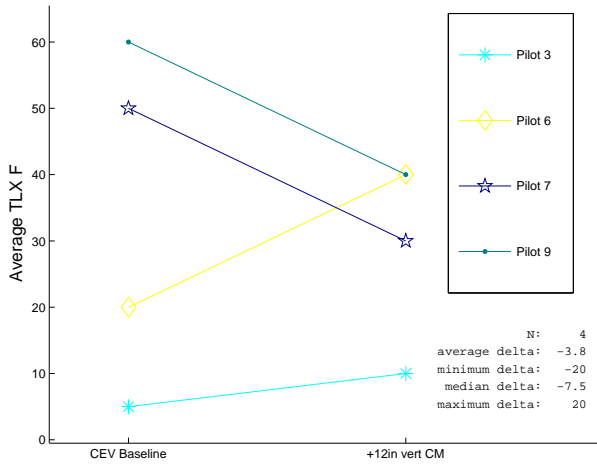
(h) Range rate at dock, ft/s



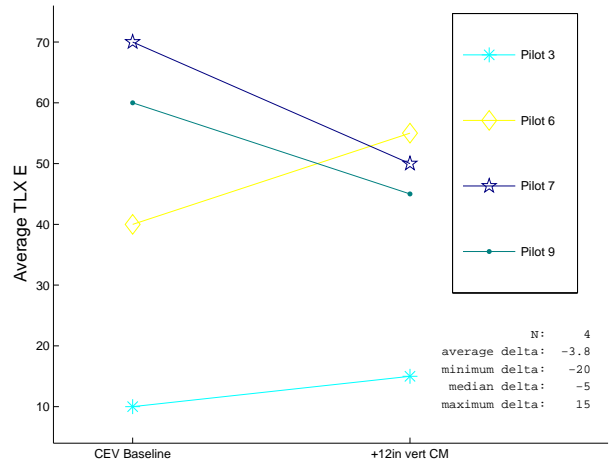
(i) Mental task load



(j) Temporal task load

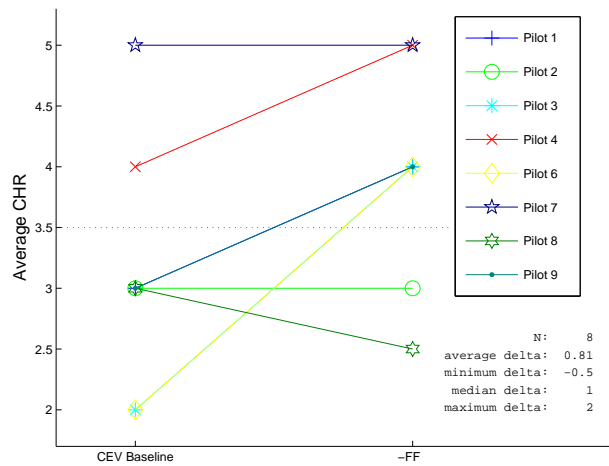


(k) Frustration

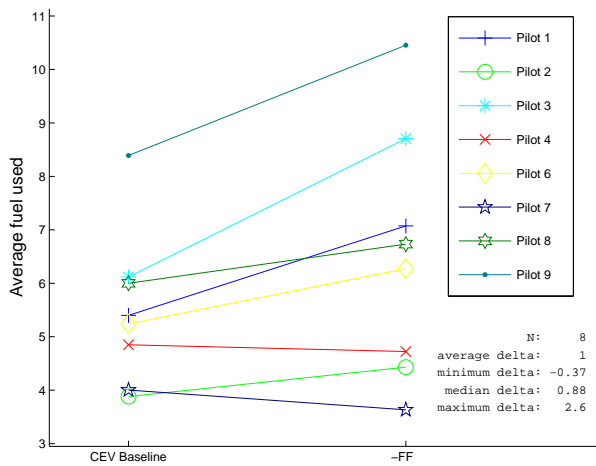


(l) Effort

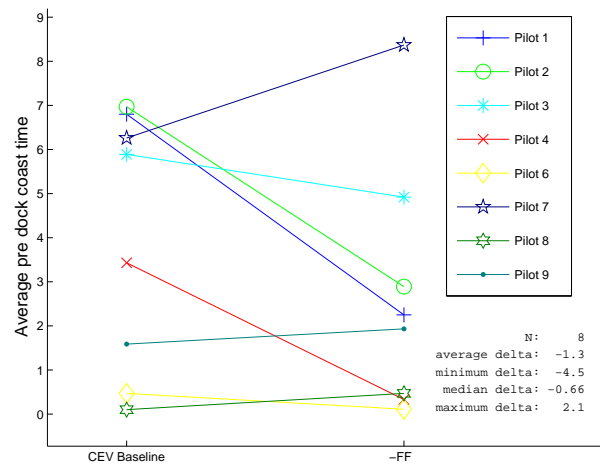
Figure A8: Effect of 12-inch vertical CM offset on baseline CEV (concluded)



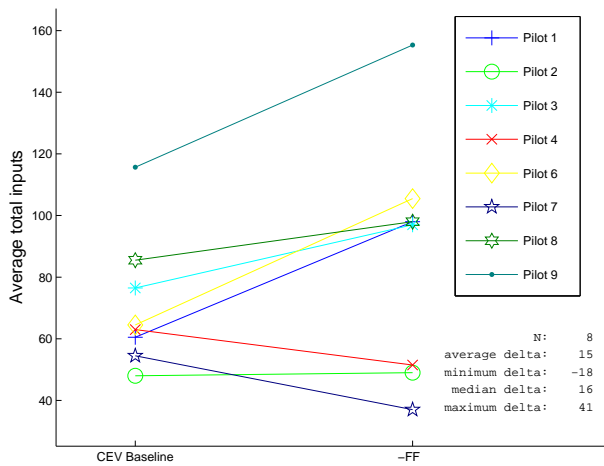
(a) Cooper-Harper rating



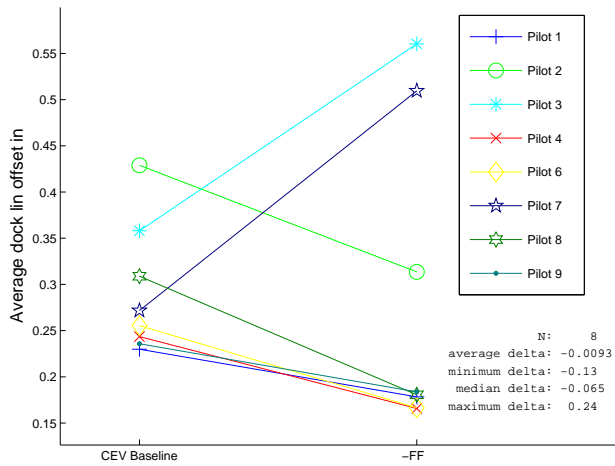
(b) Fuel use, lbm



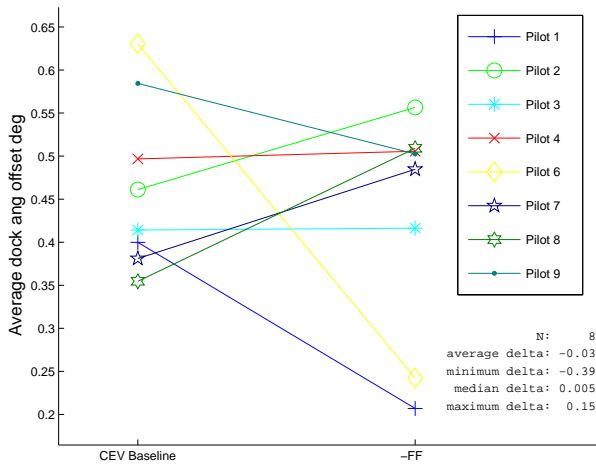
(c) Pre-dock coast time, s



(d) Number of pilot control inputs

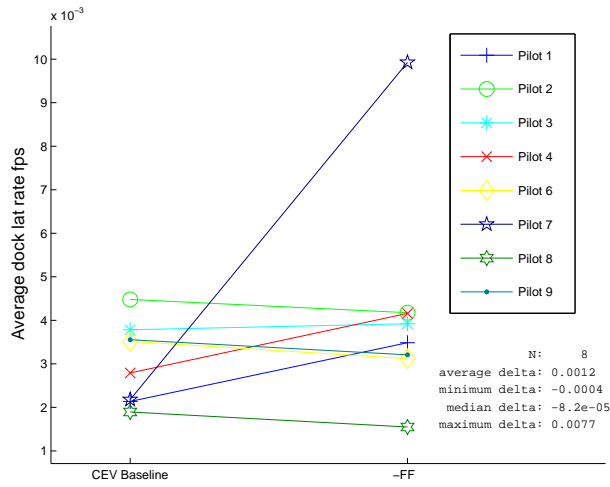


(e) Docking offset, in

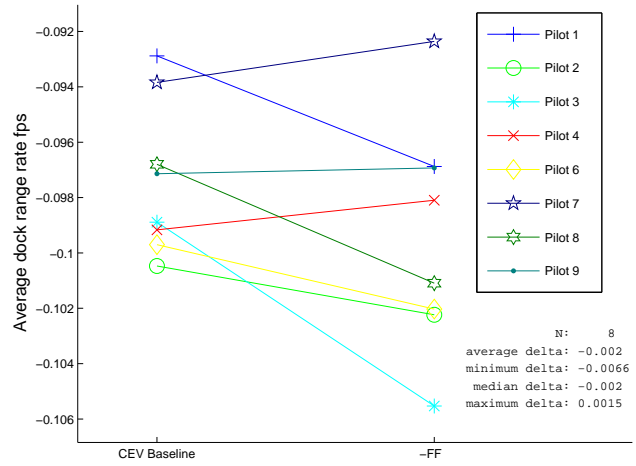


(f) Docking alignment, deg

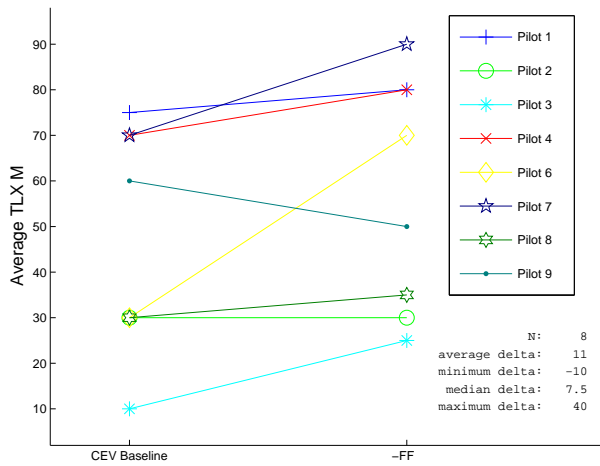
Figure A9: Effect of defeating feed-forward compensation vs. the CEV baseline



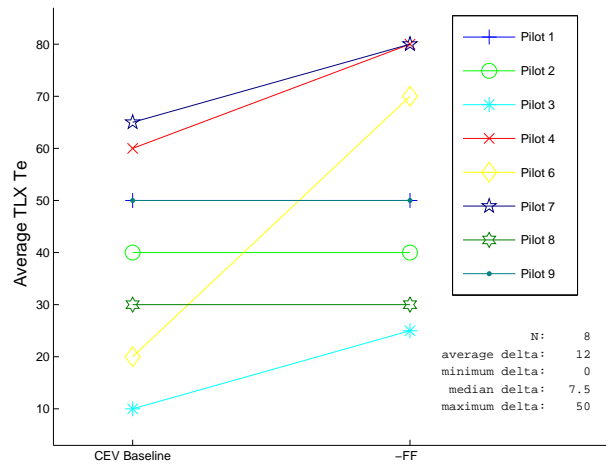
(g) Motion across dock face at dock, ft/s



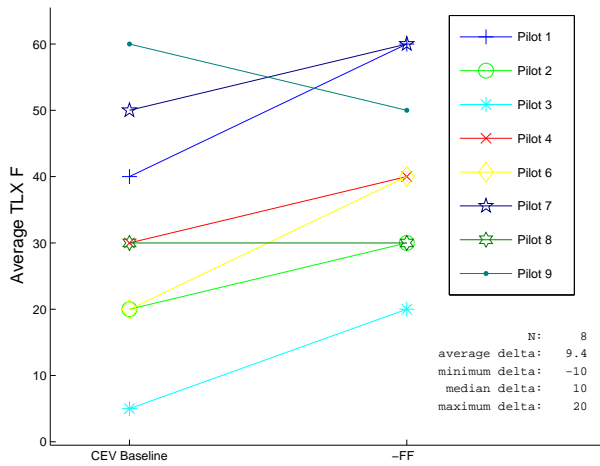
(h) Range rate at dock, ft/s



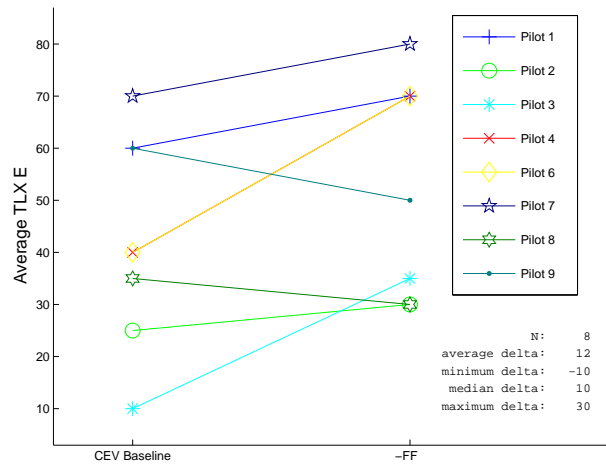
(i) Mental task load



(j) Temporal task load

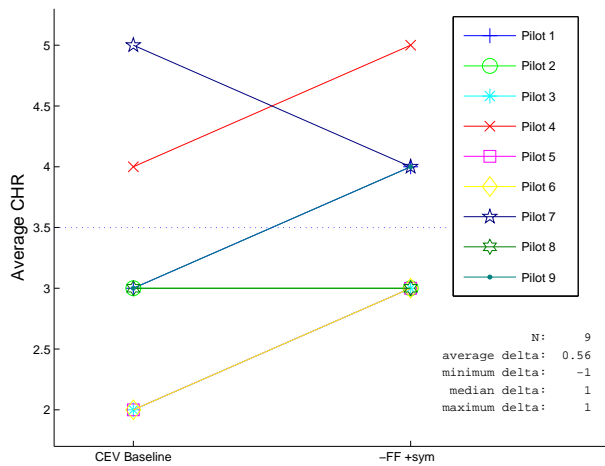


(k) Frustration

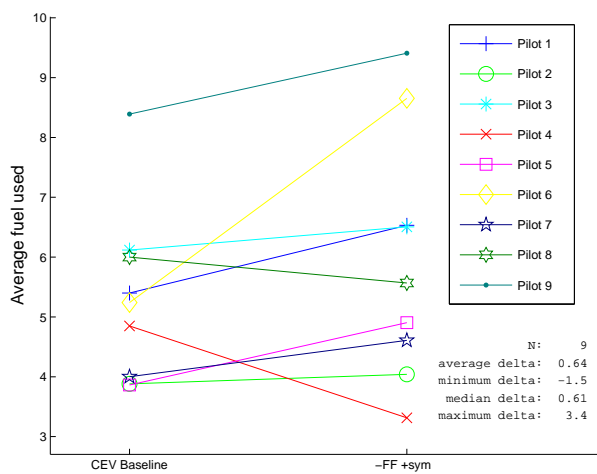


(l) Effort

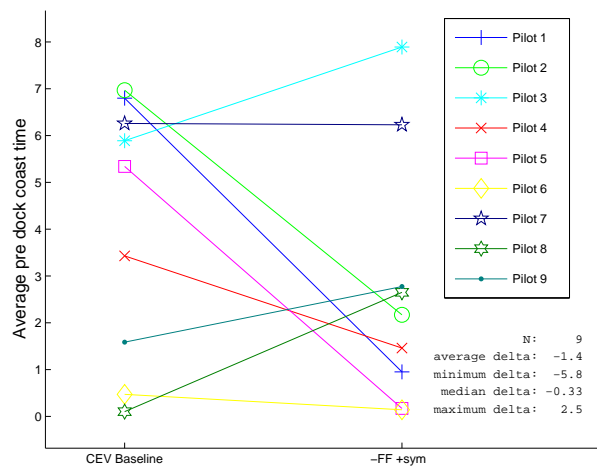
Figure A9: Effect of additional display symbology on baseline CEV (concluded)



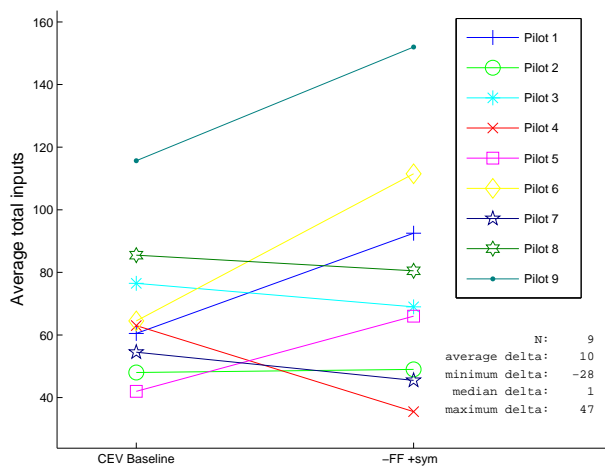
(a) Cooper-Harper rating



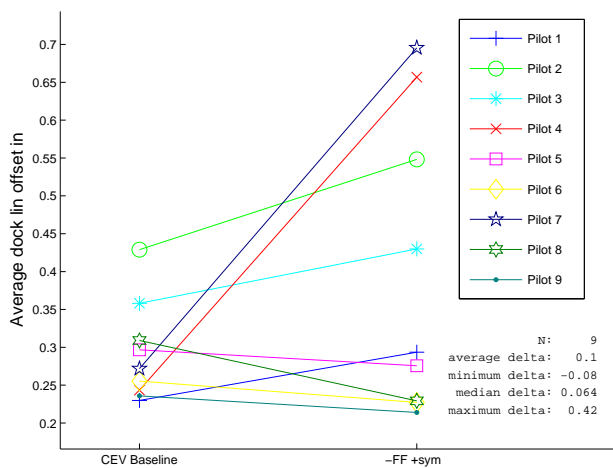
(b) Fuel use, lbm



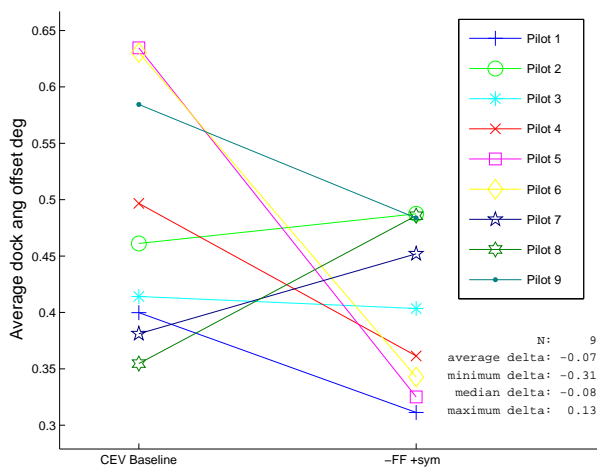
(c) Pre-dock coast time, s



(d) Number of pilot control inputs

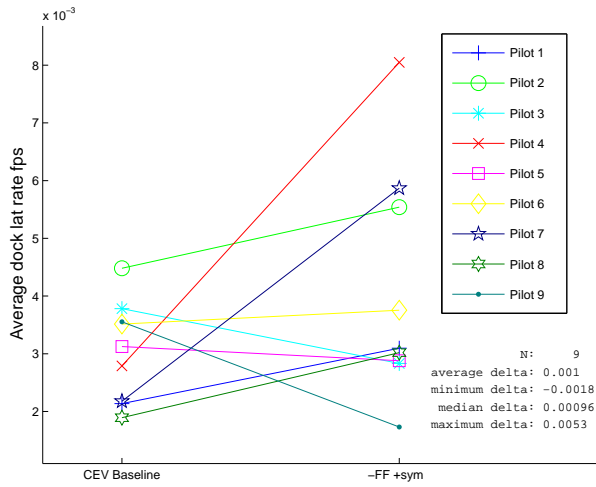


(e) Docking offset, in

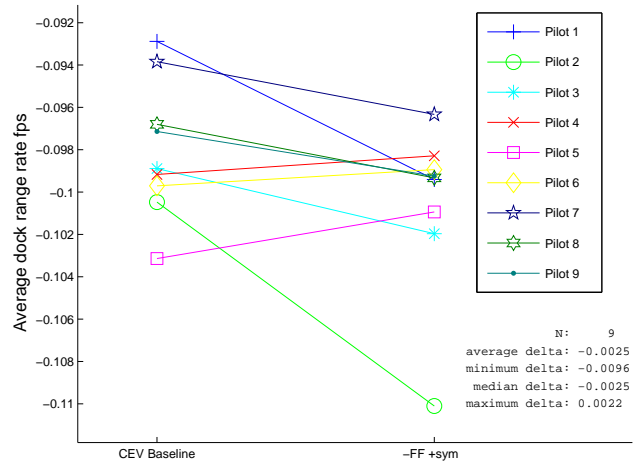


(f) Docking alignment, deg

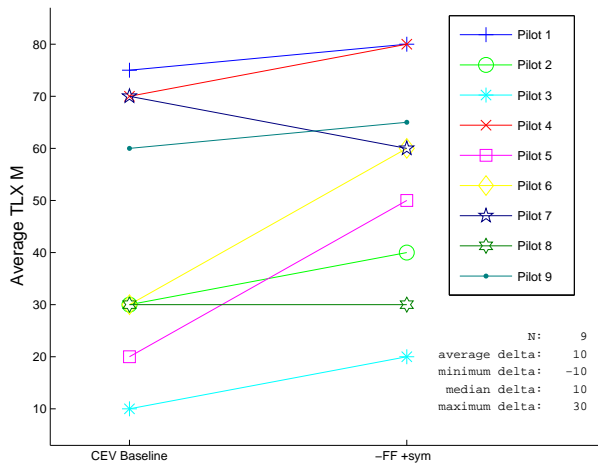
Figure A10: Effect of symbology with feed-forward mixing table disabled on baseline CEV



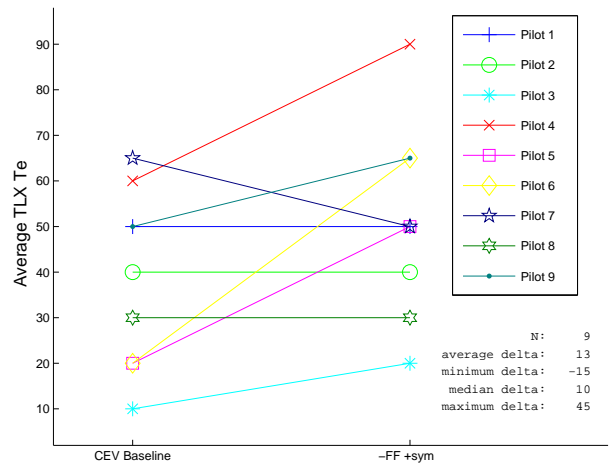
(g) Motion across dock face at dock, ft/s



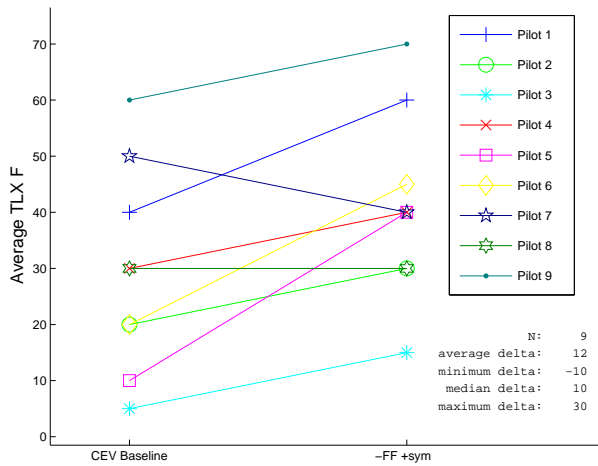
(h) Range rate at dock, ft/s



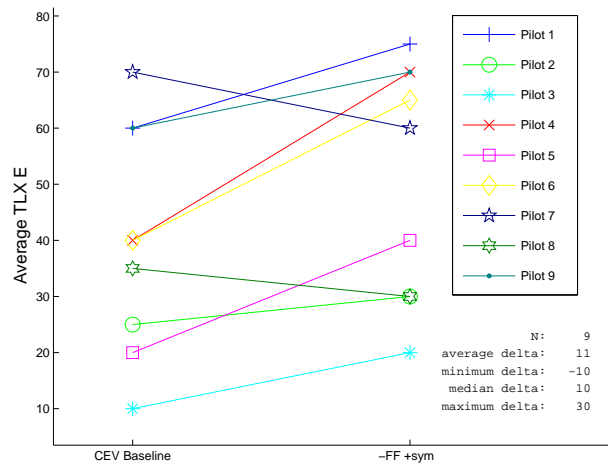
(i) Mental task load



(j) Temporal task load

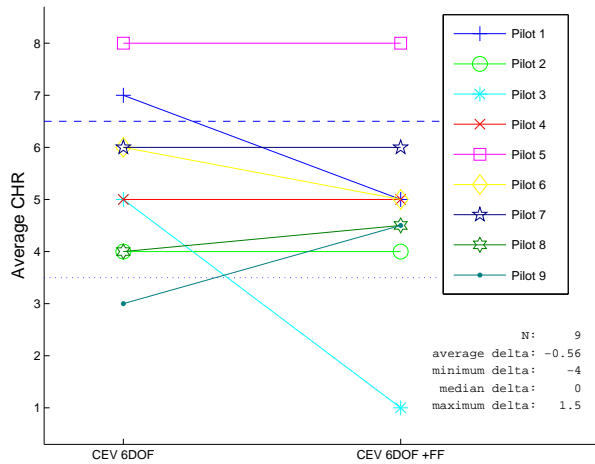


(k) Frustration

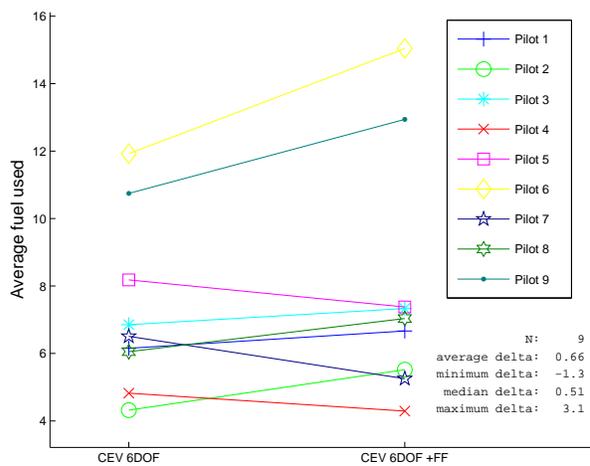


(l) Effort

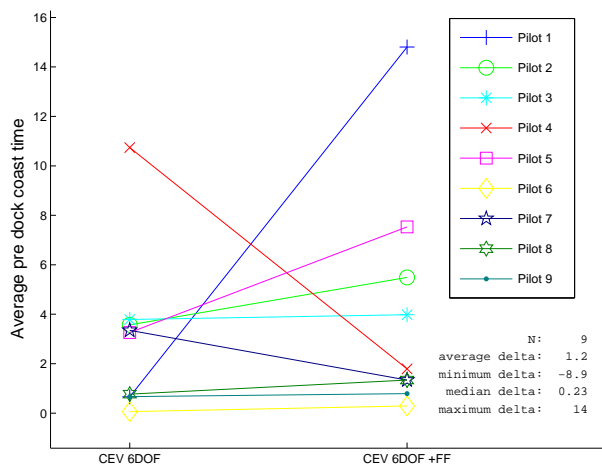
Figure A10: Effect of symbology with feed-forward mixing table disabled on baseline CEV (concluded)



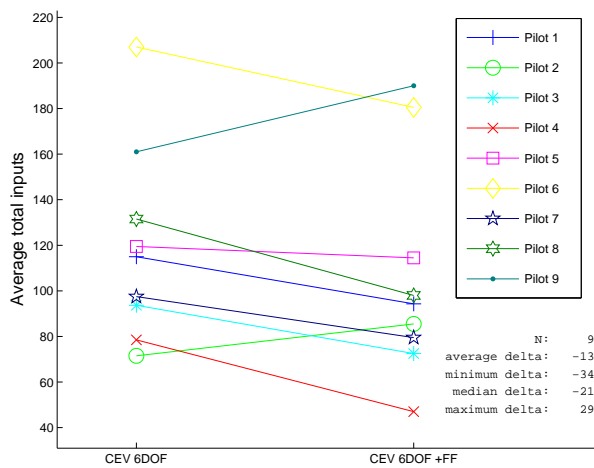
(a) Cooper-Harper rating



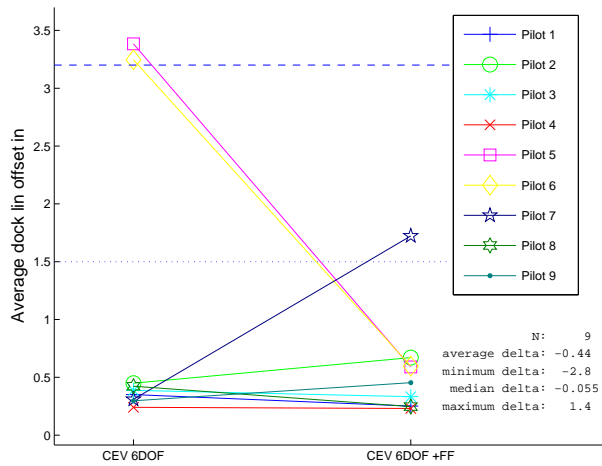
(b) Fuel use, lbm



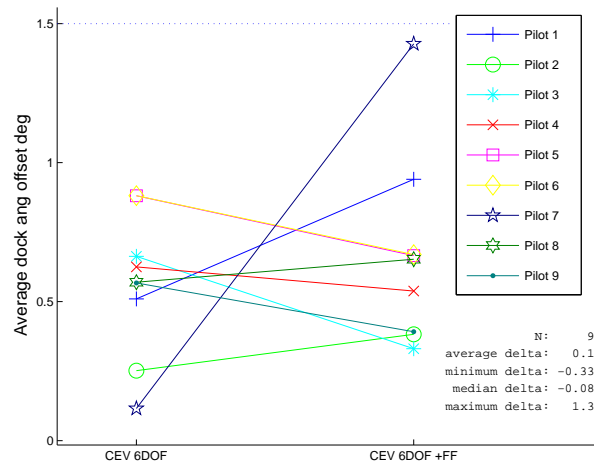
(c) Pre-dock coast time, s



(d) Number of pilot control inputs

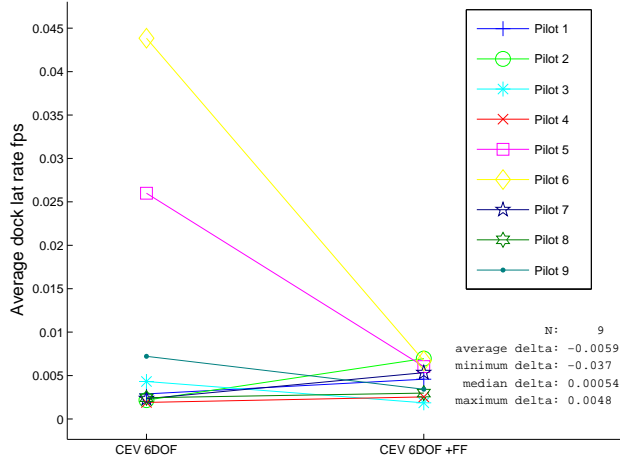


(e) Docking offset, in

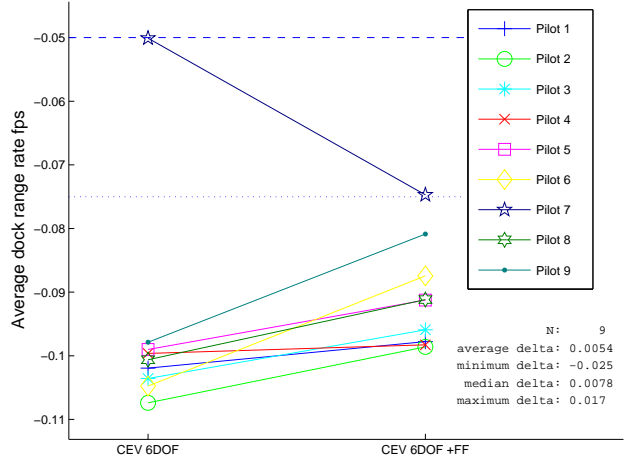


(f) Docking alignment, deg

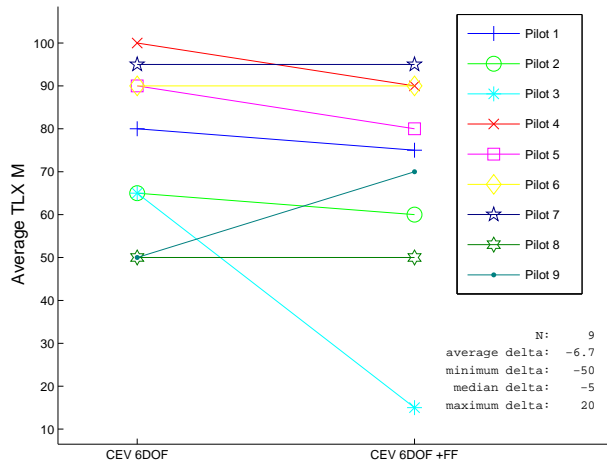
Figure A11: Effect of adding feed-forward to 6DOF configuration



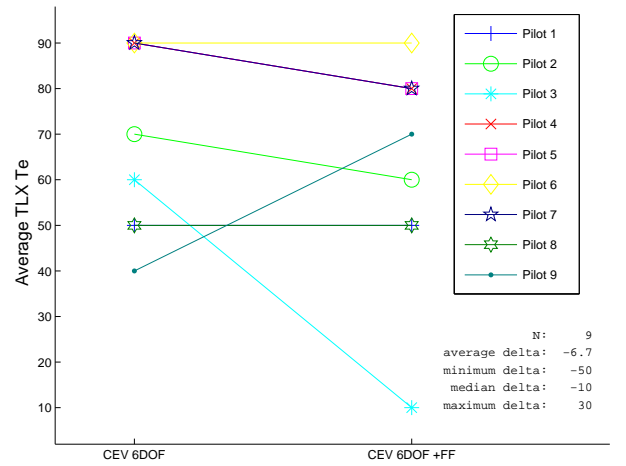
(g) Motion across dock face at dock, ft/s



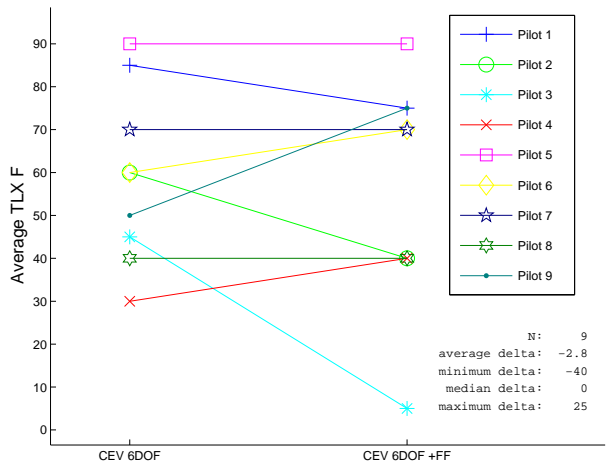
(h) Range rate at dock, ft/s



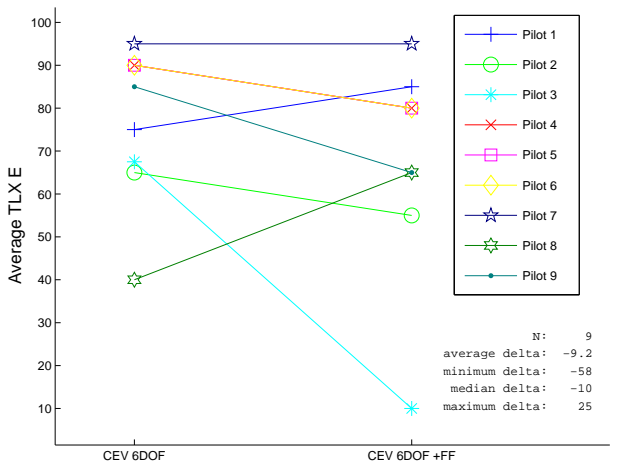
(i) Mental task load



(j) Temporal task load

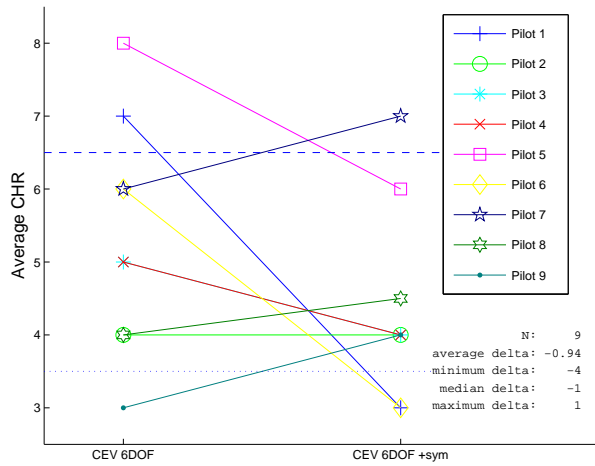


(k) Frustration

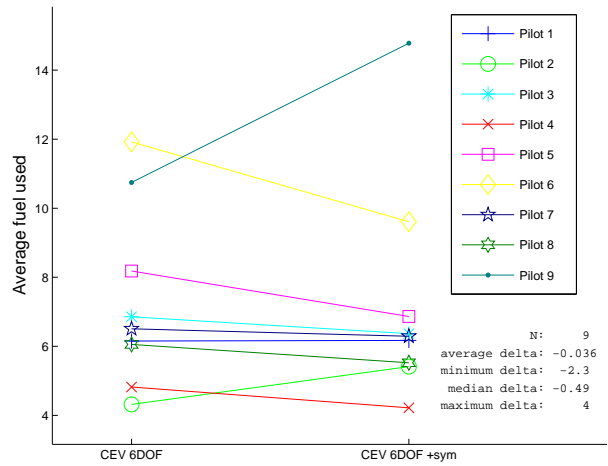


(l) Effort

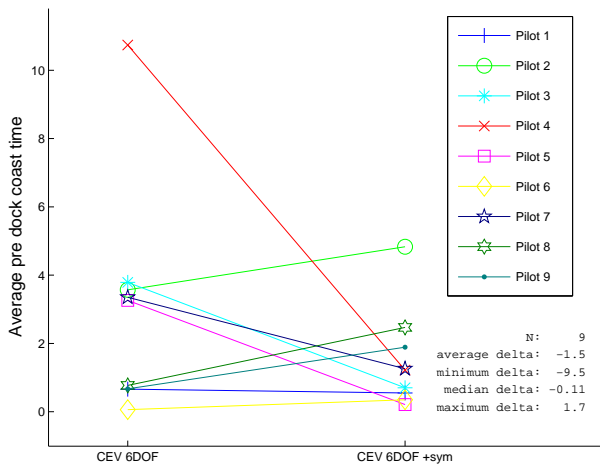
Figure A11: Effect of adding feed-forward to 6DOF configuration (concluded)



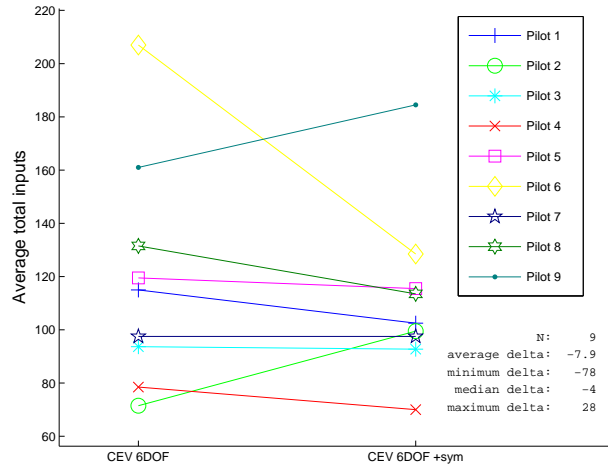
(a) Cooper-Harper rating



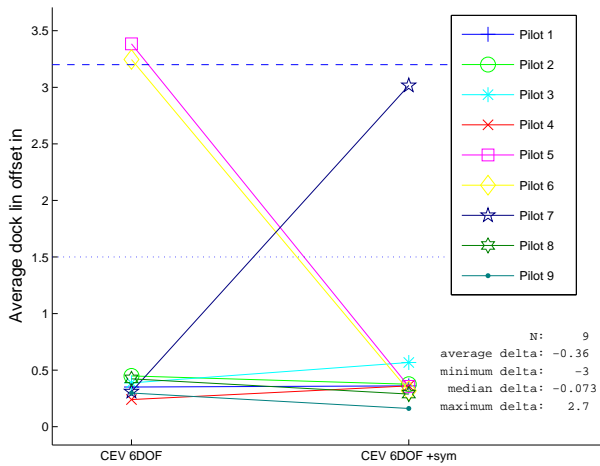
(b) Fuel use, lbm



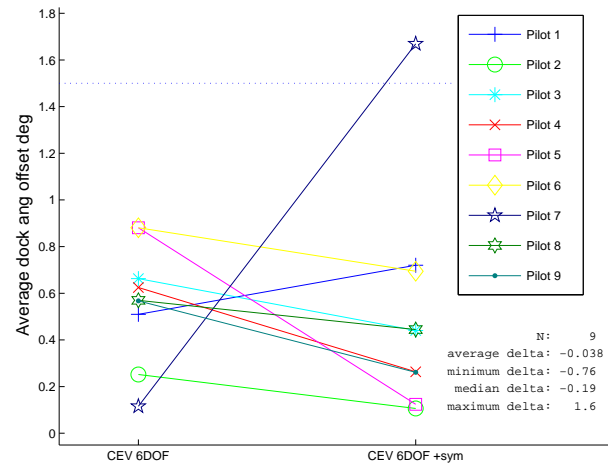
(c) Pre-dock coast time, s



(d) Number of pilot control inputs

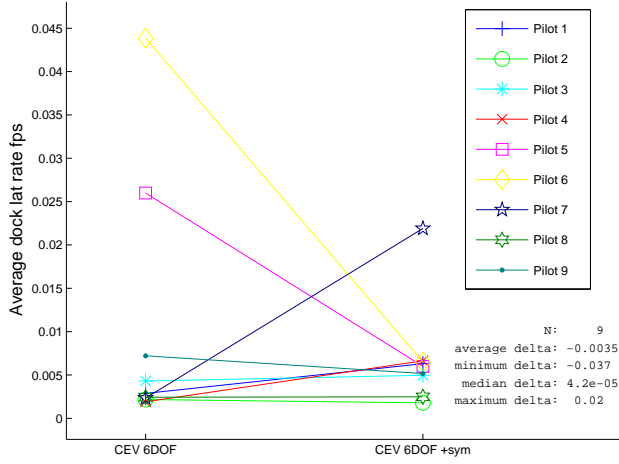


(e) Docking offset, in

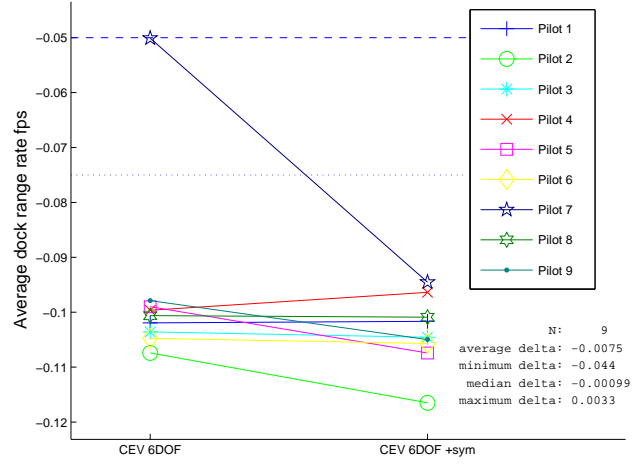


(f) Docking alignment, deg

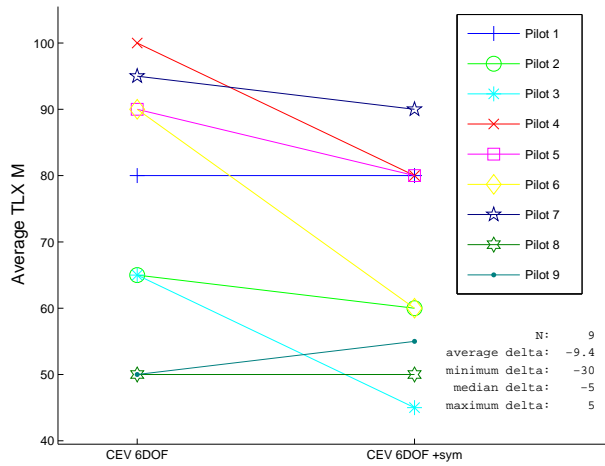
Figure A12: Effect of additional display symbology on 6DOF configuration



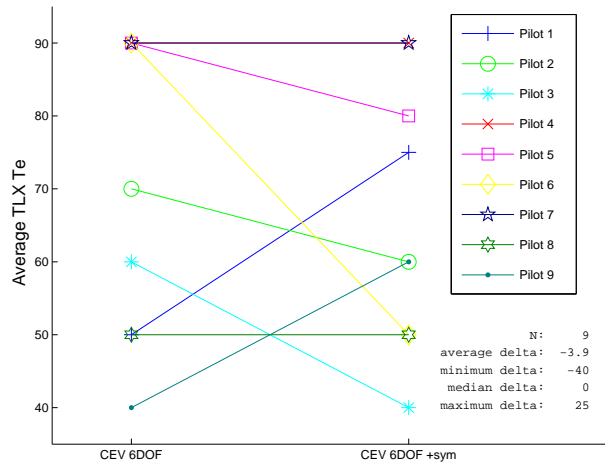
(g) Motion across dock face at dock, ft/s



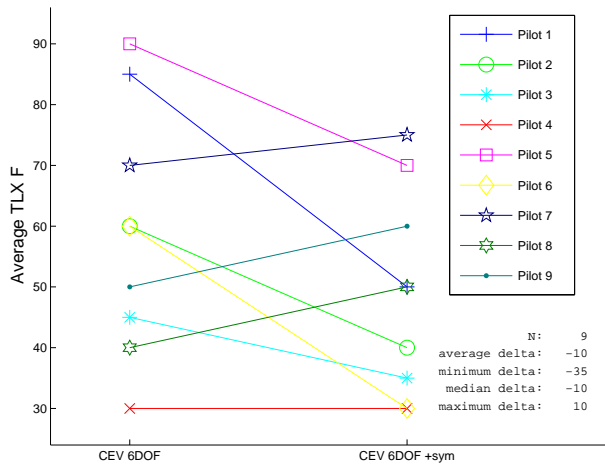
(h) Range rate at dock, ft/s



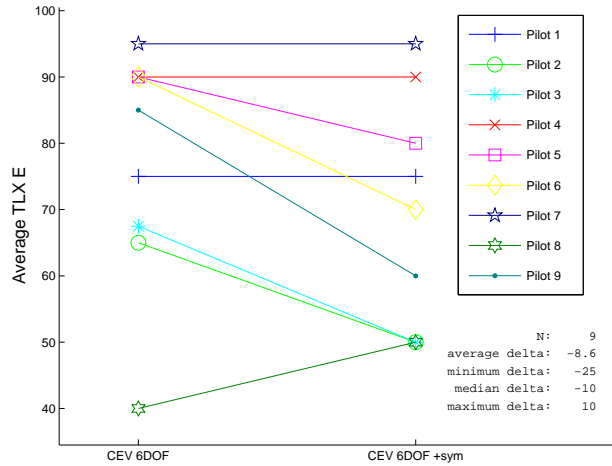
(i) Mental task load



(j) Temporal task load

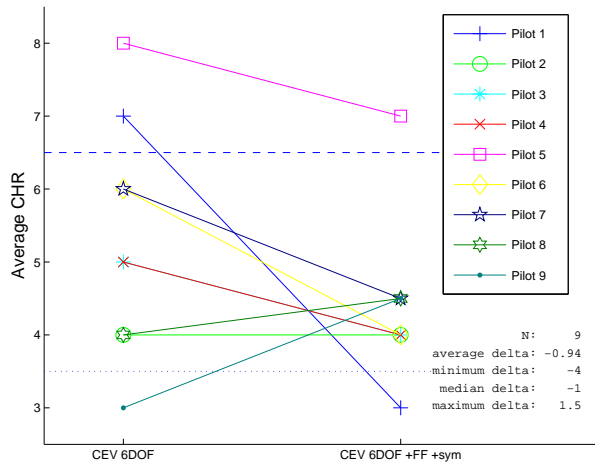


(k) Frustration

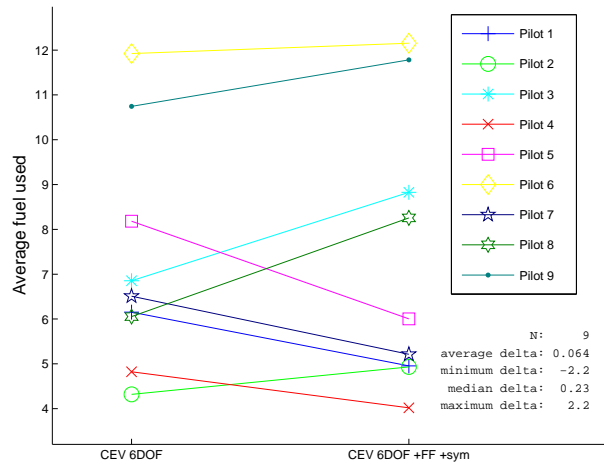


(l) Effort

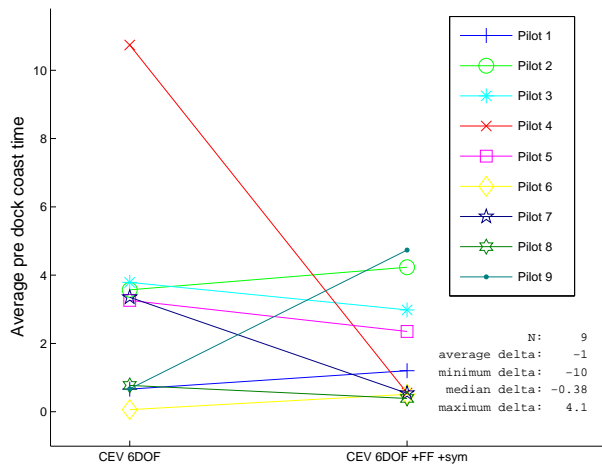
Figure A12: Effect of additional display symbology on 6DOF configuration (concluded)



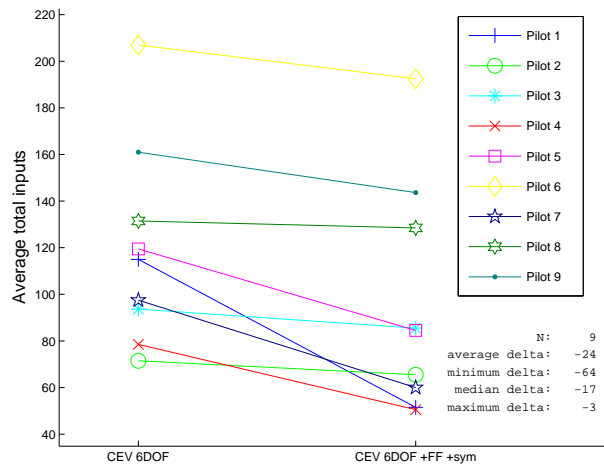
(a) Cooper-Harper rating



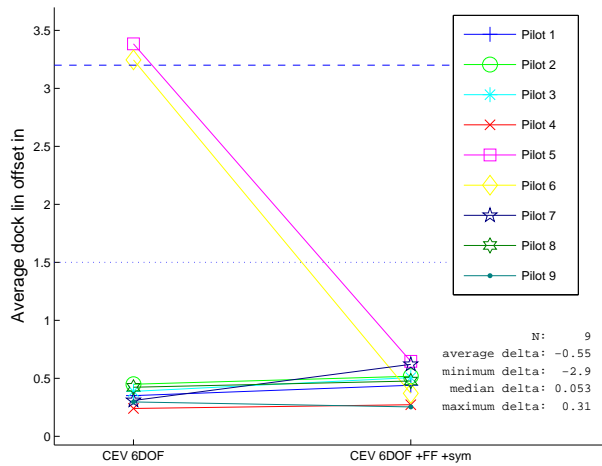
(b) Fuel use, lbm



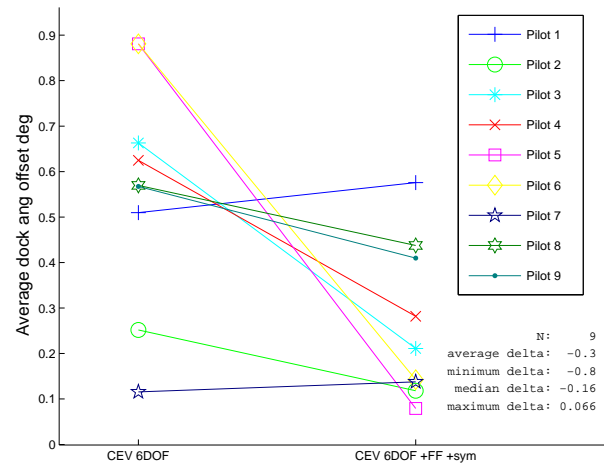
(c) Pre-dock coast time, s



(d) Number of pilot control inputs

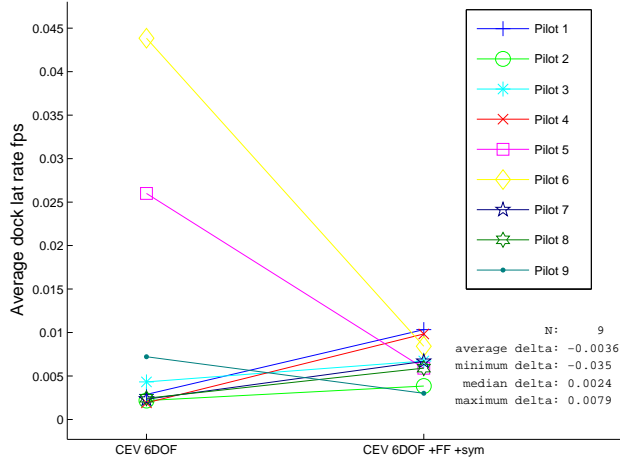


(e) Docking offset, in

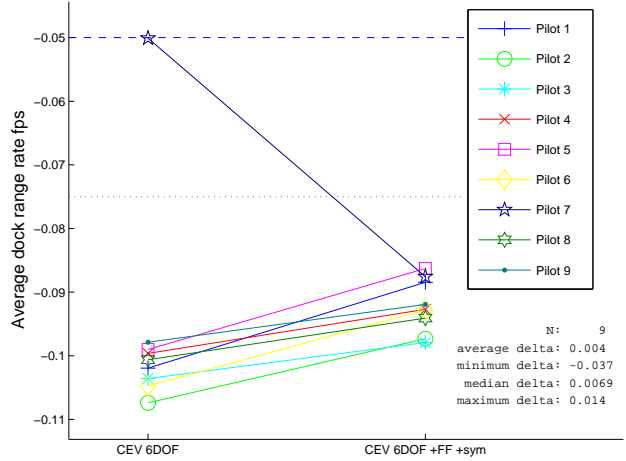


(f) Docking alignment, deg

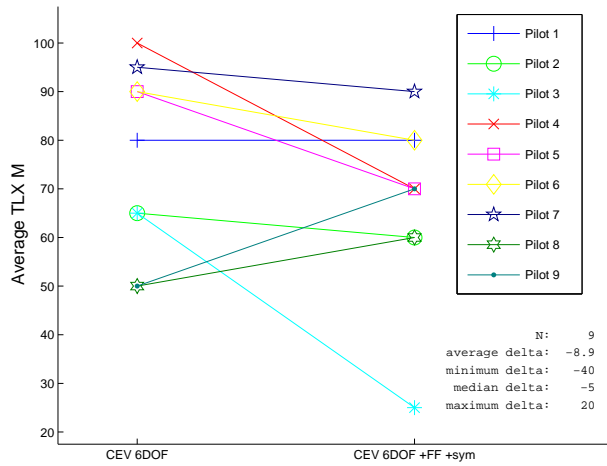
Figure A13: Effect of adding both feed-forward and symbology to 6DOF configuration



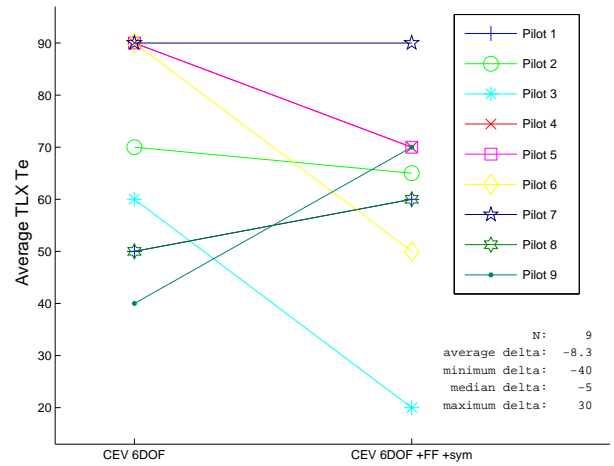
(g) Motion across dock face at dock, ft/s



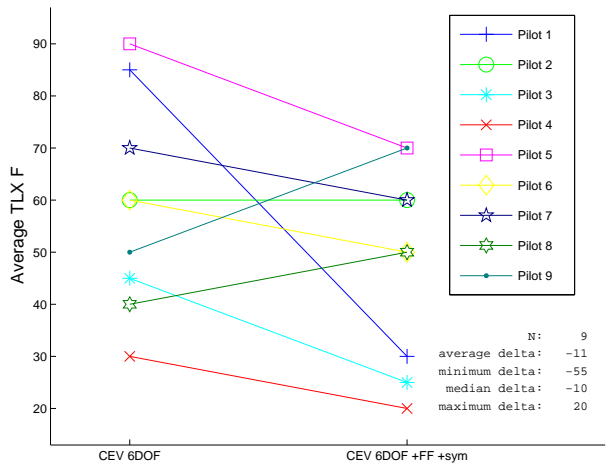
(h) Range rate at dock, ft/s



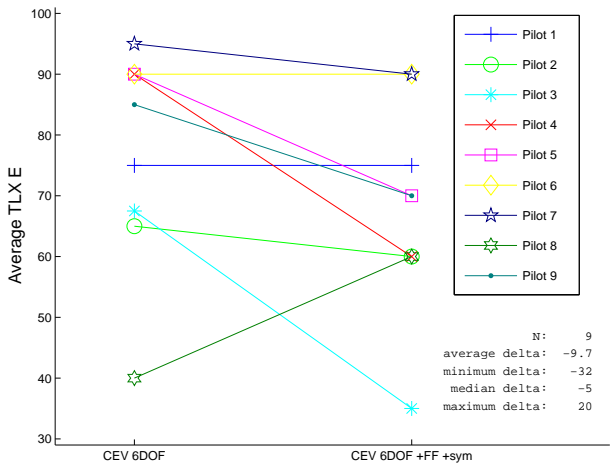
(i) Mental task load



(j) Temporal task load

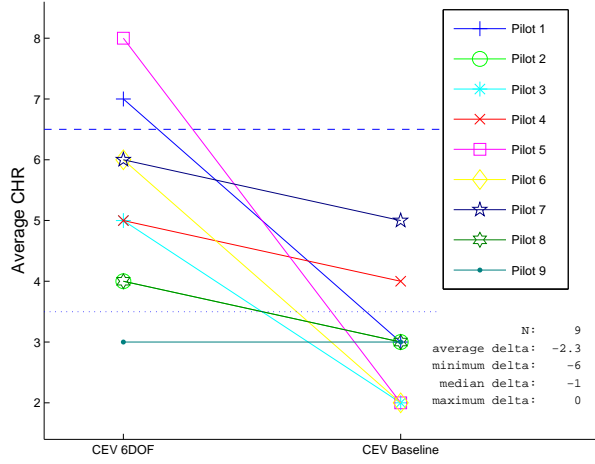


(k) Frustration

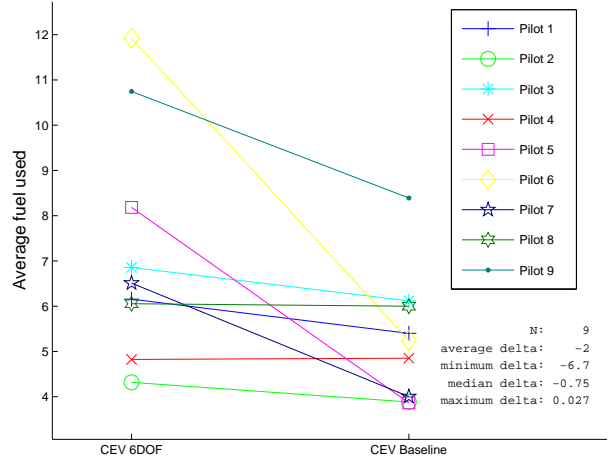


(l) Effort

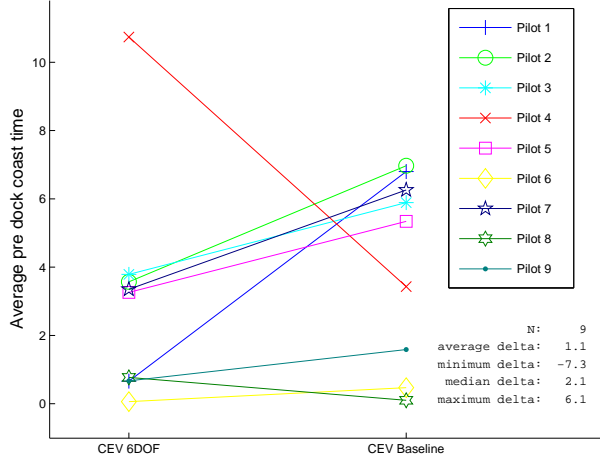
Figure A13: Effect of adding both feed-forward and symbology to 6DOF configuration (concluded)



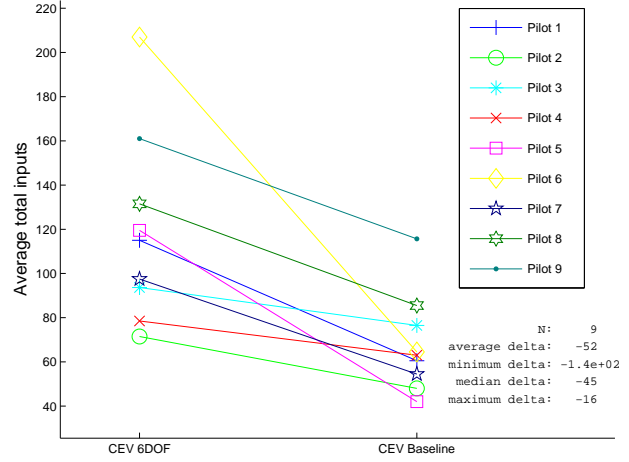
(a) Cooper-Harper rating



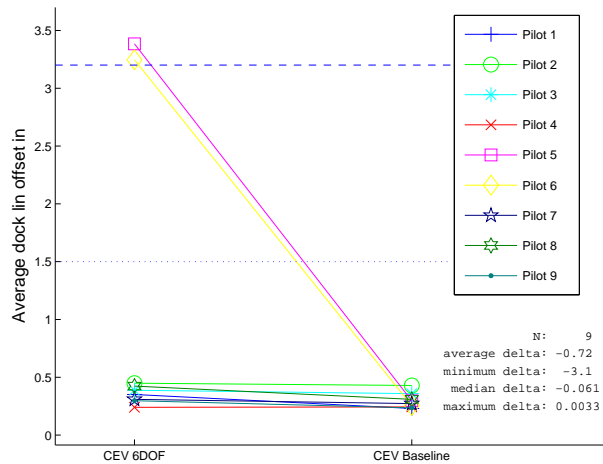
(b) Fuel use, lbm



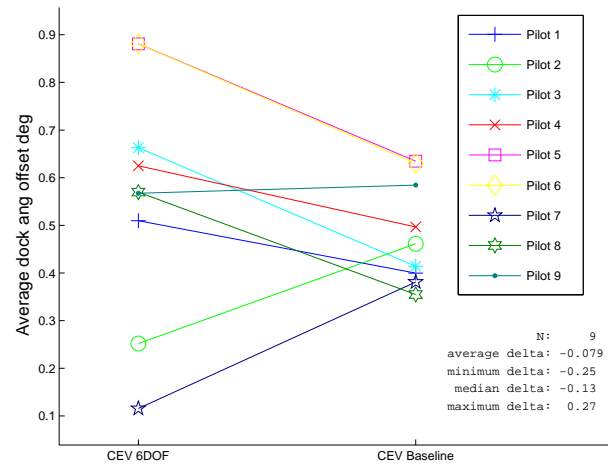
(c) Pre-dock coast time, s



(d) Number of pilot control inputs

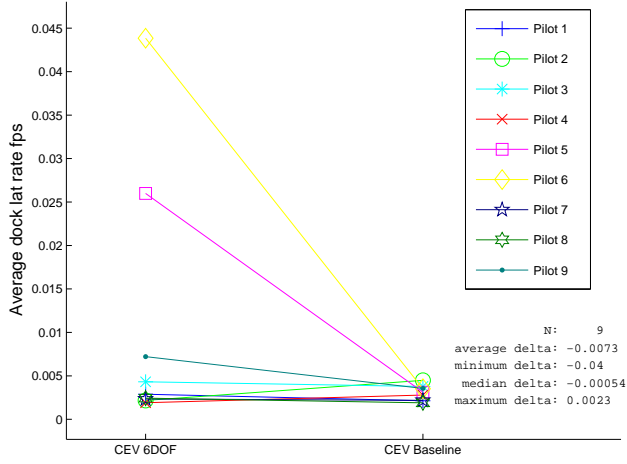


(e) Docking offset, in

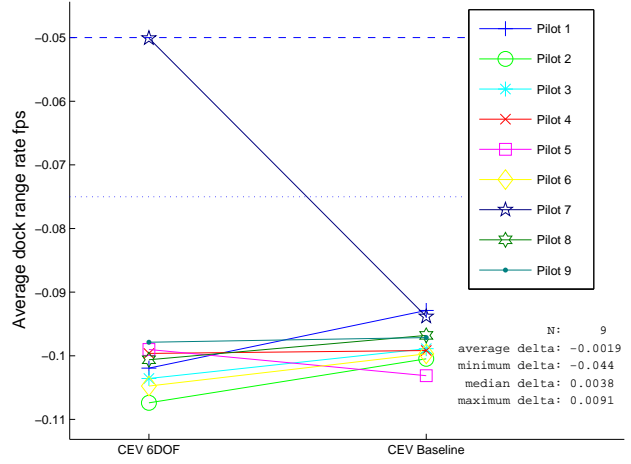


(f) Docking alignment, deg

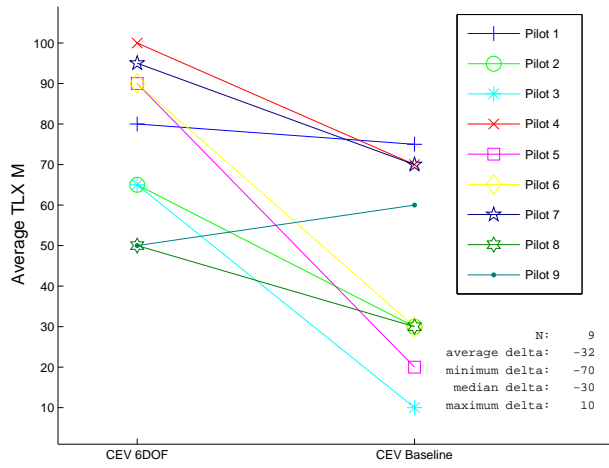
Figure A14: Effect of adding feed-forward and RCAH to the 6DOF configuration.



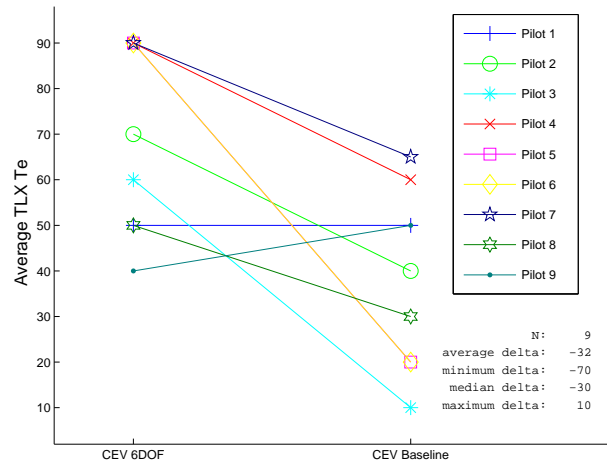
(g) Motion across dock face at dock, ft/s



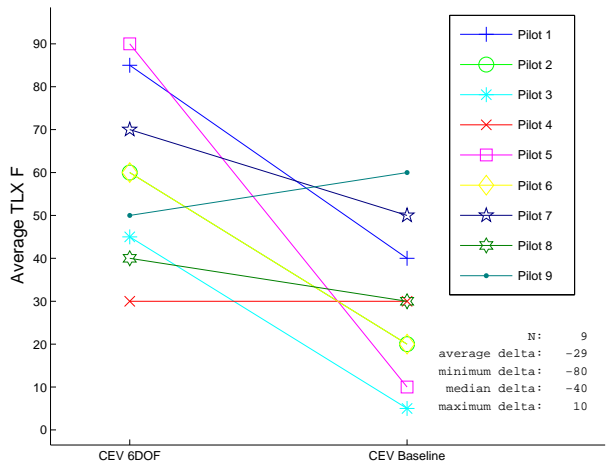
(h) Range rate at dock, ft/s



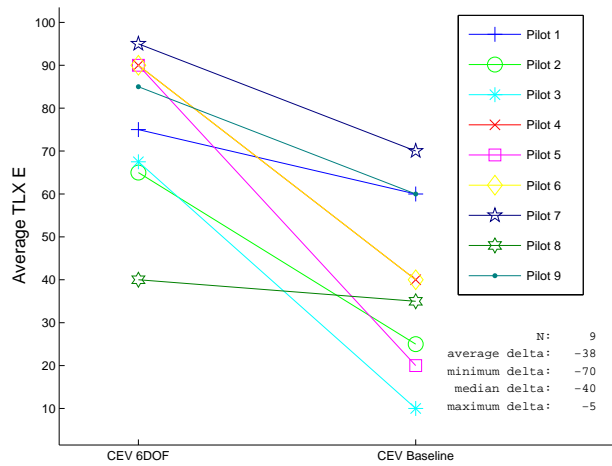
(i) Mental task load



(j) Temporal task load



(k) Frustration



(l) Effort

Figure A14: Effect of adding feed-forward and RCAH to the 6DOF configuration (concluded)

Appendix B

Autopilot Details

Introduction

This document describes the **RCS** control law control modes and **RCS** jet mixer used for the experiment. The control modes were derived from the Shuttle Rotation Hand Controller document [20]. **DAP** modes were developed to allow independent control of each axis. The current **DAP** mode selection was displayed to the test subject on the orbital **DAP** page on the **CDU** (figure B1). The test subject was able to fully control the **DAP** modes from the **CDU** during the experiment.

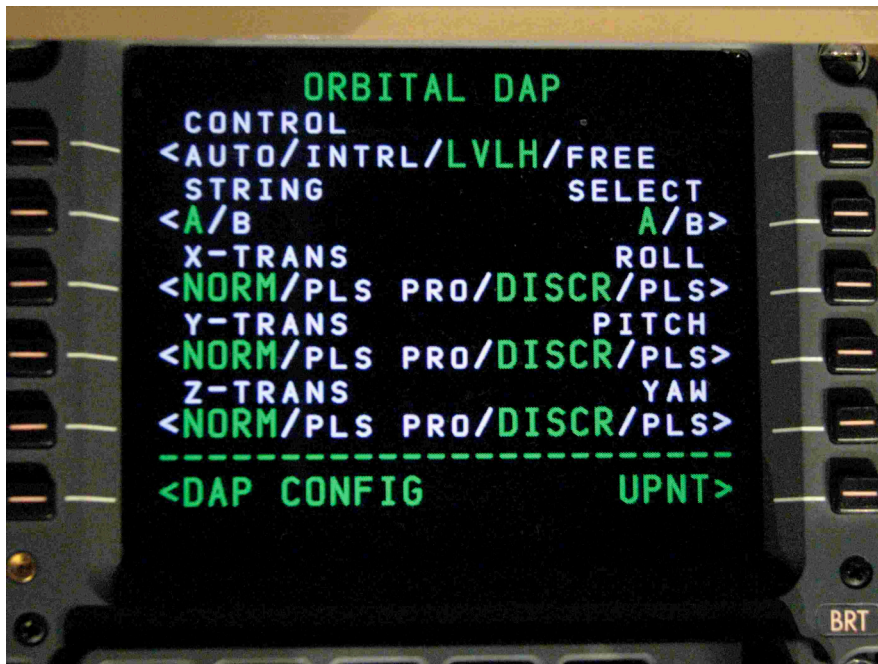


Figure B1: Photograph of the **CDU** orbital **DAP** page

Inceptor commands from the **THC** and **RHC** were sent directly to **RCS** control law to provide manual control of the vehicle. A schematic of the **RCS** control law is shown in figure B2.

DAP Configurations

The orbital **DAP** select “A” or “B” bezel button on the **CDU** determines the **DAP** configuration parameter limits for attitude dead-band, rate dead-band and desired change in velocity or rotation rate. Table B1 shows the default parameter values used in this experiment. These values provide coarse and fine attitude correction modes during orbital proximity operations. The attitude dead-band is controlled using a phase plane [13] with attitude and rate dead-bands.

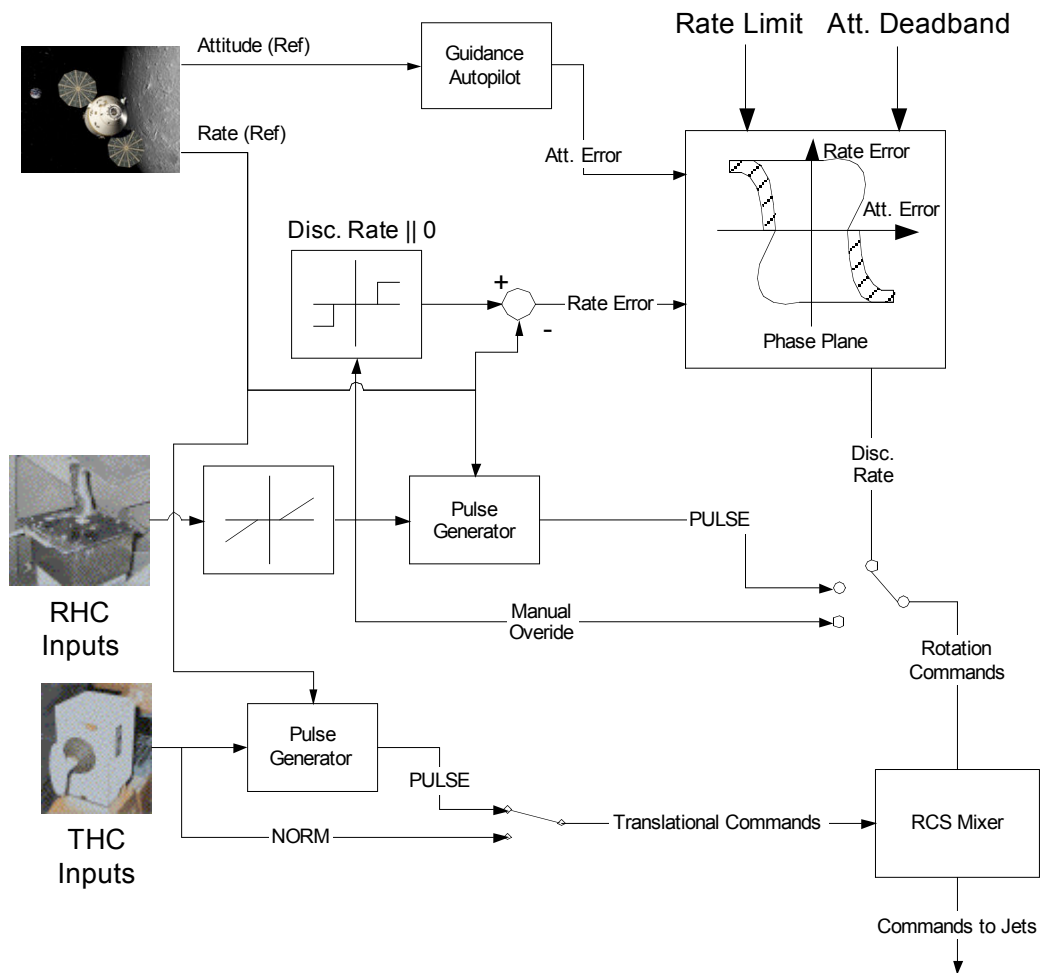


Figure B2: Schematic of RCS control law

Table B1: DAP gain set selection

Select	Rotation Rate (deg/s)	Attitude Dead-Band (deg)	Roll Rate Dead-Band (deg/s)	Pitch Rate Dead-Band (deg/s)	Yaw Rate Dead-Band (deg/s)	Rotation Pulse (deg/s)	Translation Pulse (ft/s)
A	0.05	0.5	0.02	0.04	0.04	0.10	0.01
B	0.05	0.5	0.02	0.04	0.04	0.04	0.002

Control modes

AUTO

Autopilot mode provided commands for attitude control providing autonomous docking operation. The autopilot can be overridden by manual input to the [RHC](#). The autopilot mode was implemented for test and checkout of the simulation and was not used in this experiment. Each axis was evaluated independently to determine the appropriate attitude command. Code examples for rotation (e.g. `updateRollCommand()`) and translation (e.g. `updateXTranslationCommand()`) are provided in section [B](#).

INTRL

Inertial mode provides reference and attitude hold modes to the current inertial reference frame. Manual input to the [RHC](#) will fire the [RCS](#) jets based on manual mode selection. When the [RHC](#) is returned to detent, the new inertial attitude is held when the attitude rate is within the rate dead-band. This mode was not used in this experiment.

LVLH

Local Vertical Local Horizontal (LVLH) mode provides reference and attitude hold modes to the vehicle's current [LVLH](#) reference frame. Manual input to the [RHC](#) will fire the [RCS](#) jets based on manual mode selection. Depending on manual mode selection, when the [RHC](#) is returned to detent, the new [LVLH](#) attitude is held when the attitude rate is within the rate dead-band. This was the primary mode used during this experiment.

Free

Free drift mode allows the attitude to drift freely. No jets are fired. However, when the inceptors are out of detent, jets fire continuously. When the inceptor is back in detent, free drift is continued. This mode was not used in this experiment.

Manual modes

Manual modes were provided for both rotation and translation for each axis. These were evaluated in the function `calcInceptorCommand()` shown in section [B](#).

Rotational command modes

Four rotational modes were available: Pulse, Discrete Rate, Proportional Rate, and [RHC](#) Manual Override. The effective inceptor was calculated to determine if the [RHC](#) was out of detent by using the normalized (-1 to 1) [RHC](#) inputs with a dead-band of 0.15 of full-range for noise.

Pulse Pulse mode provided the capability to rotate in any axis. Each [RHC](#) deflection resulted in a single burst of jet fire. The single firing provided the specified [DAP](#) configuration rotation pulse rate. For example, if the current rotation rate was 0.51 deg/s, with [DAP](#) configuration rotation pulse rate set to 0.1 deg/s, a single movement of the [RHC](#) fires jets to increased the rate to 0.61 deg/s. When the [RHC](#) was returned to detent the rotation rate is not nulled and attitude was allowed to drift. The experiment settings are given in table [B1](#).

This was the principal rotational command mode used for the reversionary control law scenarios (tests 1 through 4).

Discrete Rate Discrete rate mode provided the capability to rotate in any axis to provide **RCAH** capability. An **RHC** deflection resulted in a specified rate being commanded in that axis for the entire time the **RHC** was deflected. The rate was again determined by the **CDU DAP** gain selection. For example, when the **DAP** configuration rotation rate had 0.1 deg/s selected; movement of the inceptors out of detent would continuously command a rotational rate of 0.1 deg/s. When inceptors were returned to detent, the rate would be nulled and attitude hold would be re-established.

This was the principal rotational command mode used for the non-reversionary control law scenarios (tests 5 and above).

Proportional Rate Proportional mode commanded a proportional rate based on **RHC** deflection. When the inceptor was returned to detent, the rate was nulled and attitude hold was re-established. The maximum rate was set to 10 ft/s.

Proportional rate command mode was not used in this experiment.

RHC Manual Override In any mode, movement of the **RHC** past 90% of total movement would manually override any current mode of operation. This would command the appropriate jets to fire continuously until the **RHC** was moved within 90% of its total movement. When this occurred, the current mode of operation was resumed. If the mode was **PULSE**, then the new rotational rate was retained and attitude was allowed to drift.

While active for this experiment, **RHC** Manual Override was not used very often, and only in the **6DOF** vehicle case.

Translational command modes

The **THC** installed in the **RFD** was a discrete device. Two modes for translation were provided: Normal and Pulse.

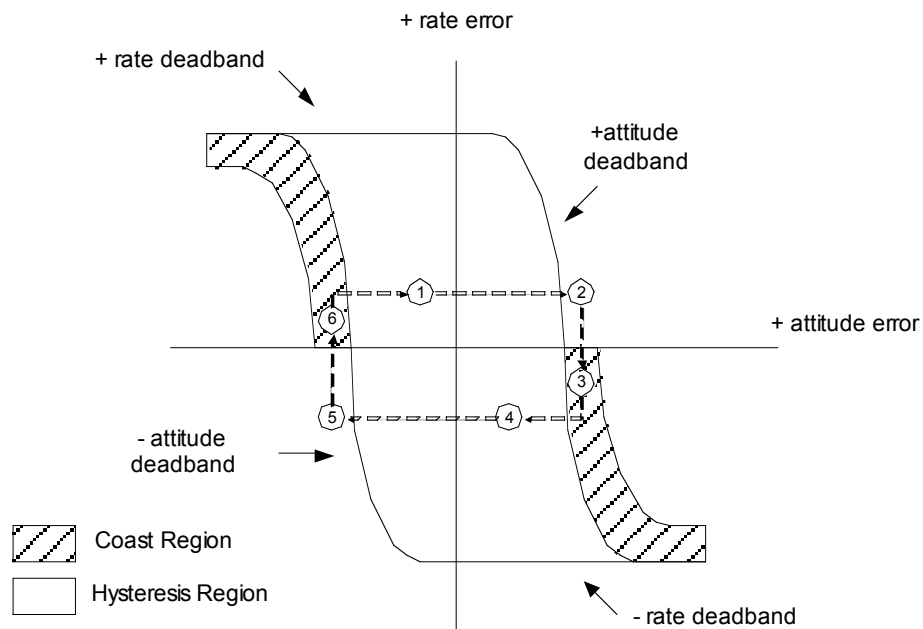
Normal Normal mode provided continuous translational acceleration commands in each axis. This mode was used only for the X_{body} axis in the rotating target scenarios (tests 16 through 19) during this experiment.

Pulse Pulse mode provided the capability to command the rate of relative translation in any axis. Each **THC** deflection resulted in a single string of **RCS** jet pulses. The single string provided the specified (via the **CDU DAP** gain selection) increase in translational rate. For example, if the current translation rate was .51 ft/s, and the **DAP** configuration translation pulse rate was set to 0.1 ft/s (**A-DAP** gain set), then a single movement of the **THC** out of detent would fire the **RCS** jets long enough to increase the rate to 0.61 ft/s. When the **THC** was returned to detent the translation rate was allowed to continue.

This was the principal translational command mode used in this experiment. The experiment settings are given in table **B1**.

Phase Plane implementation

When Discrete Rate was selected as the **DAP** manual mode, the **RCS** jets fired to maintain attitude control within the selected dead-band. The dead-band was controlled through a phase plane as depicted in figure **B3** [21], [13]. The phase plane consists of an *attitude dead-band* and a *rate dead-band*. Attitude dead-band was the allowable drift (positive or negative) that would be tolerated in any axis before the **RCS** was activated to correct the error. Rate dead-band was the allowable rate of attitude change (positive or negative) that would be tolerated before the **RCS** was activated to reduce the rate.



States during Deadbanding

- ① No jets fire since the rate error is positive, the attitude error will grow in a positive direction.
- ② Jets fire to nullify the positive rotational rate.
- ③ Jets stop firing when the deadband is crossed, but a little negative rate error is inevitable.
- ④ No jets fire with a negative rate error, the attitude error will also drift negatively.
- ⑤ Jets fire to nullify negative rate error.
- ⑥ Jets stop firing but residual positive rate error causes attitude error to go positive again and the cycle repeats.

Figure B3: RCS phase plane

Unlike the shuttle's phase plane controller, the test simulation did not implement a bias switching curve for undesirable external accelerations and disturbances [21]. This simplification allowed the control law to take advantage of symmetry. It was sufficient to specify only the positive rate error half of the phase plane, as depicted in figure B4. [13]

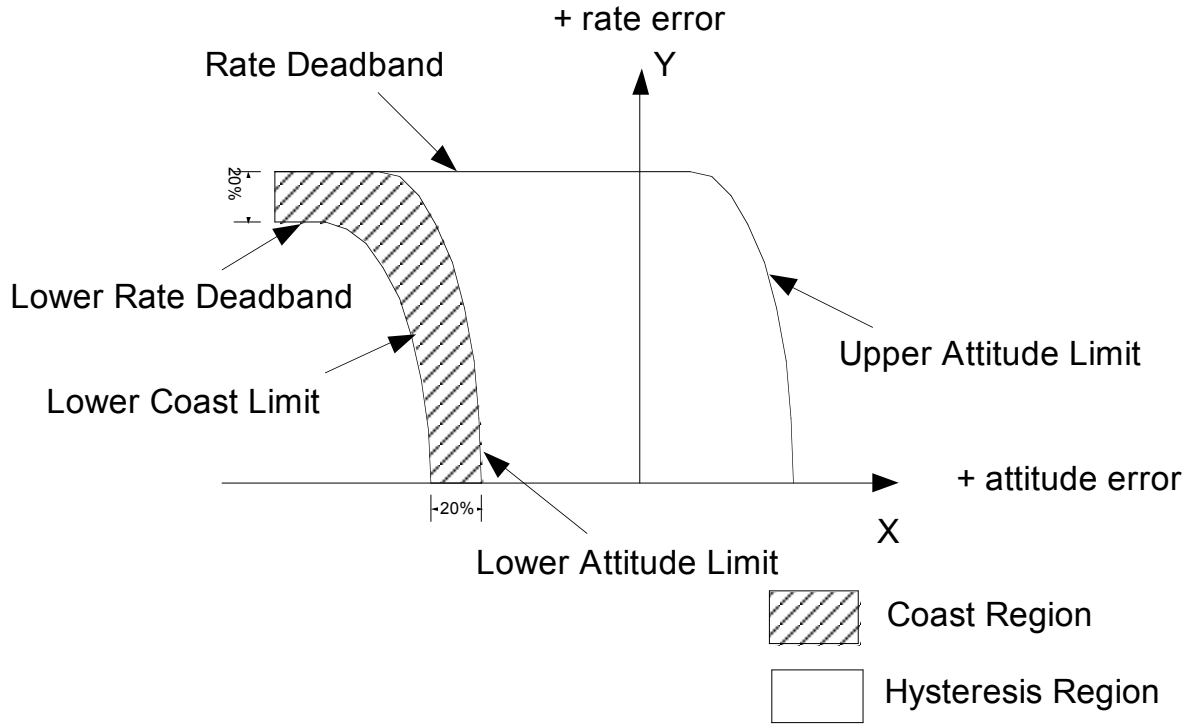


Figure B4: Positive Rate Error Phase Plane (from Cheng)

Calculations of the upper and lower attitude limits determined the bounds of the hysteresis regions and were a function of the RCS jet authority.

The upper attitude limit was calculated by:

$$\text{upper_attitude_limit} = \text{attitude_db} - \left(\frac{\text{rate_error}^2}{2 \times \text{jet_accel}} \right)$$

The lower attitude limit was calculated by:

$$\text{lower_attitude_limit} = -\text{attitude_db} - \left(\frac{\text{rate_error}^2}{2 \times \text{jet_accel}} \right)$$

The tail of the coast region was defined by the rate dead-band above and the lower rate dead-band. The lower rate dead-band was set to be 80% of the `rate_deadband`. The lower coast limit was defined as 120% of the lower attitude limit.

The following functions defined the vehicle's current position on the phase plane and took advantage of the symmetry. The vertical axis, y , is the absolute value of the rate error, and x represents the horizontal axis:

$$y = |\text{rate_error}|$$

$$x = \begin{cases} \text{att_error} & \text{if } \text{rate_error} \geq 0 \\ -\text{att_error} & \text{otherwise} \end{cases}$$

If the vehicle's attitude was outside the dead-band area, it had to be determined if the thrusters were to be fired "downward", "upward" or in the "coast" zone, by comparing current x and y position to the phase plane limits.

```

if ( y > rate_deadband || x > upper_attitude_limit )
{
    command = adjustForSymmetry(NEG_THRUST, rate_error);
}
else if ( y < (0.8 * rate_deadband) && x < (1.2 * lower_attitude_limit))
{
    command = adjustForSymmetry(POS_THRUST, rate_error);
}
else if ((y <= rate_deadband && (0.8 * rate_deadband) <= y && x <= lower_attitude_limit) ||
        (x <= lower_attitude_limit && (1.2 * lower_attitude_limit) <= x &&
        (0.8 * rate_deadband) <= y))
{
    command = ZERO_THRUST;
}
else
{
    command = ZERO_THRUST;
}

```

For a thruster firing, the thrust direction had to be adjusted for symmetry:

```

if (thrust == ZERO_THRUST || rate_error >= 0.0 )
{
    return thrust;
}
// rate_error was negative, so thruster commands must be reversed
else if (thrust == POS_THRUST)
{
    return NEG_THRUST;
}
else
{
    return POS_THRUST;
}

```

RCS mixer

The Orion Service Module [RCS](#) consists of 16 R-1E thrusters (four blocks of two thruster strings), referred to as Modified Block Swap Geometry, figure [B5](#). The 16 R-1E thrusters are rated at 25 ± 1 lbf, 220 s thrust specific impulse, and have minimum on time of 0.04 s. The mass properties for the Orion 606-C ISS 1 & 2 mission with a 0.27 lift-to-drag ratio were used for this experiment, as defined in Orion Vehicle Simulation Data Book [10].

The [RCS](#) Control Law provided body frame acceleration (P , Q , R , X , Y , and Z) sense commands (negative, zero, and positive). These commands were turned into jet commands by the [RCS](#) mixer. A [TDM RCS](#) mixer developed by one of the authors, described earlier, was implemented for this experiment. This feed-forward mixer fired some of the thrusters

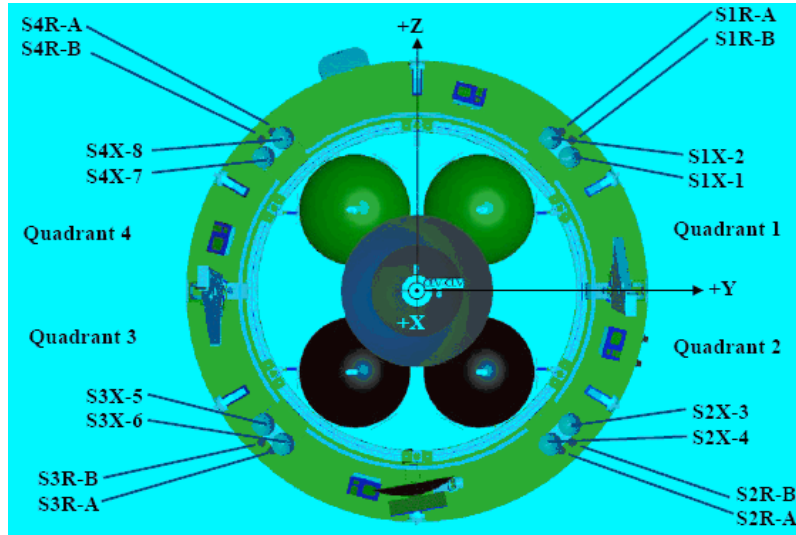


Figure B5: Cut-away aft view of the CEV Service Module looking forward

more than others to perform a single axis (uncoupled) maneuver. The resulting firings produced a translation with minimal rotational coupling (see section 6.4.2).

The TDM mixer also provided a non-feed-forward mixer option for the experiment. When this option was enabled, the mixer would provide simple four jet commands that would not prevent coupling of translation into rotation. Figure B6 shows the Simulink® model that was implemented for this experiment.

Conclusion

This appendix provided a description of the RCS control law as flown in this experiment. The control law provided the astronaut several modes for manual control of the simulated CEV during proximity operations and docking with another target spacecraft.

Code listings

updateRollCommand

```
void OrionHQRcsControlLaw::updateRollCommand()
{
    internal_att_var[ROLL]->att_error = -phi_error * deg_to_rad;

    // Check the autopilot mode see if it has changed
    if (autopilot_mode != past_autopilot_mode)
    {
        // reset the rate_command 0
        internal_att_var[ROLL]->rate_command = 0.0;
    }

    switch (autopilot_mode)
    {
        // free drift mode, use selected Attitude mode for jet firing
```

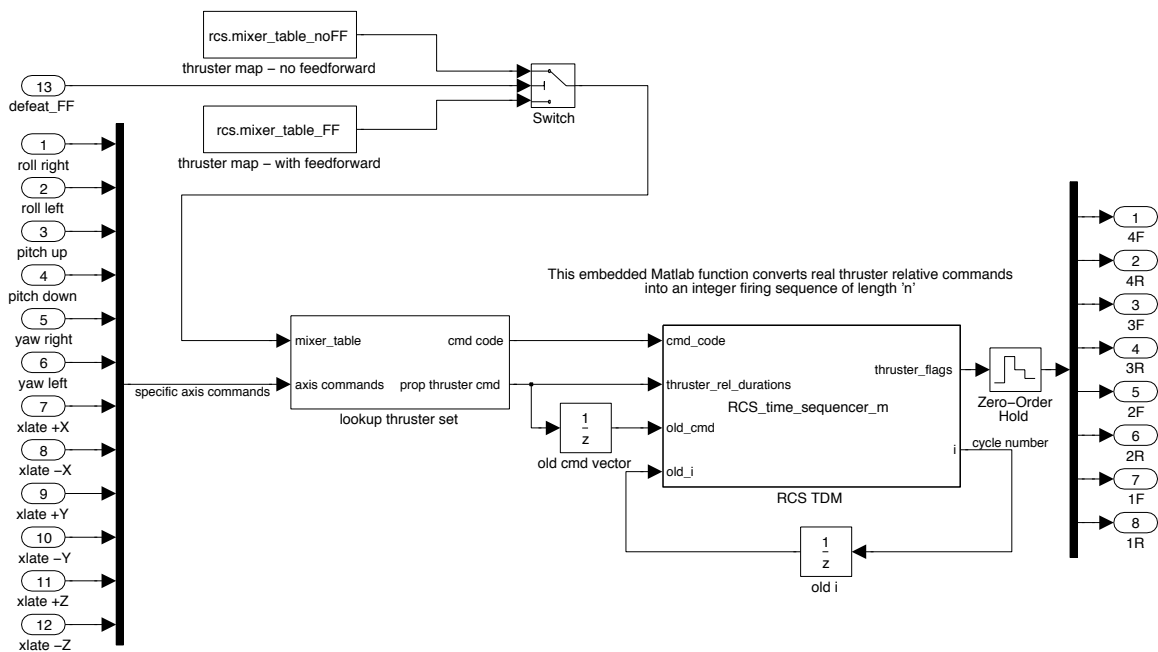


Figure B6: TDM mixer logic

```

case MANUAL:
{
  // Check for manual override by the inceptor
  if ( fabs(p_inceptor) >= 0.9 )
  {
    calcInceptorCommand(p_inceptor, internal_att_var[ROLL],
                        p_feedback,
                        config_options[rate_mode]->rotation_rate,
                        config_options[rate_mode]->roll_rate_deadband,
                        NORMAL);
  }
  else
  {
    calcInceptorCommand(p_inceptor, internal_att_var[ROLL],
                        p_feedback,
                        config_options[rate_mode]->rotation_rate,
                        config_options[rate_mode]->roll_rate_deadband,
                        roll_mode);
  }

  if (internal_att_var[ROLL]->thrust == POS_THRUST)
  {
    p_rcs_command = 1;
  }
  else if (internal_att_var[ROLL]->thrust == NEG_THRUST)

```

```

    {
        p_rcs_command = -1;
    }
    else
    {
        p_rcs_command = 0;
    }
    break;
}

case AUTO:
{
    internal_att_var[ROLL]->rate_command = p_cmd_auto;

    calcInceptorCommand(p_inceptor, internal_att_var[ROLL],
        ((autopilot_mode == LVLH) ?
         lvlh_p_feedback : p_feedback),
        (roll_mode == PULSE ?
         config_options[rate_mode]->rotation_pulse :
         config_options[rate_mode]->rotation_rate),
        config_options[rate_mode]->roll_rate_deadband,
        roll_mode);

    break;
}

case INERTIAL:
case LVLH:
{
    if (autopilot_mode == INERTIAL)
    {
        internal_att_var[ROLL]->rate_command = 0.0;
    }
    else if (autopilot_mode == LVLH)
    {
        if (roll_mode != PULSE)
        {
            internal_att_var[ROLL]->rate_command = 0.0;

            // Check to see if to reset the hold att
            if ( internal_att_var[ROLL]->in_detent &&
                 fabs(lvlh_p_feedback) <=
                 config_options[rate_mode]->roll_rate_deadband )
            {
                roll_lvlh_first_pass = true;
            }
        }
    }

    if ( roll_lvlh_first_pass && !internal_att_var[ROLL]->att_hold)
    {
        internal_att_var[ROLL]->att_hold = true;
        reset_att_hold = true;
    }
}

```

```

        roll_lvlh_first_pass = false;
    }
}

// Check for manual override by the inceptor
if ( fabs(p_inceptor) >= 0.9 )
{
    calcInceptorCommand(p_inceptor, internal_att_var[ROLL],
                        ((autopilot_mode == LVLH) ?
                         lvlh_p_feedback : p_feedback),
                        config_options[rate_mode]->rotation_rate,
                        config_options[rate_mode]->roll_rate_deadband,
                        NORMAL);
}
else
{
    calcInceptorCommand(p_inceptor, internal_att_var[ROLL],
                        ((autopilot_mode == LVLH) ?
                         lvlh_p_feedback : p_feedback),
                        (roll_mode == PULSE ?
                         config_options[rate_mode]->rotation_pulse :
                         config_options[rate_mode]->rotation_rate),
                        config_options[rate_mode]->roll_rate_deadband,
                        roll_mode);
}

if (internal_att_var[ROLL]->thrust == POS_THRUST)
{
    p_rcs_command = 1;
}
else if (internal_att_var[ROLL]->thrust == NEG_THRUST)
{
    p_rcs_command = -1;
}
else
{
    p_rcs_command = 0;
}
break;
}

default:
    break;
}
}

```

updateXTranslationCommand

```

void OrionHQRcsControlLaw::updateXTranslationCommand()
{
    switch (autopilot_mode)

```

```

{
// free drift mode, use selected Attitude mode for jet firing
case MANUAL:
case INERTIAL:
case LVLH:
{
// translational commands are disable in landing programs
if ( ( program < 60 ) ||
      ( program >=70 ) )
{
// Assumes a speedbrake handle input is used (0 forward to 1.0 aft)
// 0 to 0.25 -> forward    0.25 to 0.75 -> neutral    0.75 to 1.0 -> aft
double temp_inceptor = 0.0;
if (x_inceptor < 0.25)
{
temp_inceptor = 1.0;
}
else if (x_inceptor > 0.75)
{
temp_inceptor = -1.0;
}
else
{
temp_inceptor = 0.0;
}

// calculated the accumulated velocity based on the feedback
// acceleration
x_feedback += getTimer().getTimeStep() * nx * earth_reference_gravity;

calcInceptorCommand(temp_inceptor, internal_att_var[X_TRANS],
                    x_feedback,
                    config_options[rate_mode]->translation_pulse,
                    0.0,
                    x_trans_mode);

if (internal_att_var[X_TRANS]->thrust == POS_THRUST)
{
x_rcs_command = 1;
}
else if (internal_att_var[X_TRANS]->thrust == NEG_THRUST)
{
x_rcs_command = -1;
}
else
{
x_rcs_command = 0;
x_feedback = 0;
}
break;
}
}
}

```

```

    case AUTO:
    {
        x_rcs_command = x_cmd_auto;
        break;
    }

    default:
        break;
}

if ( x_rcs_command != 0 )
{
    rcs_sound = true;
}
}

```

calcInceptorCommand

```

void OrionHQRcsControlLaw::calcInceptorCommand(double      inceptor,
                                                InternalVar* attitude_var,
                                                double      rate_feedback,
                                                double      pulse_rate,
                                                double      rate_deadband,
                                                AttitudeMode att_mode)
{
    double effect = 0.0;

    // Calculate the effective inceptor position after accounting for noise
    if (fabs(inceptor) < attitude_var->noise)
    {
        effect = 0.0;
    }
    else if (inceptor > attitude_var->noise)
    {
        effect = (inceptor - attitude_var->noise) / (1.0 - attitude_var->noise);
        attitude_var->att_hold = false;
        reset_att_hold = false;
    }
    else if (inceptor < -attitude_var->noise)
    {
        effect = (inceptor + attitude_var->noise) / (1.0 - attitude_var->noise);
        reset_att_hold = false;
        attitude_var->att_hold = false;
    }

    // Based on the attitude mode, calculate the attitude command
    switch (att_mode)
    {
        case NORMAL:
        {

```

```

    if ( inceptor < 0.0 )
    {
        attitude_var->thrust = NEG_THRUST;
    }
    else if ( inceptor > 0.0 )
    {
        attitude_var->thrust = POS_THRUST;
    }
    else
    {
        attitude_var->thrust = ZERO_THRUST;
    }
    break;
}

case DISC_RATE:
{
    if ( effect < 0.0 )
    {
        attitude_var->rate_command = -pulse_rate;

        if (attitude_var->rate_command <= rate_feedback)
        {
            attitude_var->thrust = NEG_THRUST;
        }
        else
        {
            // apply zero thrust to maintian the rate
            attitude_var->thrust = ZERO_THRUST;
            attitude_var->rate_command = 0.0;
        }
    }
    else if (effect > 0.0 )
    {
        attitude_var->rate_command = pulse_rate;

        if (attitude_var->rate_command >= rate_feedback)
        {
            attitude_var->thrust = POS_THRUST;
        }
        else
        {
            // apply zero thrust to maintain the rate
            attitude_var->thrust = ZERO_THRUST;
            attitude_var->rate_command = 0.0;
        }
    }
    else
    {
        // calculate the rate error
        attitude_var->rate_error = rate_feedback;
    }
}

```

```

double rate_error = limit(attitude_var->rate_error * deg_to_rad,
                          -0.1, 0.1);

attitude_var->thrust =
    static_cast<ThrustType>(calcRcsControlCommand(attitude_var->att_error,
                                                  rate_error,
                                                  attitude_var->accel,
                                                  rate_deadband));
}
break;
}

case PULSE:
{
    if ( attitude_var->in_detent )
    {
        // This will start the pulse. The command is the commanded rate to drive
        // to for this one pulse.
        if ( effect < 0.0 )
        {
            attitude_var->rate_command = rate_feedback - pulse_rate;
            attitude_var->thrust = NEG_THRUST;
            attitude_var->increase_pulse = false;
        }
        else if ( effect > 0.0 )
        {
            attitude_var->rate_command = rate_feedback + pulse_rate;
            attitude_var->thrust = POS_THRUST;
            attitude_var->increase_pulse = true;
        }
    }

    // Pulse rate needs to be stopped when the feedback ~ = command
    if ( (attitude_var->increase_pulse &&
          rate_feedback >= attitude_var->rate_command) ||
          (!attitude_var->increase_pulse &&
           rate_feedback <= attitude_var->rate_command) )
    {
        attitude_var->thrust = ZERO_THRUST;
    }
    break;
}

case PROPORTIONAL:
{
    // pitch rate command after shaping
    attitude_var->shaped_rate = (1.0 - attitude_var->shaping) * effect +
        attitude_var->shaping * effect * fabs(effect);

    // pitch rate command
    attitude_var->rate_command =
        attitude_var->maximum * attitude_var->shaped_rate;
}
}

```

```

double rate_error =
    limit(-(attitude_var->rate_command - rate_feedback) * deg_to_rad,
          -0.1, 0.1);

attitude_var->thrust =
    static_cast<ThrustType>(calcRcsControlCommand(attitude_var->att_error,
                                                  rate_error,
                                                  attitude_var->accel,
                                                  rate_deadband));

    break;
}
}
}

```

calcRcsControlCommand

```

int OrionHQRcsControlLaw::calcRcsControlCommand(double att_error,
                                                double rate_error,
                                                double accel,
                                                double rate_deadband)
{
    double command;

    calcPhasePlanPosition(att_error, rate_error, accel);

    // Calculate the coordinate for plotting
    double y = fabs(rate_error);
    double x = (rate_error >= 0.0 ? 1 : -1) * att_error;

    if ( y > (rate_deadband * deg_to_rad) ||
        x > fire_ftc1 )
    {
        command = adjustForSymmetry(NEG_THRUST, rate_error);
        deadband_hit = true;
    }
    else if ( y < (0.8 * rate_deadband * deg_to_rad) &&
             x < 1.2 * coast_ftc2)
    {
        command = adjustForSymmetry(POS_THRUST, rate_error);
        deadband_hit = true;
    }
    else if ((y <= (rate_deadband * deg_to_rad) &&
             (0.8 * rate_deadband * deg_to_rad) <= y &&
             x <= coast_ftc2) ||
             (x <= coast_ftc2 &&
             (1.2 * coast_ftc2) <= x &&
             (0.8 * rate_deadband * deg_to_rad) <= y))
    {
        command = ZERO_THRUST;
    }
    else

```

```

    {
        command = ZERO_THRUST;
    }

    return command;
}

```

calcPhasePlanPosition

```

void OrionHQRCsControlLaw::calcPhasePlanPosition(double att_error,
                                                  double rate_error,
                                                  double accel)

{
    if ( accel != 0.0 )
    {
        fire_ftc1 = -(rate_error * rate_error / (2.0 * accel)) +
                    (config_options[rate_mode]->attitude_deadband * deg_to_rad);

        coast_ftc1 = (rate_error * rate_error / (2.0 * accel)) +
                    (config_options[rate_mode]->attitude_deadband * deg_to_rad);

        fire_ftc2 = (rate_error * rate_error / (2.0 * accel)) -
                    (config_options[rate_mode]->attitude_deadband * deg_to_rad);

        coast_ftc2 = -(rate_error * rate_error / (2.0 * accel)) -
                    (config_options[rate_mode]->attitude_deadband * deg_to_rad);
    }
    else
    {
        TerminalIO::applicationError("OrionHQRCsControlLaw::calcPhasePlanPosition()",
                                     "Jet Acceleration == 0.0! Please check io "
                                     "connections.",
                                     true,
                                     true);
    }
}

```

adjustForSymmetry

```

int OrionHQRCsControlLaw::adjustForSymmetry(ThrustType thrust,
                                             double rate_error)

{
    if (thrust == ZERO_THRUST || rate_error >= 0.0 )
    {
        return thrust;
    }
    // rate_error was negative, so thruster commands must be reversed
    else if (thrust == POS_THRUST)
    {
        return NEG_THRUST;
    }
    else

```

```
{  
  return POS_THRUST;  
}
```

Appendix C

Pilot Briefing Slides



SHaQ LaRC-2 Evaluation Pilot Briefing Guide

Co-PIs:

Randall E Bailey (D-318)

Bruce Jackson (D-316)

Ken Goodrich (D-316)

Al Ragsdale (D-107)

24 July 2008

Outline



- Spacecraft Handling Qualities (SHaQ) background
 - Experiment Objectives
- Simulation Overview
 - Controls and Displays
- Test Overview
 - Procedures
 - Data

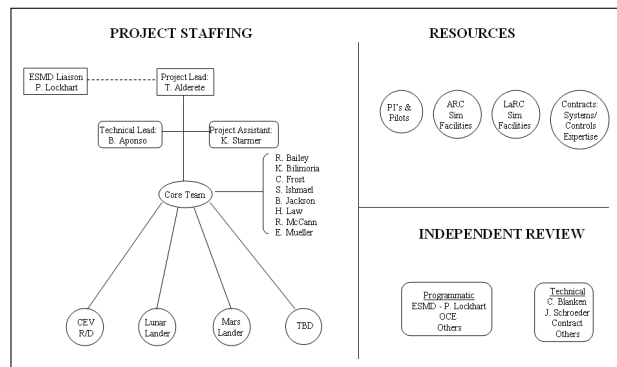
LaRC-2 EP Briefing Guide

Slide 2

Spacecraft Handling Qualities (SHaQ)



- ESMD - directed by Doc Horowitz - to undertake the development of a Spacecraft Handling Qualities Manual.
- Multi-Center Effort



LaRC-2 EP Briefing Guide

Slide 3

SHaQ Philosophy



- Goal:
 - To provide data and guidelines for the design, development, test and evaluation of all future NASA manned spacecraft
 - Provide options to Exploration for spacecraft GNC ideas
- Support CEV Handling Qualities evaluations
- Develop “Generic” Spacecraft Handling Qualities Requirements (long-term, low-effort, at present)
 - Using representative (Apollo, LM, CEV-like) models
 - Span “Crew Exploration Vehicle (CEV)-Type” issues to assist CEV (et al) development where possible and practical.

LaRC-2 EP Briefing Guide

Slide 4

Experiment Objectives

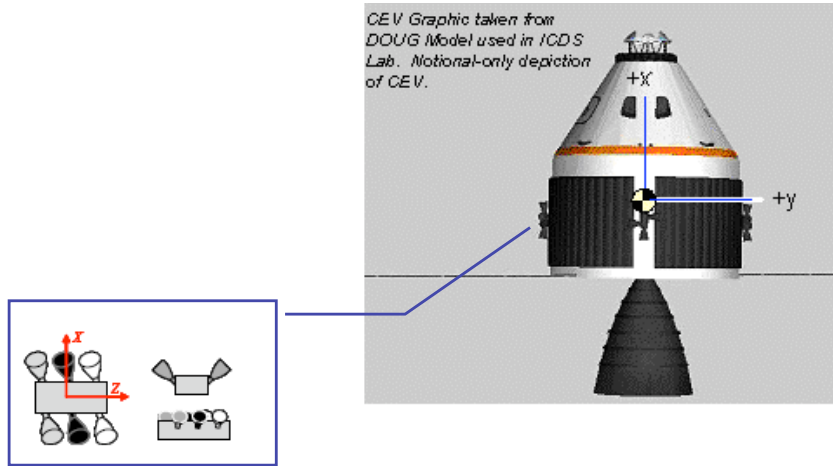


- Address shortcomings found in LaRC-1/Ames-2 for ‘coupled’ vehicles
 - Without some form of compensation, vehicles with RCS nozzles not aligned with vehicle center-of-mass exhibit ‘coupling’ where lateral translation RCS firings cause uncommanded rotations
 - Evaluate **feed-forward RCS mixing** to cancel rotations
 - Evaluate changes to **control laws for attitude** control
 - Evaluate novel **display cues** on centerline camera
- Investigate effect of target motion
 - Evaluate capability to manually dock with rotation target
 - Pitch, yaw separately and in combinations

LaRC-2 EP Briefing Guide

Slide 5

Reaction Control System (RCS)



Jackson, M. and Gonzalez, R., " Orion Orbit Reaction Control Assessment," paper presented at AIAA Guidance, Navigation and Control Conference and Exhibit, 20 - 23 August 2007, Hilton Head, South Carolina, AIAA Paper No. 2007-6684

LaRC-2 EP Briefing Guide

Slide 6

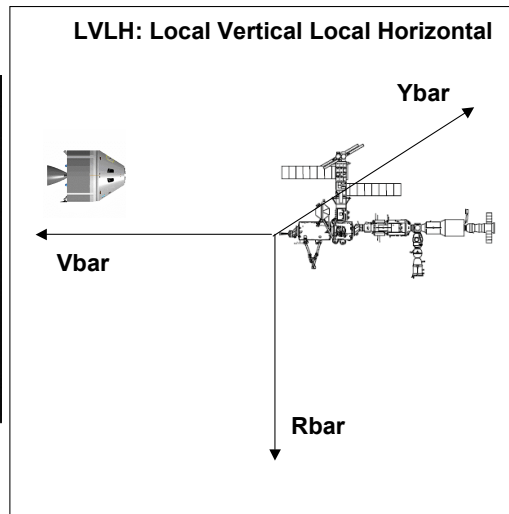
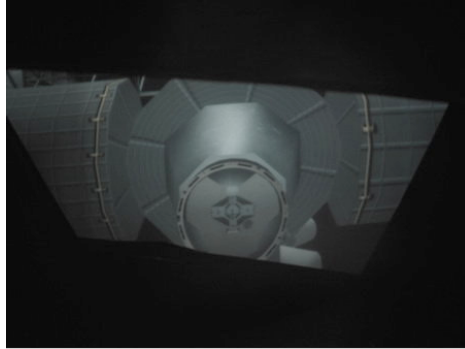


Simulation Overview

Prox. Ops and Docking



Vbar Docking Evaluation



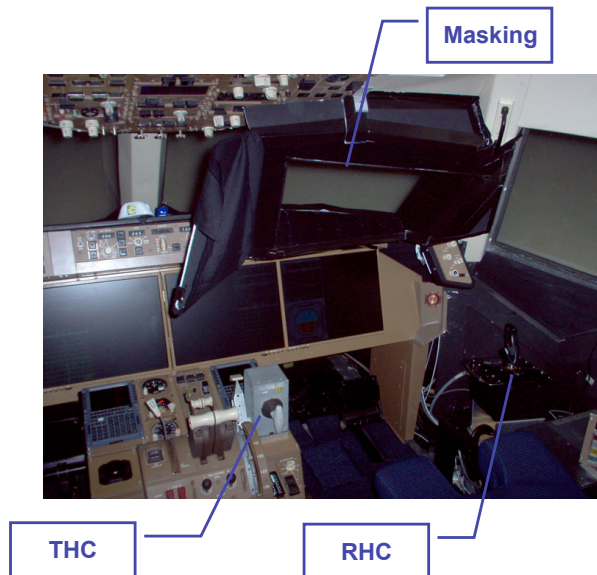
LaRC-2 EP Briefing Guide

Slide 8

RFD Simulator



- Test Conducted in RFD Simulator
 - Right Hand Seat
 - Installation of Rotational Hand Controller (RHC) and Translational Hand Controller (THC)
 - Window Masking Added



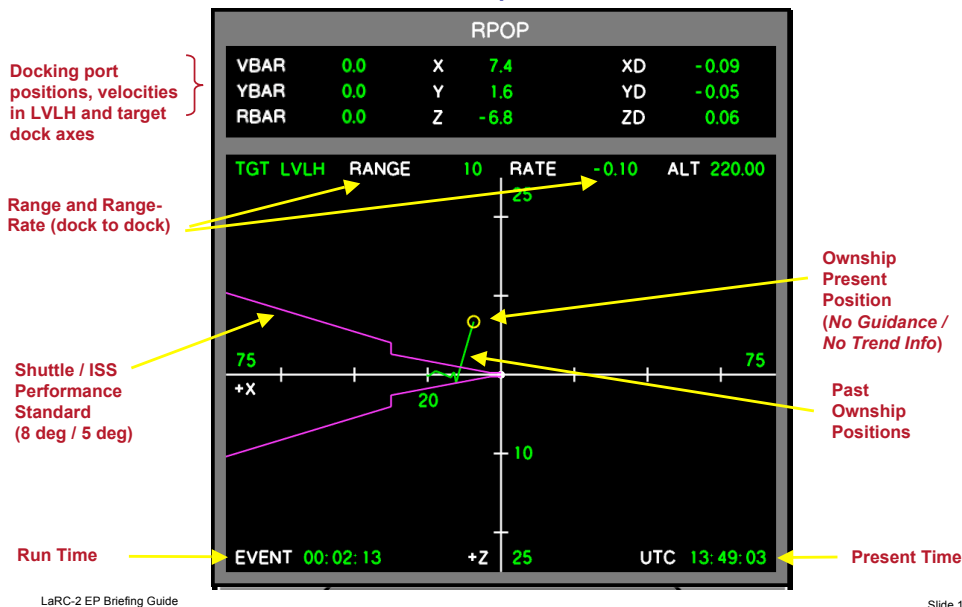
LaRC-2 EP Briefing Guide

Slide 9



Pseudo-RPOP

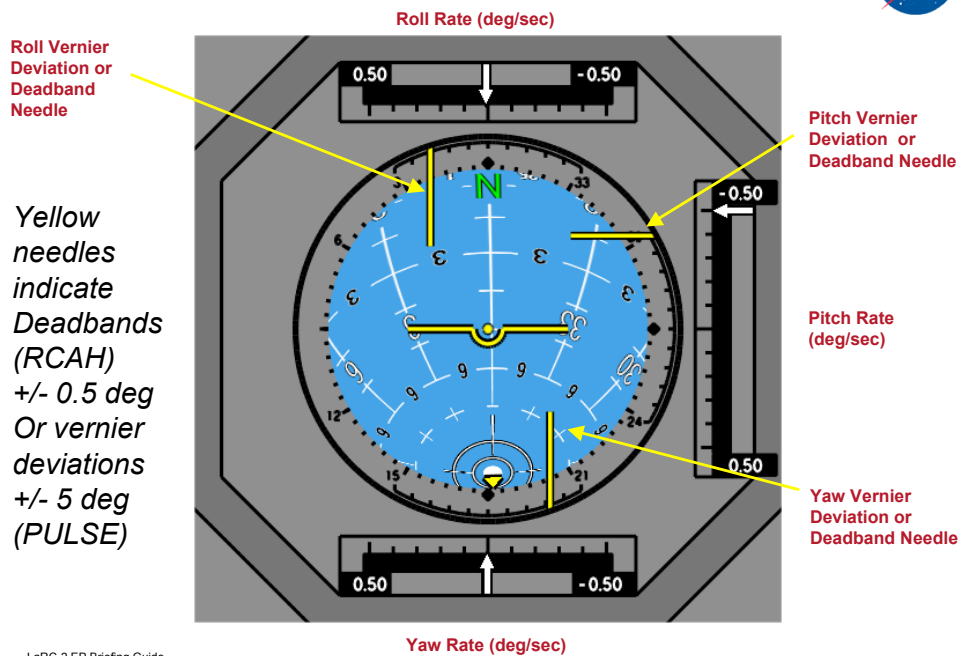
Pseudo-RPOP: Not A Replicate of Shuttle RPOP



LaRC-2 EP Briefing Guide

Slide 12

ADI (Default: LVLH)



LaRC-2 EP Briefing Guide

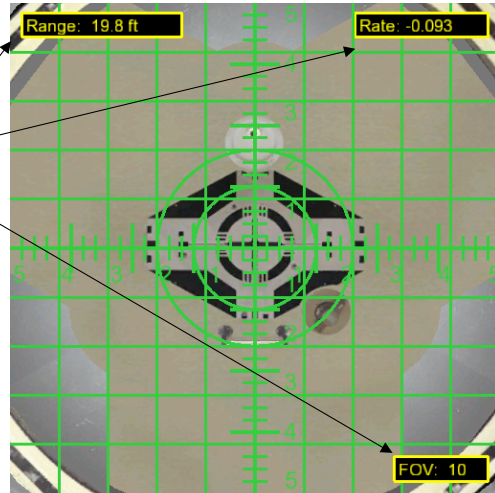
Slide 13

Centerline Camera Symbology



Minimal symbology shown

Range to Dock
Range Rate
Current Field of View



LaRC-2 EP Briefing Guide

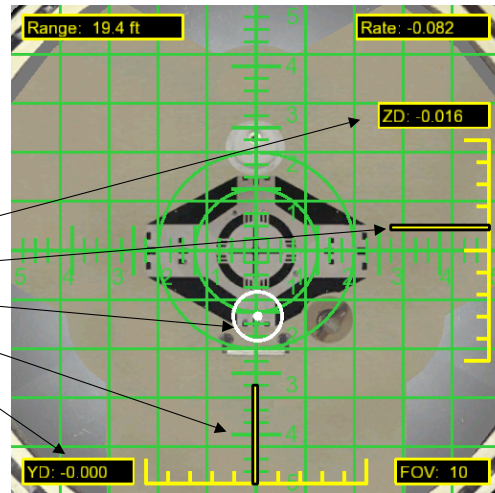
Slide 16

Centerline Camera Symbology (cont'd)



RHC DISCRETE mode symbology shown

Vertical velocity readout
Pitch dead-band scale
Impact Predictor
Yaw dead-band scale
Lateral velocity readout



LaRC-2 EP Briefing Guide

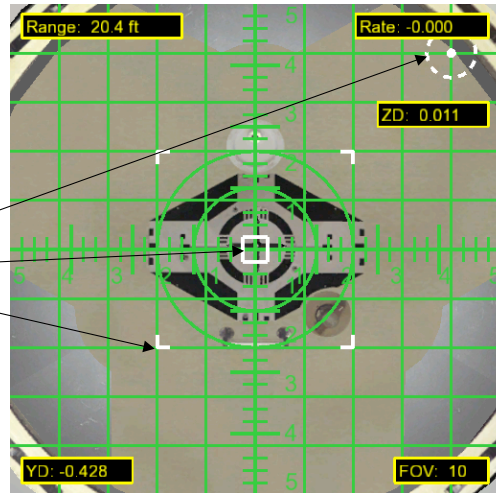
Slide 17

Centerline Camera Symbology (cont'd)



RHC PULSE mode symbology shown

Impact Predictor (limited)
Attitude Status indicator
Attitude Limits ($\pm 1^\circ$) box



LaRC-2 EP Briefing Guide

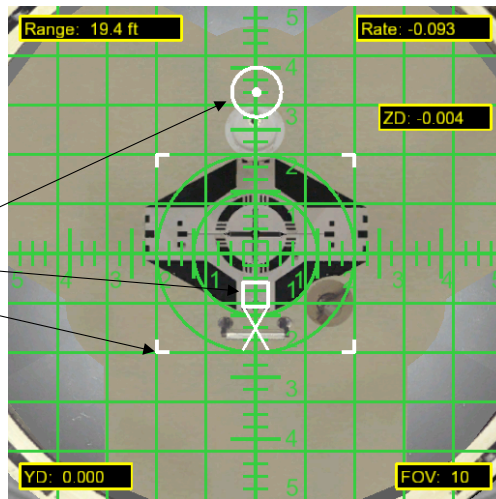
Slide 18

Centerline Camera Symbology (cont'd)



RHC PULSE mode symbology shown

Impact Predictor
Attitude Status indicator
Attitude Limits ($\pm 1^\circ$) box



LaRC-2 EP Briefing Guide

Slide 19

Centerline Camera Symbology (cont'd)



- Impact Predictor
 - Estimates where center of ownship docking ring will land on target
 - Includes 'droop' compensation for orbital effects

Here the Impact Predictor indicates eventual docking several inches outside the adequate bounds



Sometimes contradicts current alignment and translation due to orbital effects

LaRC-2 EP Briefing Guide

Slide 20

Centerline Camera Symbology (cont'd)



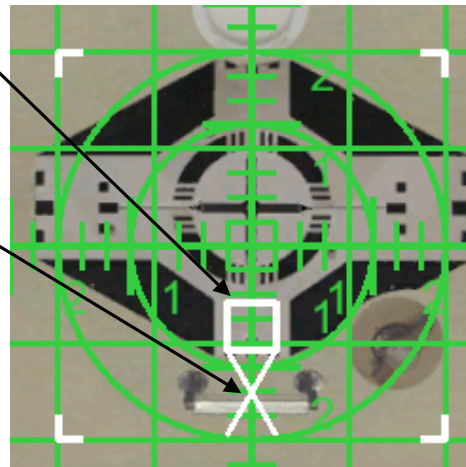
Attitude Status Indicator

Shows current attitude error relative to dead-band limits (corner ticks), as well as current angular rates.

Angled lines cross when rate reaches maximum desired rate.

Here the ASI indicates

- ~0.4 degree nose-low pitch angle,
- pitching nose-down, at about
- twice the docking limit



LaRC-2 EP Briefing Guide

Slide 21

Scorecard



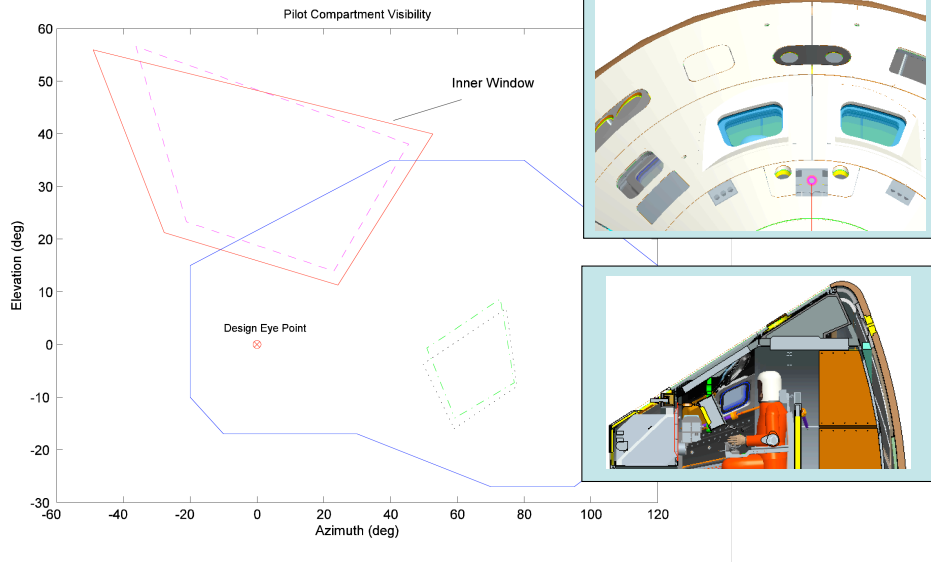
- Gives performance numbers for approach and docking phases
- Assists pilot in providing subjective ratings about difficulty of task

DOCKING EVENT 19-JUN-08 13:55Z		CONFIG 2101	
		RUN 00013	
	MIN	MAX	RATING
APPROACH:			
RDOT	-0.06	-0.11	ADEQUATE
DOCKING:			
LINEAR OFFSET		0.53	DESIRED
LINEAR RATE		0.00	DESIRED
RDOT		-0.06	ADEQUATE
PHI		-0.47	DESIRED
PHIDOT		0.00	DESIRED
THETA		-0.48	DESIRED
THETADOT		0.01	DESIRED
PSI		0.39	DESIRED
PSIDOT		0.04	DESIRED
ZDOT		-0.01	DESIRED
YDOT		0.00	DESIRED

LaRC-2 EP Briefing Guide

Slide 22

CEV-Like Window Size & Location



LaRC-2 EP Briefing Guide

Slide 23



Test Overview

Overview / Method

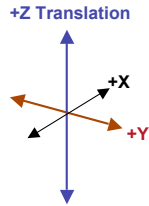


- Using CEV 606C model
 - ISS 1&2 0.27 'First Docking Attempt' inertias
- Two RCS mixers
 - Four-jet combos with some coupling
 - Feed-forward mixer with minimal coupling
- Control Laws
 - Two modes for translation (THC)
 - PULSE: Each THC input adds 0.01 or 0.002 ft/s per axis (A/B)
 - NORMAL: Continuous firing when out of detent
 - Two modes for rotation (RHC):
 - PULSE: Each RHC input adds 0.04 deg/s (free-drift)
 - DISCRETE (RCAH) holds LVLH attitude (closed-loop) within
 - 0.50 deg attitude deadband
 - 0.04 deg/s rate deadband

Translational Control Law



Translational Hand Controller



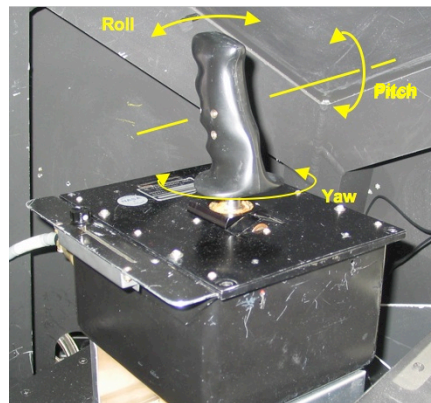
- Controller Closes a Discrete Switch
- Normal Mode
 - Fires Continuous Translational Jets; not used
- Pulse Mode
 - Adds pilot-selectable delta-V in each axis (0.01 or 0.002 fps)

Rotational Control Laws

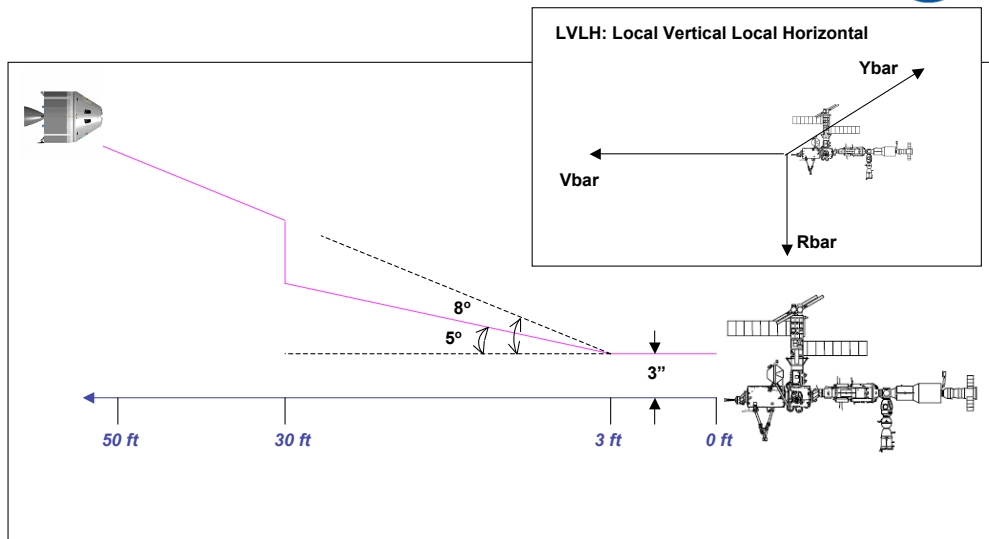


- DISCRETE (aka “RCAH”) mode
 - Discrete rate commanded beyond inner (15%) deadband
 - Exceeding 90% control authority causes continuous firings
 - Return to neutral holds attitude reached when rotation stops
- PULSE Mode
 - Input beyond inner (15%) deadband commands incremental rate
 - Exceeding 90% control authority causes continuous firings
 - Must return to neutral before another pulse can be generated
 - Rate delta is 0.04 deg/s

Rotational Hand Controller



Side View of +Vbar Docking Task



LaRC-2 EP Briefing Guide

Not Drawn to Scale.
Only "+Vbar" Profile performance shown.
Desired Approach "Corridors" based on RPOD ISS Requirements

Slide 28

Task 1 - ISS Docking



- Stationary ISS Docking Target
- Initial condition:
 - 20 ft from docking port along +Vbar
 - Closure rate -0.1 ft/s
 - Offset from docking centerline
 - Ybar and/or Zbar +/- 3 ft
 - Zero Angular Offsets
 - Zero Angular Rates
- Experiment variables:
 - **Feedforward**: off; ideal; 4% thruster variations; CG variations
 - **RHC mode**: RCAH off (PULSE); on (DISCRETE)
 - **Symbology**: off; on (slight differences depending on RHC mode)

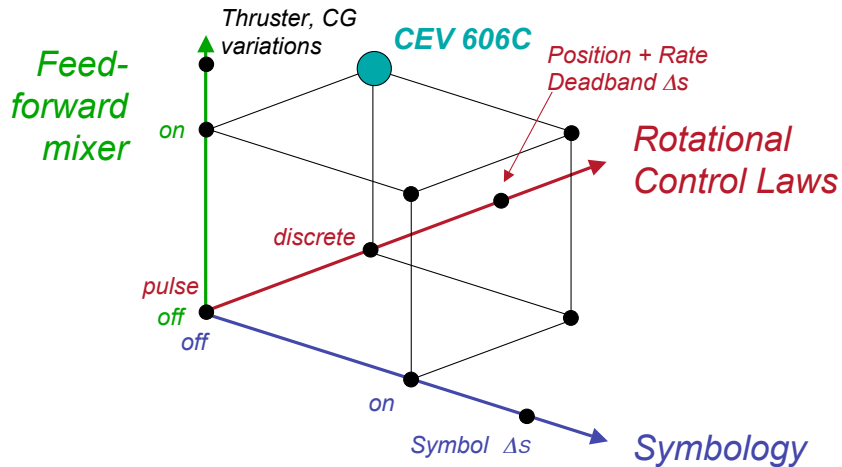
LaRC-2 EP Briefing Guide

Slide 29

Task 1: Docking - Test Dimensions



Test matrix is a 3-D cube (eight points) with additional explorations along each axis:



LaRC-2 EP Briefing Guide

Slide 30

Task 2 - Apollo CSM Docking



- Rotating CSM Docking Target
 - Pitching and/or yawing about inertial axis at constant rate
 - Rate to be determined by experiment; blind to EP
- Initial conditions
 - 20 ft from docking port along +Vbar
 - Initial closure rate 0.1 ft/s
 - No initial misalignments or lateral offsets
- Experimental variables
 - Pitch and/or yaw rates of 0.4 deg/sec (program requirement)
 - In two axes: both 0.4 root-sum-squared and 0.4 each axis



LaRC-2 EP Briefing Guide

Slide 31

Procedures



- Configuration Details - Task 1, ISS docking
 - Mixer type (either feed-forward or simple jet groups) - blind
 - Symbology on/off - obvious
 - Rotational mode (Pulse or Discrete/RCAH) - briefed
- Configuration Details - Task 2, CSM docking
 - Feed-forward mixer - briefed
 - Selected symbology - obvious
 - Yaw axis in PULSE; pitch & roll in DISCRETE - briefed
- Aural Range Call-Outs
 - 20, 15, 10, 9, 8, ... 1
- For Each Configuration:
 - One run for practice / familiarization
 - Two runs for “data”
 - Optional third run at pilot request
 - Pilot Rating and Comment / Questionnaire data

LaRC-2 EP Briefing Guide

Slide 32

Docking Task Performance Standards



	<i>Desired</i>	<i>Adequate</i>
Radial Offset	1.5 in	1.5 to 3.2 in
Roll and Pitch+Yaw Angle	±1.5 deg	±1.5 to ±3.0 deg
Axial Closure Rate	0.075 to 0.125 fps	0.05 to 0.075 fps 0.125 to 0.15 fps
Radial (Linear) Rate	0.075 fps	0.075 to 0.15 fps
Roll/Pitch/Yaw (Angular) Rate	±0.075 deg/s	±0.075 to ±0.15 deg/s

Closure Rate on Approach Also “Graded”

LaRC-2 EP Briefing Guide

Slide 33

Comment Card

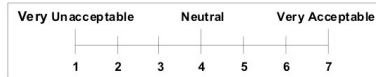
SHAQ Pilot Comment Card



1) Assign Cooper-Harper Pilot Ratings

2) Translational Control

Rate Acceptability of Translational Control for Mission/Task:

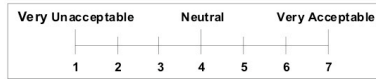


Please Comment On:

- a. Translational Control Power / Sensitivity?
- b. Ability to Precisely Control / Maintain Position & Closure

3) Rotational Control (If Applicable)

Rate Acceptability of Rotational Control for Mission/Task:

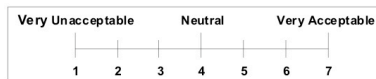


Please Comment On:

- a. Rotational Control Power / Sensitivity?
- b. Ability to Precisely Control / Maintain Attitude

4) Control Coupling:

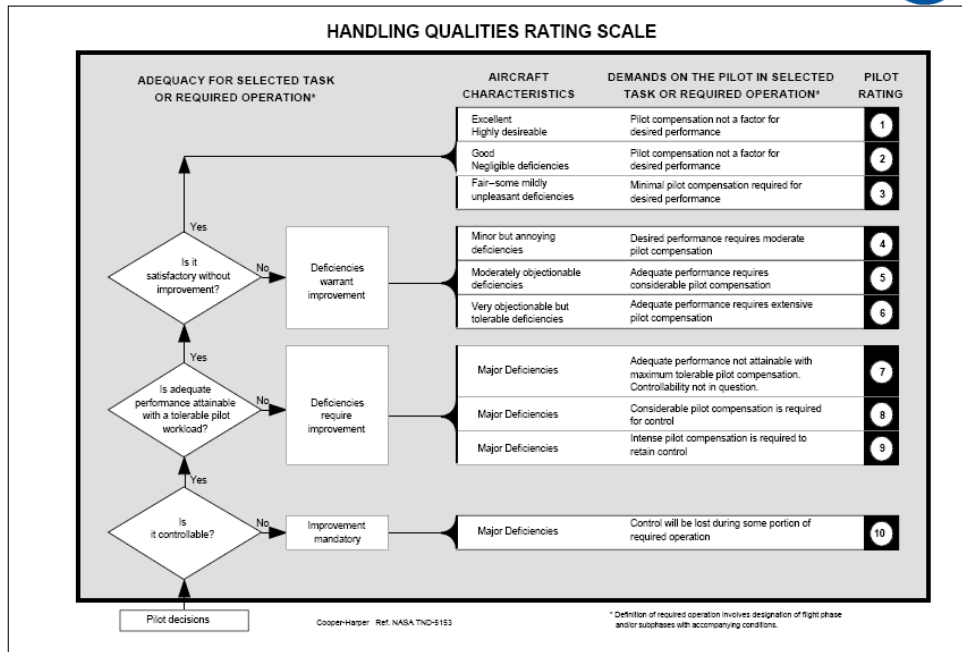
Rate Acceptability of Coupling for Mission/Task:



5) Summary / Overall Comments

- a. Any Change in Pilot Rating?
- b. TLX Rating

Cooper-Harper Pilot Rating Scale



NASA TLX Workload Scale



Subject ID: _____ Study ID: _____

Verbalize your rating for each scale:

Title	Descriptions
MENTAL DEMAND	How much mental and perceptual activity was required (e.g., thinking, deciding, calculating, remembering, looking, searching, etc.)? Was the task easy or demanding, simple or complex, exacting or forgiving?
PHYSICAL DEMAND	How much physical activity was required (e.g., pushing, pulling, turning, controlling, activating, etc.)? Was the task easy or demanding, slow or brisk, slack or strenuous, restful or laborious?
TEMPORAL DEMAND	How much time pressure did you feel due to the rate or pace at which the tasks or task elements occurred? Was the pace slow and leisurely or rapid and frantic?
PERFORMANCE	How successful do you think you were in accomplishing the goals of the task set by the experimenter (or yourself)? How satisfied were you with your performance in accomplishing these goals?
EFFORT	How hard did you have to work (mentally and physically) to accomplish your level of performance?
FRUSTRATION LEVEL	How insecure, discouraged, irritated, stressed and annoyed versus secure, gratified, content, relaxed and complacent did you feel during the task?

MENTAL DEMAND

0 _____ 50 _____ 100

Low _____ High

PHYSICAL DEMAND

0 _____ 50 _____ 100

Low _____ High

TEMPORAL DEMAND

0 _____ 50 _____ 100

Low _____ High

PERFORMANCE

0 _____ 50 _____ 100

Poor _____ Good

EFFORT

0 _____ 50 _____ 100

Low _____ High

FRUSTRATION

0 _____ 50 _____ 100

Low _____ High

LaRC-2 EP Briefing Guide

Slide 36

Schedule



- In Sim
 - Nominal Schedule:
 - 1 Hour Blocks with 15 min. Breaks Between
 - Can Call For Breaks Whenever Desired
- Training
 - 2 One Hour Sessions
 - 15 Min Break Between
 - Displays, Controllers, Control Laws, Task
- Data
 - One Hour Sessions
 - 15 Min Breaks Between
 - As Long As Possible!

LaRC-2 EP Briefing Guide

Slide 37



Questions?

REPORT DOCUMENTATION PAGE

*Form Approved
OMB No. 0704-0188*

The public reporting burden for this collection of information is estimated to average 1 hour per response, including the time for reviewing instructions, searching existing data sources, gathering and maintaining the data needed, and completing and reviewing the collection of information. Send comments regarding this burden estimate or any other aspect of this collection of information, including suggestions for reducing this burden, to Department of Defense, Washington Headquarters Services, Directorate for Information Operations and Reports (0704-0188), 1215 Jefferson Davis Highway, Suite 1204, Arlington, VA 22202-4302. Respondents should be aware that notwithstanding any other provision of law, no person shall be subject to any penalty for failing to comply with a collection of information if it does not display a currently valid OMB control number.
PLEASE DO NOT RETURN YOUR FORM TO THE ABOVE ADDRESS.

1. REPORT DATE (DD-MM-YYYY) 01-02-2010			2. REPORT TYPE Technical Memorandum		3. DATES COVERED (From - To)	
4. TITLE AND SUBTITLE Investigation of Control System and Display Variations on Spacecraft Handling Qualities for Docking with Stationary and Rotating Targets					5a. CONTRACT NUMBER	
					5b. GRANT NUMBER	
					5c. PROGRAM ELEMENT NUMBER	
6. AUTHOR(S) Jackson, E. Bruce; Goodrich, Kenneth H.; Bailey, Randall E.; Barnes, James R.; Ragsdale, William A.; Neuhaus, Jason R.					5d. PROJECT NUMBER	
					5e. TASK NUMBER	
					5f. WORK UNIT NUMBER 825855.04.03.04.05	
7. PERFORMING ORGANIZATION NAME(S) AND ADDRESS(ES) NASA Langley Research Center Hampton, VA 23681-2199					8. PERFORMING ORGANIZATION REPORT NUMBER L-19801	
9. SPONSORING/MONITORING AGENCY NAME(S) AND ADDRESS(ES) National Aeronautics and Space Administration Washington, DC 20546-0001					10. SPONSOR/MONITOR'S ACRONYM(S) NASA	
					11. SPONSOR/MONITOR'S REPORT NUMBER(S) NASA/TM-2010-216194	
12. DISTRIBUTION/AVAILABILITY STATEMENT Unclassified - Unlimited Subject Category 08 Availability: NASA CASI (443) 757-5802						
13. SUPPLEMENTARY NOTES						
14. ABSTRACT This paper documents the investigation into the manual docking of a preliminary version of the Crew Exploration Vehicle with stationary and rotating targets in Low Earth Orbit. The investigation was conducted at NASA Langley Research Center in the summer of 2008 in a repurposed fixed-base transport aircraft cockpit and involved nine evaluation astronauts and research pilots. The investigation quantified the benefits of a feed-forward reaction control system thruster mixing scheme to reduce translation-into-rotation coupling, despite unmodeled variations in individual thruster force levels and off-axis center of mass locations up to 12 inches. A reduced rate dead-band in the phase-plane attitude controller also showed some promise. Candidate predictive symbology overlaid on a docking ring centerline camera image did not improve handling qualities, but an innovative attitude status indicator symbol was beneficial. The investigation also showed high workload and handling quality problems when manual dockings were performed with a rotating target. These concerns indicate achieving satisfactory handling quality ratings with a vehicle configuration similar to the nominal Crew Exploration Vehicle may require additional automation.						
15. SUBJECT TERMS Spacecraft; Thrust vectoring; Handling qualities; Flying qualities; Docking; RPOD; RCS						
16. SECURITY CLASSIFICATION OF:			17. LIMITATION OF ABSTRACT	18. NUMBER OF PAGES	19a. NAME OF RESPONSIBLE PERSON	
a. REPORT	b. ABSTRACT	c. THIS PAGE			19b. TELEPHONE NUMBER (Include area code)	
U	U	U	UU	124	STI Help Desk (email: help@sti.nasa.gov) (443) 757-5802	

